UNIVERSITEIT VAN PRETORIA
UNIVERSITY OF PRETORIA
YUNIBESITHI YA PRETORIA

INTERNAL VIBRATION MONITORING OF A PLANETARY GEARBOX

by

Marc Ryan de Smidt

Submitted in partial fulfilment of the requirement
for the degree

Master of Engineering

in the

Department of Mechanical and Aeronautical Engineering

Faculty of Engineering, the Built Environment and Information Technology

University of Pretoria

March 2009

© University of Pretoria

UNIVERSITEIT VAN PRETORIA
UNIVERSITY OF PRETORIA
YUNIBESITHI YA PRETORIA

Internal vibration monitoring of a planetary gearbox

by

Marc Ryan de Smidt

Supervisor: Prof P. S. Heyns
Department: Mechanical and Aeronautical Engineering
Degree: Master of Engineering

Abstract

Vibration monitoring is widely used to determine the condition of various mechanical systems. Traditionally a transducer is attached to the structure under investigation and the vibration signal recorded. This signal is then processed and the required information extracted from the signal. With epicyclic gearboxes this traditional approach is not advisable. This is in part due to the fact that the planet gears rotate internally on a planet carrier. Special techniques are therefore required to extract a viable data signal from the measured vibration signal. These techniques require an additional post-processing step in which a compiled data signal is extracted from the measured data signal.

This work investigates the possibility of mounting transducers internally on the rotating planet carrier. Mounting transducers at this location removes the relative motion seen in traditional measurement techniques. An epicyclic gearbox is modified to facilitate the internal mounting of the accelerometers. A number of implementation problems are highlighted and solutions to these problems are discussed.

A large portion of the work is dedicated to implementing and qualifying the epicyclic time synchronous averaging technique which is traditionally used to evaluate epicyclic gearboxes. As this technique forms the basis to evaluate the data obtained from internal measurements, it is of fundamental importance that the technique is implemented correctly.

It is shown that vibration data can be reliably measured internally, by means of accelerometers mounted on the planet carrier. The internally measured data is compared

to data obtained by traditional techniques and shown to be equally adept in detecting deterioration of a planet gear tooth.

Simple condition indicators were used to compare the vibration data of the two techniques. It was seen that the data obtained from the internally mounted accelerometers was equally, and in certain cases, slightly more sensitive to planet gear damage. This implies that the technique can be used successfully to evaluate epicyclic gearbox damage. There are a number of practical implementation problems that will limit the use of this technique. As the technology becomes available to transmit measured vibration signals wirelessly, the application of the internal measurement technique will become more viable.

A preliminary investigation was also launched into the relationship between a planetary gearbox with a single planet gear and one with multiple planet gears. It is illustrated that vibration data, measured from a gearbox containing a single planet gear, shows an increased sensitivity to planet gear damage. Although a special test rig might be required, the increased sensitivity to damage can provide a method to test planet gears in critical applications such as aircraft gearboxes.

KEYWORDS

Epicyclic gearbox, planet gear, ring gear, sun gear, damage detection, internally mounted transducers

TABLE OF CONTENTS

TABLE OF ILLUSTRATIONS
FIGURES

TABLES

UNIVERSITEIT VAN PRETORIA
UNIVERSITY OF PRETORIA
YUNIBESITHI YA PRETORIA

EXPRESSIONS OF THANKS

My Creator and saviour, Jesus Christ – A firm foundation in the trying times that it took to complete this thesis

Nerina de Smidt, my wife – Without your support, love and patience I would not have been able to complete this research

Neil and Shann de Smidt, my parents – Your love and commitment has carried me through difficult times

Prof Stephan Heyns – For your continued patience, support and advice

John Hofmeyr – For your time and input and experience have been greatly appreciated

Danie Els – For the leeway you gave me to put extra time into my studies

5ASU VCC Staff – For the extra that you put in to allow me to finish my studies

At du Preez – For the advice and equipment that you let me use on such a regular basis

Willem Ras – For the help you are always willing to give

Jan Brand – For the design and manufacturing advice that was integral to my work

Frans Windell – For your time and help in maintaining the measurement equipment

A number of companies and persons assisted in the development of this research. Special thanks to the individuals and companies who assisted:

COMPANY	INDIVIDUAL	ASSISTANCE WITH
Bonfiglioli Power Transmissions (Pty) Ltd	Tony dos Santos	Calculation and sizing of required epicyclic gearbox Design specifications for manufacture
Flender Power Transmission (Pty) Ltd	Mike Hoepper Peter Boxall	Frequency calculation of epicyclic gearboxes Practical vibration monitoring pitfalls on epicyclic gearboxes Discussion regarding epicyclic gearboxes
M-Tek	Martin	Donation of slip rings Operational specification of slip rings Design verification of slip ring mounting
Pretoria Instrument Makers	Johan Binedell	Assistance in design Manufacturing of components
	Goestaf Binedell	Manufacturing of components
South African Air Force	AO Johan von Biljon	Selection of shaft steel Material specification for shaft steel
	Conraad Snyman	Microscope investigation Material testing and element specification
SKF Pretoria	Meshak Mahlangu	Sizing of bearings and seals
Textron Power Transmissions	ColinThornton Damas Gomes	Epicyclic gearbox requirements

NOMENCLATURE

Abbreviations

CF	Crest Factor
CI	Condition Indicators
DFT	Discrete Fourier Transform
ED	Extremely Damaged Tooth on Planet Gear
EO	Energy Operator
EpiTSA	Epicyclic Time Synchronous Averaging
ER	Energy Ratio
$FM0^e$	Zero-Order Figure of Merit
$FM4^e$	Fourth-Order Figure of Merit
GMF	Gear Mesh Frequency
lcm	Lowest Common Multiple
mod	Modulus - signed remainder after division
NK	Normalized Kurtosis
OEM	Original Equipment Manufacturer
P1	Planet Gear 1
P2	Planet Gear 2
P3	Planet Gear 3
PPF	Planet Pass Frequency
PSOA	Particle Swarm Optimization Algorithm
RD	Relatively Damaged tooth on planet gear
RMS	Root Mean Squared
SD	Slightly Damaged tooth on planet gear
SDev	Standard Deviation
SI	Sideband Indicator
SLF	Sideband Level Factor
T#	Planet Tooth #
TMP	Tooth Mesh Period
TSA	Time Synchronous Averaging
UD	Undamaged Planet gear
VCC	Vibration Control Centre
WVD	Wigner-Ville Distribution

NOMENCLATURE

Symbols

f_{shaft}	Shaft rotational frequency
L	Window length
m	Harmonic number
n	Number of revolutions
N_g	Number of teeth on gear of interest
N_n	Number of data sets
$N_{n,g}$	Tooth number engaged on gear of interest
N_p	Number of teeth on planet gear
N_r	Number of teeth on ring gear
$n_{Reset,g}$	Number of planet revolutions to same tooth re-mesh on gear of interest
$n_{Reset,p}$	Number of planet revolutions to same tooth re-mesh on planet gear
$n_{Reset,s}$	Number of planet revolutions to same tooth re-mesh on sun gear
N_s	Number of teeth on sun gear
P	Number of planet gears present in the gearbox
P_i	Position on planet gear i
p	Planet under investigation
Q_{ims}	Phase contribution to the spectrum
s	Sideband number
T_{shaft}	Period of a single shaft revolution
Δf	Frequency resolution
ω	Rotational speed

Chapter 1 - Introduction and literature study

1.1. Introduction to epicyclic gearboxes

The concept of an epicyclic gearbox was developed by James Watt in 1781 *http://www.princeton.edu/~humcomp/bikes/design/desi_87.html* (Accessed 01 May 2006) for use with steam engines.

Later in 1902 Sturmey and Archer *http://www.princeton.edu/~humcomp/bikes/design/desi_87.html (Accessed 01 May 2006)* used the concept to develop a multi-speed rear bicycle hub, which initially had two speeds but was upgraded to three speeds soon thereafter.

An epicyclic or planetary gearbox consists of 3 main components. These components are illustrated in figure 1.1.

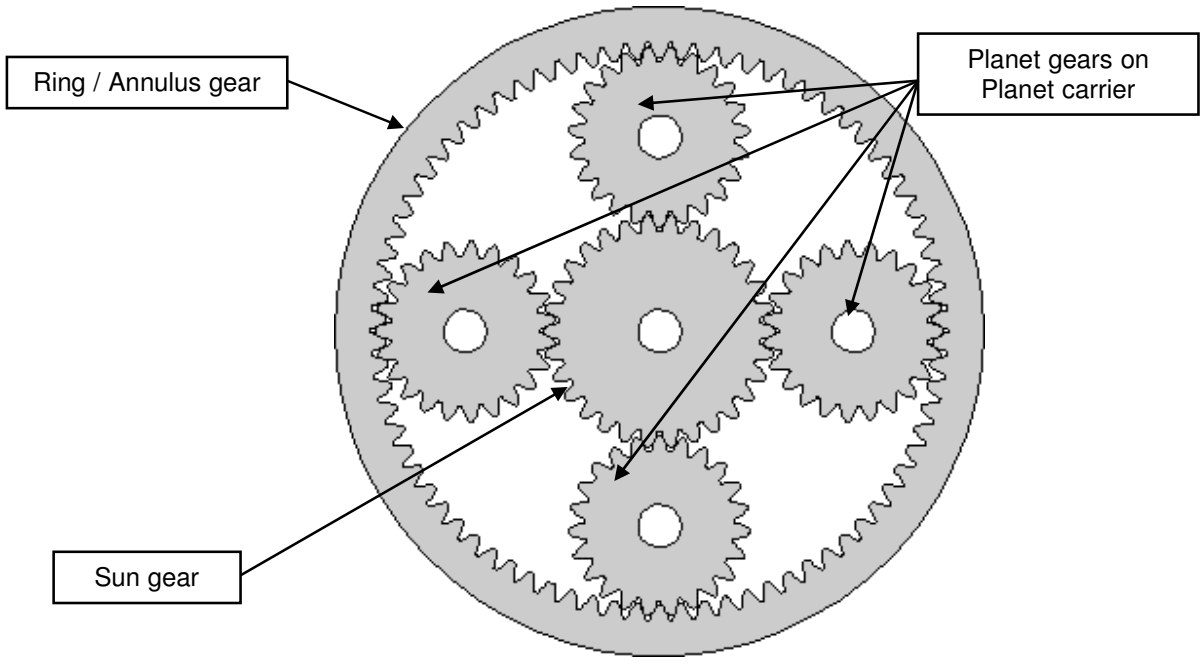

Figure 1.1 - Basic layout of an epicyclic gearbox

The epicyclic gearbox has in rare cases one, but in most applications multiple, planet or epicyclic gears that mesh and rotate around the central sun gear. The same planet gears are meshed and

rotate inside an internal ring gear. The planet gears are attached to a planet carrier which rotates around the same centre as the sun gear but at a different speed.

The advantages of using an epicyclic gearbox include the fact that a large speed / torque ratio is obtainable in a compact gearbox. Furthermore the fact that the input and output shafts lie on the same axis, means that the incoming shaft supplying drive to the gearbox and the outgoing shaft from the gearbox, align with each other. This means that equipment can be mounted on the same central axis without having an offset as would be the case if a non-aligned gearbox is used. This characteristic of an epicyclic gearbox considerably simplifies design. It is also well known that epicyclic gearboxes have low noise and vibration characteristics.

The epicyclic gearbox can operate in a number of different manners of which two are illustrated in figure 1.2. The planet carrier, sun gear or ring gear can be used as an input with any one of the other components being used as an output. Other configurations using one input and two outputs or two inputs and one output are possible. The left hand side gearbox in figure 1.2 has the ring gear fixed with the sun gear and planet carrier as input/output. The right hand side gearbox in figure 1.2 has the planet carrier fixed with the sun and ring gear as input/output. In most applications the sun gear is used as an input with the planet carrier being used as an output while the ring gear is kept stationary.

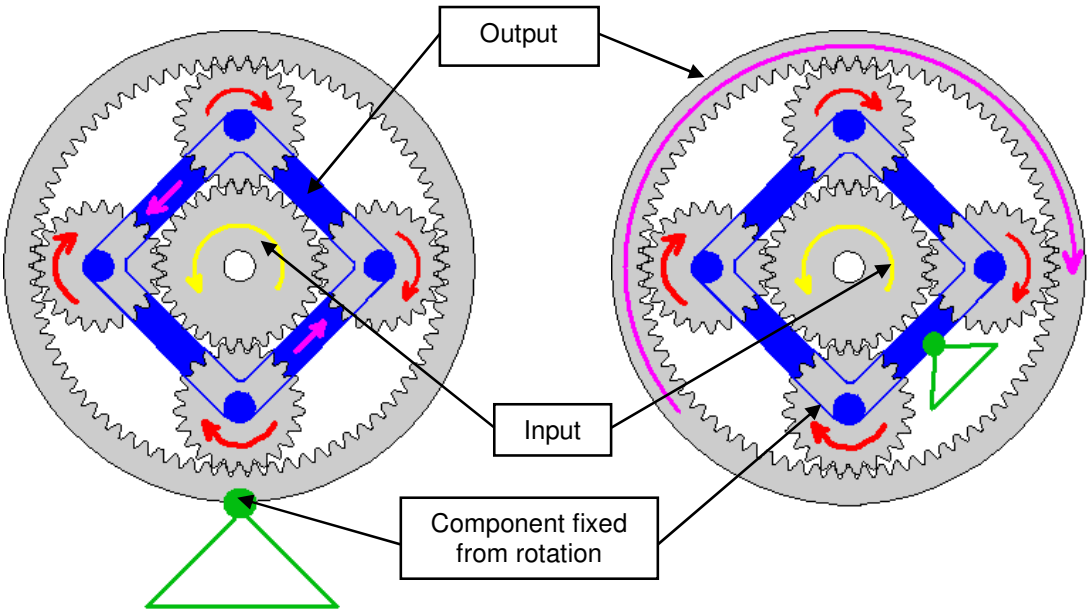

Figure 1.2 - Different operational applications of an epicyclic gearbox

Epicyclic gearboxes have the ability to adapt to different speed and torque ratios from the same planetary set, depending on which inputs and outputs are used and which gears remain stationary. This ability of the epicyclic gearbox makes it ideal for use in automatic vehicle transmissions, as well as other assemblies such as all-wheel drive transfer cases and axle differentials.

Epicyclic gearboxes are also extensively used in winch and lifting applications where high speed to torque conversion is required in a small space. Many other such applications for epicyclic gearboxes exist. Industry makes extensive use of epicyclic gearboxes and thus requires accurate monitoring capabilities for these gearboxes.

1.2. Vibration monitoring of gearboxes in general

Vibration monitoring is a commonly used method for determining faults in gear transmissions. Many different techniques exist to determine the condition of gears as well as determining other faults including cracks, damaged bearings, imbalance and other faults in these transmissions.

Vibration monitoring when correctly applied can be used not only to predict damage in a gearbox but also to monitor degradation, thus providing optimal use of equipment and scheduling of maintenance. Vibration monitoring is well described and researched.

Epicyclic gearboxes however cannot be monitored using the traditional techniques due the complexity of the gearbox. Specialized techniques are thus required to monitor these gearboxes.

There is however, limited research in the practical monitoring of epicyclic gearboxes. Thus research is required to expand the knowledge base in terms of vibration measurement of these gearboxes.

1.3. Aeronautical use of epicyclic gearboxes

The fact that epicyclic gearboxes enable large speed / torque ratios, have co-axial input and output shafts and have relatively large torque to mass ratios (Kahraman, 2001) makes these gearboxes ideal for use in aircraft applications. The helicopter environment makes extensive use of epicyclic

gearboxes as final drives to the rotors. It is well known that a helicopter gearbox is one of the most safety critical components and it is thus crucial that faults emanating from the gearbox can be identified before catastrophic failure occurs.

Epicyclic gearboxes are mainly used in the final drive of helicopters and final drive of propellers on fixed-wing aircraft. Figure 1.3 is the first stage planetary set used in the Oryx helicopter which has eight planet gears while figure 1.4 is that of the second planetary stage of the gearbox with nine planet gears.

Figure 1.3 - Oryx first stage planetary set

Figure 1.4 - Oryx second stage planetary set

These figures clearly show the complexity of an aeronautical epicyclic gearbox and also illustrate the compounding problem of identical planet gears. In the second stage a fault on a planetary gear will be masked by nine similar signals.

McAdams and Tumer (2002) state that failures in rotating machines on high risk aerospace applications are unacceptable. In certain applications gearbox failure with catastrophic results can occur without causing excessive damage or causing loss of life. In such applications failure prediction is not essential, however there are certain applications - especially in the helicopter environment - where gearbox failure cannot be allowed to occur as the effect of such failure would most likely result in the loss of the aircraft, but more importantly the loss of life of the people on board. Thus the monitoring of these critical gearbox components, to predict internal damage before failure occurs is of utmost importance in these high-risk applications.

Raithby and Baillie (2004) point out that a high five times propeller speed vibration level was found on a T56 Reduction Gearbox of a C-130 Hercules. After inspection it was found that the secondary planetary reduction system was damaged. The gear system has five planets and a correlation to the five times prop speed was made.

The practical monitoring of epicyclic gearboxes in industry is grossly underdeveloped. Guesses and attempts at diagnostics often lead to misdiagnosis resulting in gearboxes being withdrawn from service. Such mistakes are financially expensive as well as being expensive time wise as the entire systems must be withdrawn from service for replacement of a gearbox that is not damaged. Should the gearbox be misdiagnosed as being serviceable while there is in fact severe damage that would lead to catastrophic failure, the cost, both in human lives as well as financially, makes this misdiagnosis extremely dangerous and increases the tendency to remove undamaged gearboxes from service.

It can clearly be seen from the above discussion that a more accurate and reliable fault identification system for epicyclic gearboxes is highly desirable, especially to the aircraft industry.

1.4. Literature study

Howard (1990) as well as Forrester and Blunt (2003) point out that conventional vibration monitoring techniques cannot easily be applied to epicyclic gear transmissions, as these transmissions have multiple and time-varying vibration transmission paths, as well as multiple planet gears producing similar vibration signatures. McAdams and Tumer (2002) point out that a high rate of false alarms and missed failures occur with vibration monitoring especially on epicyclic gearboxes.

Most vibration monitoring techniques are valid for gears that are fixed to a stationary shaft under constant loads. Techniques to monitor under varying load and speed conditions have been developed by Stander, Heyns and Schoombie (2002) and have proved to be effective in determining transmission degradation under these conditions. The problem with these techniques however is that they relate to gears with fixed vibration transfer paths from the source of the vibration to the sensor. With planetary gears this path is not fixed but subject to variation.

Buyukataman and Kazerouian (1994) discuss experimental and analytical methods to ensure identification of system and component vibrations thus enabling isolation of the components or systems. Buyukataman and Kazerouian separate an epicyclic gearbox into three different levels of system and component dynamics. These levels can be described as given in table 1.1:

Table 1.1 - Epicyclic gearbox levels of system dynamics

Level	Description	Mechanisms
1	Components	Sun Gear
		Planet Gears
		Ring Gear
2	Sub Systems	Sun & Planet
		Ring & Planet
3	System	Entire Gearbox

Buyukataman and Kazerouian furthermore point out that the four main sources of excitation forces in an epicyclic gearbox are the sun gear mesh frequencies, the relative sun – planet gear mesh frequencies, the relative ring – planet gear mesh frequencies and the input and output shaft rotation.

McFadden and Smith (1985) state that in most standard gearboxes the tooth meshing frequencies and their harmonics dominate the vibration spectrum. In many epicyclic gearboxes however, the main component of the spectrum is not the GMF (Gear Meshing Frequency). McFadden and Smith show that for a single planetary gear, symmetrical sidebands about the tooth mesh frequency occurs. Under certain circumstances, when more than one planetary gear is present as would be in any practicable epicyclic gearbox, the different phase angles for different planets may cause asymmetry of the spectrum. This fact is often overlooked when investigating the asymmetry of sidebands and suppression of gear meshing frequency often seen with epicyclic gearboxes.

Asymmetry may also be caused by the interaction between amplitude and frequency modulation. Individually, amplitude or frequency modulation will result in symmetrical sidebands, but when these components are superimposed the sidebands can be reinforced on the one side and cancelled on the other side due to different phase relationships. As there is a modulation of the vibration signal

at the PPF (Planet Pass Frequency) this can cause asymmetry of the GMF side bands. This, however, does not account for the suppression of the GMF that is common with epicyclic gearboxes.

It is thus clear as set out in the work done by McFadden and Smith (1985) that the design of the gearbox will determine whether the GMF will be suppressed. If the number of teeth on the ring gear is directly divisible by the number of planet gears GMF suppression will not occur.

McNames (2002) expands on the work done by McFadden and Smith and investigates the asymmetric nature of a spectrum and suppression of the GMF found in epicyclic gearboxes. Using a continuous-time Fourier series analysis, McNames finds that the total vibration will not have any components at the meshing frequency unless the number of teeth on the ring gear N_r, is an integer multiple of the number of planet gears P as was found by McFadden and Smith. McNames further finds that the PPF will be the fundamental frequency should the number N_r not be exactly divisible by P. As each planet gear meshes with the ring and sun gear, a characteristic vibration pattern is produced. This occurs for P planet gears, each producing its own vibration signal. These signals should be similar as the gears are identical with the same GMF. Thus, the total vibration measured at a single sensor contains P copies of a planet gear meshing with the ring gear. The asymmetrical nature of the sidebands can furthermore be explained by investigating the non-zero continuous-time Fourier series analysis which are not aligned with the meshing frequency when N_r is not exactly divisible by P. This resulting shape can vary depending on how the non-zero coefficients are aligned.

A signal averaging technique was developed by Howard (1990) to window the signal as each planet passes the transducer and using this windowed signal an artificial planetary and sun gear signal average is determined. This technique has been proven to increase the sensitivity of the vibration analysis to certain gear faults.

Forrester and Blunt (2003) point out that the only feasible location for a transducer is on the outside of the ring gear but that is subject to planet pass modulation. To overcome this problem Forrester and Blunt developed a planet separation technique by incorporating a selective time filter into the signal averaging process. This method is patented and often referred to as the “Australian patent” technique.

McFadden and Howard (1990) investigate the use of signal averaging on epicyclic gearboxes. Signal averaging is a known signal processing technique which assists in extracting periodic waveforms from a noisy signal. This technique is most useful in condition monitoring where the meshing frequency of interest can be extracted from the total vibration of a large system or gearbox. The signal average obtained can be processed using other signal processing techniques to enhance the damage detection ability.

There are factors that limit the use of signal averaging when applied to epicyclic gearboxes. These factors include the fact that there is the relative motion of the planet gears to the sun and ring gears; there are also multiple contact regions between the different components of the epicyclic gearbox. Any vibration measurement from a single accelerometer mounted on the outside of the gearbox, when synchronized with either the planet or sun gear, will present a composite signal of the vibration from all of the planet gear meshes.

Thus, vibration levels from a damaged planet gear contribute only a fraction of the number of planet gears to the measured vibration signal. If, for example, there are eight planet gears, the signal average from a damaged planet gear will be averaged to only one eighth of the original magnitude, with the other seven-eighth contributed from the undamaged planet gears. This implies that damage levels must be considerably higher before detection is possible.

McFadden and Howard use the modulation effect of the planets rotating relative to a fixed accelerometer as basis for the development of a signal averaging technique. A signal can be sampled for a short time when the planet is closest to the transducer. The main component of the signal obtained will be from the planet gear which is closest to the transducer. After one complete carrier revolution, the same planet will again be closest to the transducer.

It can be assumed that over the width of a window as described above, the transfer function between the accelerometer and the region of tooth contact will remain constant. Thus, the data for a window size around the planet can be obtained for each revolution of the carrier. Furthermore the planet gear teeth in mesh can be determined at each revolution, and the window of data can be stored in a position corresponding to the tooth in mesh. This process is then repeated N_p times to obtain a window for each tooth on the planet gear. The compiled data set is stored and the process re-started.

For a number of averages N_a of the compiled data sets as obtained above, there are N_a windows for each tooth on the planet gear. These windows can be averaged over N_a samples to obtain a signal average of the vibration of the particular planet gear. The process described is illustrated in the block diagram given in figure 1.5.

Samuel, Conroy and Pines (2004) point out that there are a number of issues that affect the accuracy of the signal averaging technique. Samuel et al. (2004:6) point out that a high sampling rate during digitization is essential for improving performance. A minimum sampling rate of 26.8 samples per TMP (tooth mesh period) is suggested with the TMP given by equation 1.1

$$\text{TMP} = \frac{1}{\text{Number of Teeth} \times \omega} \qquad \textbf{(1.1)}$$

Another factor which affects signal averaging as described by Samuel et al. is interpolation. A signal from a rotating gear is sampled at time instants defined by the sampling rate. When signal averaging is performed, it is calculated not in terms of the time domain but in terms of angle of rotation of the gear under investigation. Thus, at a given sampling frequency the samples per rotation become a function of the revolution speed of the gear in question.

To average signals in the angular domain, data points must exist at identical angular intervals. Measured signals must be transformed from the time domain to the angular domain, and in so doing redefine the sampling frequency as a function of angle. If gear rotation speed varies with time, the sampling frequency in the angular domain will not correspond. This is seen in figure 1.6 where a sample rate of 10 samples per second is used to sample a gear rotating at 2 and 4 revolutions per second respectively.

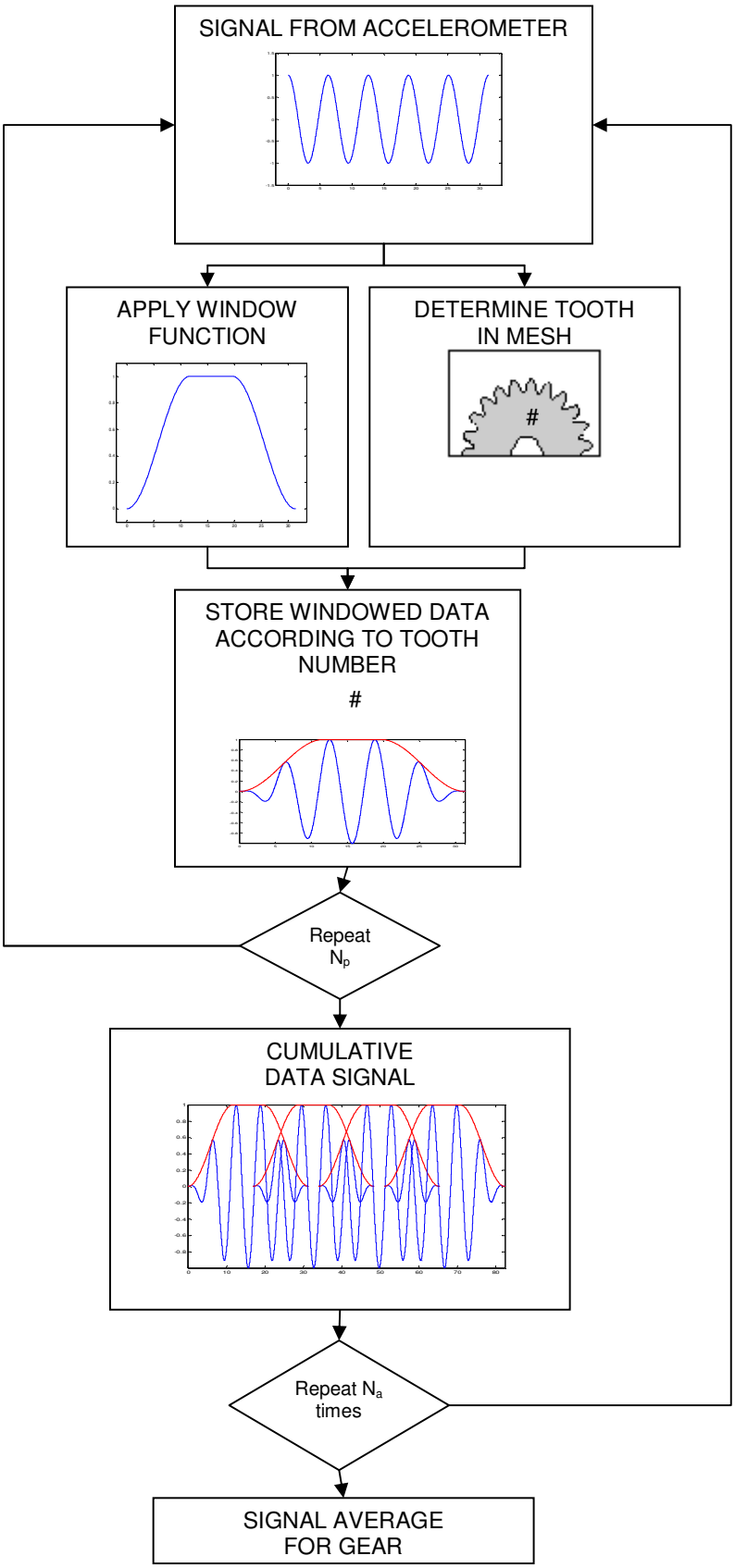

Figure 1.5 - Block diagram of the planet separation technique

When the same sampling points are then transferred to the angular domain, it is seen that for the faster rotating shaft there are certain rotational angles where no data is available. Should the two samples be averaged it can clearly be seen that additional data is required from the 4 revolutions per second signal to enable averaging with the slower rotational speed. Thus integration is required to determine the "missing" data points.

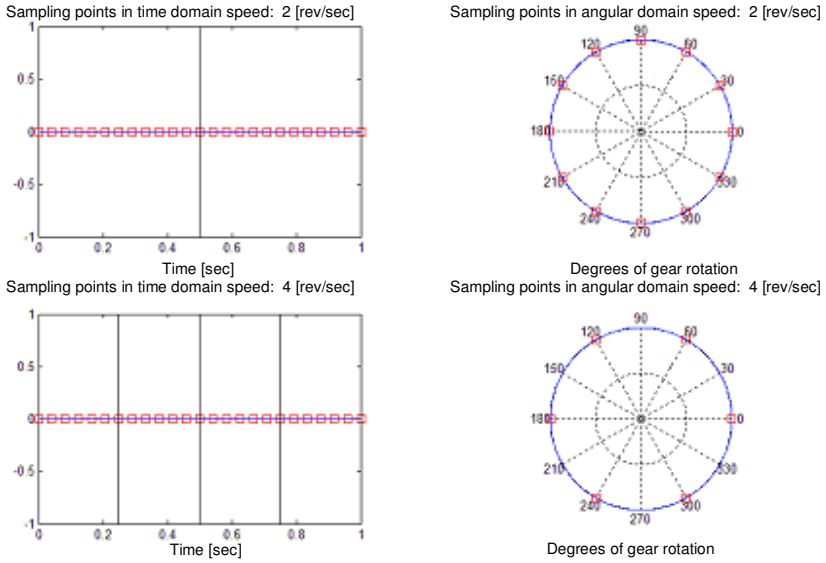

Figure 1.6 - Time domain to angular domain transformation

Samuel et al. discuss different interpolation techniques that are available and used to determine the required data points. It is assumed by the transmission diagnostic community in general, that variation of revolution speed is negligible for a single rotation of the rotating component under investigation. This assumption makes application of interpolation possible.

Samuel et al. point out that a reference signal connected to the rotational speed of the component of interest must also be recorded to enable the window period to be extracted at the correct position. The synchronous reference signal should ideally contain the waveform of the window that is to be extracted. This is not always possible, and thus a minimum of one pulse per revolution can be used, but the more pulses per revolution, the more robust the system will be against speed variation within a single rotation.

TSA (time synchronous averaging) can be directly applied to planetary gearboxes but Samuel et al. highlight the fact that additional complexities are introduced when applied to these gearboxes. As

was discussed earlier, when vibration measurements are averaged by making use of a number of sampling instants during a single revolution, the vibration signal can be averaged over a single revolution. This technique cannot directly be applied to an epicyclic gearbox. Two factors complicate TSA on an epicyclic gearbox, these being the fact that transducers can only practically be attached on the gearbox housing and that the rotational axes of the planet gears are not fixed, but move relative to the housing and transducer attached to the housing. Sun gear vibration is transferred through the planet gears to the ring gear before it can be detected by a transducer. These complicating factors must therefore be resolved before TSA can be applied to the signal obtained from a planetary gearbox.

The fundamental assumption of the vibration separation algorithm as stated by Samuel et al. is that when a given planet gear is near a transducer, the vibrations measured by the transducer are dominated by the meshing of that specific planet gear with the sun and ring gears. Based on this assumption, a small window of data can be collected during each pass of a planet gear and TSA performed as discussed by McFadden and Howard (1990).

Samuel et al. however, point out that there are limitations when using only a single transducer to obtain data for the TSA. These limitations include the fact that certain gearbox geometries exist where the capture of data for all the gear teeth is not possible. Another limitation is that the quantity of data required to calculate the TSA from a single transducer is large. The time required to develop the TSA is controlled by the number of averages required, the time it takes for each tooth to pass through mesh and the number of teeth on the ring gear. Another limitation is that a single transducer set up is susceptible to noise contamination as it can only measure data at a single angular position. Therefore, any external disturbance synchronous with the gear under investigation in the angular direction of the accelerometer will be enhanced by averaging, thus corrupting the TSA.

The multiple transducer technique, an extension of the single transducer technique of McFadden and Howard, is discussed by Samuel et al. The basic principles of application of the multiple transducer technique are the same as that of the single transducer. Instead of using a single transducer to obtain a signal for TSA, multiple transducers are used. Each transducer captures data in the same way as for a single transducer and averages the signal to the corresponding tooth in mesh. By doing so, a number of transducers can be used to record the vibration signal from the gearbox.

One of the advantages of using multiple transducers according to Samuel et al. is that the time required to obtain a TSA is reduced. A TSA using two accelerometers will require half the time of a TSA with a single transducer and using three accelerometers will further reduce the time to a third. A further advantage of using multiple transducers as explained by Samuel et al. is that multiple transducers will eliminate synchronized noise due to the fact that measurement is taken in multiple axes. This provides increased accuracy for the TSA signal.

Signals obtained from four accelerometers placed on a ring gear of a planetary transmission are compared by Samuel et al. The single planet gear planet separation technique was applied using each accelerometer individually. The results for a single tooth mesh period were then compared. Clear differences in the signal are evident. Samuel et al. thus rejected this technique for application to their work but points out that there are definitely benefits associated with the use of this technique.

The window that is used to window tooth data is another factor that affects the accuracy of the TSA process. Samuel et al. explain that the minimum window width is one TMP and that the sum of the windows in the TSA process must remain constant to prevent artificial amplitude modulation. Furthermore, the window width and window shape must be adjusted to obtain an optimum overlap period and shape. They investigate five different windows and compare them to a narrow rectangular window. The windows under investigation are the wide rectangular window, triangular window, Hanning window, Tukey window and the Forrester window given by equation 1.2 with the planet under investigation, p and the number of planets, P

$$w_p(t) = \left[a\left(1 - \cos(2\pi f_c t - \frac{p2\pi}{P})\right)\right]^{P-1} \quad \textbf{(1.2)}$$

The generalized equation for a Tukey window with the ratio of taper to constant sections, α as given by Mathworks (http://www.mathworks.com/access/helpdesk/help/toolbox/signal/tukeywin.html) is given in equation 1.3 for a window length, L

$$w(n) = \begin{cases} 1.0 & 0 \le |n| \le \alpha \dfrac{L-1}{2} \\ \dfrac{1}{2}\left[1+\cos\left(\pi \dfrac{n-\alpha\frac{L-1}{2}}{2(1-\alpha)\frac{L-1}{2}}\right)\right] & \alpha\dfrac{L-1}{2} \le |n| \le \dfrac{L-1}{2} \end{cases} \quad \textbf{(1.3)}$$

After investigation of signals obtained from damaged and undamaged gear teeth, Samuel et al. select the Tukey window with α = 0.8 as an optimum trade off between calculation speed and accuracy. The main factors influencing the selection being the fact that the Tukey window has smooth shoulders and represents a rectangular window during the critical period of tooth mesh, which is seen in figure 1.7

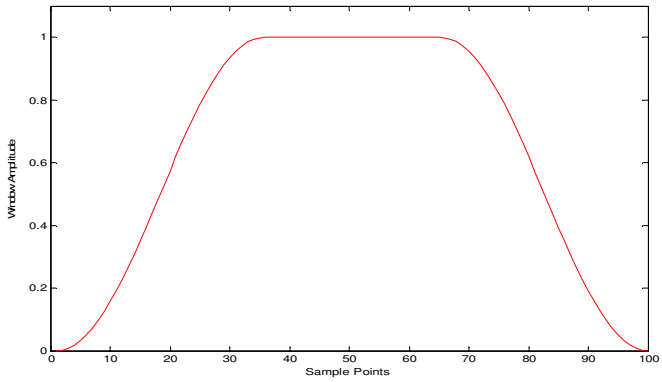

Figure 1.7 - Shape of Tukey window with α = 0.8

McFadden (1994) states that there are two conditions which must be met before a window scheme can be applied to planetary gearbox time domain averaging. The first condition is that the minimum window width to produce a valid time domain average is a single tooth width. The second condition is that the window shape must be such that, when mapped, the windows sum to a constant value. The simplest window to satisfy these conditions is the rectangular window. When a rectangular window is used to map data, a small error term will be created. A rectangular window has been used successfully in the past but quantification of the error term is required. McFadden states that windows such as the Hamming, Kaiser-Bessel and Blackman-Harris window cannot be used due to the fact that their tapered ends are not antisymmetric and when mapped will not sum to unity. Windows such as the rectangular, triangular and Tukey windows or combinations thereof are suitable and can be used. From these, the Tukey window gives the lowest error term in the time

domain average. Thus, the increased computation time required is acceptable when the decreased error is taken into consideration.

McFadden (1987) examined a technique for the signal processing of the time domain average of the vibration produced by meshing gears. A regular signal which contains the tooth meshing harmonics can be extracted from the time domain average of the vibration signal from a gear. The regular signal defines the time domain average of the meshing vibration of a single gear tooth. The residual signal can then be obtained by subtracting the regular signal from the original time domain average. This residual signal is the departure of the vibration of a gear tooth from what would be average. This ability to determine the departure of a gear tooth from average simplifies the ability to identify a fault on a gear tooth. McFadden however, points out that narrow band techniques eliminate much of the pitch and profile variation signal, and should thus give better discrimination than what is obtainable using the regular and residual signal.

McFadden (1990) describes the WVD (Wigner-Ville Distribution) as a tool to provide a powerful means to represent a signal in the time-frequency domain. The WVD was used to compare a number of different signals. WVD of the time domain average was compared to the WVD of the residual signal of the time domain average. The WVD of the time domain average is able to detect damage to a gear. The WVD of the residual is, however, more sensitive and gives a more detectable indication of damage. McFadden illustrates the use of the WVD on, amongst other gears, an epicyclic gearbox. The data was obtained from a Whirlwind helicopter epicyclic gearbox run on a test rig with induced damage on planet gear teeth. The WVD of the time domain average illustrates the difficulty in interpreting the WVD as well as interference lines that are evident. The WVD of the residual signal of the time domain average is easier to interpret. In both the above cases a fault is seen. The damage induced was 30% removal of one tooth. McFadden comes to the conclusion that the WVD may not necessarily be the optimum technique for the detection of a gear fault as the WVD has a tendency to illustrate more frequencies than those that would be seen with other techniques, and this makes fault identification more difficult using the WVD.

Keller and Grabill (2003) investigate the plausibility of using standard CIs (Condition Indicators) to detect a crack in a planet carrier of a UH-60A Blackhawk main transmission. It is however, clearly stated that the CIs can be used with pre-determined vibration limits but this requires vibration data and extended periods during which the gearbox damage increases. CIs used were modified to account for the vibration characteristics of a planetary gearbox as has been discussed by McFadden and Smith (1985). The modified CIs included NK (Normalized Kurtosis), CF (Crest

Factor), ER (Energy Ratio), SLF (Sideband Level Factor), SI (Sideband Index), $FM0^e$ (Zero-Order Figure of Merit) and $FM4^e$ (Fourth-Order Figure of Merit). Data obtained from an aircraft, as well as test cell data for the UH-60A main transmission was used. Data was measured at different torque settings. After the CIs were calculated and interpreted, it was clear that the SI and SLF were only successful in determining fault conditions at high torque. Low torque results were not as clear as high torque results, thus making the determination of fault conditions at low torque levels complex. None of the CIs were able to detect faults from the on-aircraft vibration data. This is a clear indication of the complexity of vibration analysis on the epicyclic gearbox and the difficulty of determining fault conditions, in such a gearbox.

Wu, Saxena, Khawaja, Patrick and Vachtsevanos (2004) expand the use of the CIs to include Harmonic Index around the 5^{th} and 10^{th} harmonic and Intra-Revolution Energy Variance. These features were evaluated using a 2-sample Z-test, that compares the average of two groups and determines whether there is a statistical difference between them. This test provides an elegant measure of the difference between two distributions of data.

From this test it was seen that none of the features had a consistent advantage over the others. It was, however, apparent that the Harmonic Index as well as the Intra-Revolutionary Energy Variance was able to distinguish between data from damaged and un-damaged planetary gears. It was stated that further investigation into the use of these CIs as fault detection parameters was required. Wu et al. make use of raw data instead of the TSA. It is claimed that the raw data provides better results with the planetary gear data that was available. It is stated that the TSA could be used if new data were available. to

Wu, Saxena, Patrick and Vachtsevanos (2005) further investigate the use of the Harmonic Index and Intra-Revolutionary Energy Variance. As described, the use of the TSA was questioned and an alternative approach used. This involved the use of the DFT (Discrete Fourier Transform) during each revolution of the vibration data, thus no interpolation was required. The ensemble average of the complex numbers including amplitude and phase was performed for corresponding indices. This was done due to the fact that the frequency resolution, Δf of the DFT is given by equation 1.4.

$$\Delta f = \frac{1}{T_{shaft}} = f_{shaft} \tag{1.4}$$

T_{shaft} is the period of each individual revolution and may vary from one revolution to the next. If the period of a revolution increases from the previous one the data volume sampled in that revolution is greater, thus causing a finer frequency resolution with the same sampling frequency, which results in a higher number of frequency indices. In the frequency domain, the indices of the meshing frequency and sidebands do not change. These common frequencies can be used during averaging with the extra frequencies of higher indices being discarded. This procedure results in TSA data in the frequency domain or alternatively the DFT of the TSA without the interpolation and re-sampling required with TSA. This process is less computationally complex and is simpler and faster than re-sampling vibration data, especially if the data sampling frequency is high. When phase information is not required, averaging of the DFT can be conducted using the amplitudes of the DFT only. This technique is useful when CIs such as the Harmonic Index are used.

McInerny, Hardman, Keller and Bednarczyk (2003) modify the definitions of tonal and residual components of the TSA for application with planetary gears. The modified energy ratio was able to identify the fault under full torque conditions. A metric was developed and found to be highly responsive to the presence of a crack on the planet carrier. This metric made use of the number of planets multiplied by the revolution speed to reflect the deviation of the TSA. This may provide a possible monitoring method for a crack and could confirm the findings of Raithby & Baillie (2004).

Mosher, Pryor and Huff (2002) use the CIs to investigate gear faults in the OH-58C gearboxes. These metrics include FM0, FM4, N6A, N8A, NA4 and NB4. The focus of the investigation was the input pinion gear and no investigation of the epicyclic gearbox was undertaken, as the metrics that were being investigated were not designed for detecting damage of complex gear systems such as an epicyclic gear system. It is interesting to note that during the investigation it was found that significant variation in torque and rotor rpm occurred in the course of test flights, even when the aircraft was flown under controlled steady flight conditions with highly proficient test pilots.

Decker (2002) directly compare different CI parameters such as RMS, CF, ER, EO (Energy Operator), FM0, FM4, Kurtosis and various other parameters. The tests were conducted on a spur gear test stand using aerospace quality gears. Gear teeth were notched to induce damage and then run to damage while vibration data was recorded. The different parameters were then calculated and compared to determine crack progress. The results of these experiments illustrate that none of the techniques were robust or accurate enough to repeatedly detect gear fractures. Only when severe secondary damage, such as a loss of a tooth occurred, were the techniques reliable. Thus, high levels of damage are required when using such techniques.

Decker and Lewicki (2003) use the CIs to monitor damage on an OH-58 Main Rotor Transmission spiral bevel input pinion. Damage was induced by means of a notch in the fillet region of one of the spiral bevel pinion teeth. The metric that best illustrated damage was the NA4 or improved FM4 metric. The kurtosis was found to be highly responsive to torque variations which occurred during early testing. The kurtosis also provided a clear indication of gear damage, once advanced damage was present.

Polyshchuk, Choy and Braun (2002) develop and test the NP4 parameter which is based on the WVD and kurtosis of a signal. The advantage of the NP4 parameter is that it does not compare a measured gear vibration signal with an undamaged one. This means that the NP4 parameter will work for fault detection where a long recorded history is not available. This provides an ideal monitoring technique. The NP4 parameter was not tested on an epicyclic gearbox but on spiral bevel gears and would need to be tested on an epicyclic gearbox.

Samuel and Pines (2001) use a normalized energy metric to classify faults seeded on an OH-58A helicopter main transmission. A self-organizing Kohonen neural network classifier is used to map elements of the normalized energy metric to a two-dimensional grid. This information is then used in a feed forward, back propagation, neural network, to classify different faults. The classification results would seem to indicate robustness against false alarms for certain gearbox faults. The results proved that bevel gear faults can be sufficiently identified using this technique. The seeded sun gear faults were, however, difficult to identify. The position of the accelerometer used to measure data significantly affected the results obtained. False alarms were also found to be high for the sun gear faults. Samuel and Pines point out that while there is room for improvement, the results are promising.

Samuel and Pines (2003) investigate the use of a constrained adaptive lifting technique to diagnose faults in the planetary stage of helicopter gearboxes. The adaptive lifting technique is based on the wavelet transform where the fundamental basis function can be adapted to construct an optimum function. The transform thus has a choice of fundamental bases which can be applied. The technique uses the fundamental bases to construct a set of wavelets that best represent the vibration signals of a gearbox operating in an undamaged condition. The technique has to be constrained on certain characteristics to enhance detection of local wave shape changes caused by certain types of gear damage. The results from the constrained adaptive lifting techniques show that there is potential benefit for diagnostics but that further investigation into the validation of the

performance algorithm is required in conjunction with a method to better quantify the output of the algorithm.

Meltzer and Ivanov (2003) initially investigate time frequency analysis as a method to recognize faults during run-up, run-down testing of passenger car gear drives. These drives consist of three planetary stages each containing three planet gears. An incremental sender and ordinary impulse generator was used to tune the sampling of the vibration signal. Fourier-spectrum and Fourier-cepstrum analysis was used for time-frequency analysis of the data obtained with the ordinary impulse generator. The signal obtained in combination with the incremental sender was used with different smoothing kernels in the Choi-Williams distribution, thus enabling fault diagnosis of machines with unsteady rotational speed. Faults at different tooth flanks were identified using both methods. Meltzer and Ivanov (2003) expand their research to include the time-quefrency approach. This approach allowed the detection and identification of faults and damages without the implementation of an incremental sender to determine the rotational angle. This is a substantial improvement on the existing techniques, as the equipment required to monitor the gearbox is dramatically reduced.

Samuel and Pines (2004) evaluate a number of different vibration based diagnostic techniques. From this comparison it is clear that each of the different parameters and techniques have certain conditions to which they are suited, but do not perform well when used under different circumstances. Samuel and Pines come to the conclusion that there is certainly no single technique that works under all conditions and that there are still significant improvements required in the development of damage detection techniques especially of helicopter transmissions. Samuel and Pines furthermore point out that there is currently no standard method to evaluate the different techniques and that a standard method would be of great importance to the research community. This would enable the direct comparison of the different techniques with each other.

Parker (2000) makes reference to the fact that experimental verification of existing analytical models is limited. The design of epicyclic gearboxes has thus been based on empirical development without a sufficient basis of dynamic analysis and experimental verification. Experimental verification for epicyclic gearboxes is thus of utmost importance in providing such a foundation. The design strategies of epicyclic gearboxes include tooth-shape modification, gear geometry changes, a reduction in tolerances during manufacturing, the use of floating sun gears as well as floating carriers, vibration isolation and planet phasing. Parker continues to explain that dynamic modeling of tooth forces has not been fully resolved even for single-mesh gear pairs, let

alone multiple meshes of planetary gears. Parker continues his investigation into planet phasing based on an empirical model, and does not base his investigation on experimental verification.

Howard (1995) discusses the use of MATLAB® for vibration signal processing. He accentuates the excellent ability of the program when used to refine existing vibration monitoring techniques and where new methods are to be developed to monitor vibration data. The features of MATLAB® which are important include the fact that the program is interactive, has a range of built in functions, incorporates graphic capability, is extendable, has multi-platform capability and uses standardized data formats.

These factors make MATLAB® specially suited to an environment where high frequencies and time synchronous signal averaging is applied.

1.5. Scope of research work

From this discussion of the literature, it is apparent that the main focus of current work on epicyclic gearboxes makes use of the planet separation technique. The technique often forms the basis for further research and comparative work. This technique was implemented in a number of cases, having direct application in various research fields. The technique is based on the fundamental premise that the only feasible position to place an accelerometer for vibration monitoring is on the outside of a gearbox. It is also clear that there is no epicyclic gearbox vibration monitoring technique that in itself is suitable for use under all conditions.

None of the CIs used to identify faults were seen to be reliable under all fault conditions. Under large torque or high damage conditions certain of the CIs were able to predict faults. The complexity of the CIs used does not seem to have a direct effect on the general reliability of the prediction technique. Thus, CIs that are simple and easy to calculate may perform equally well, compared to complex CIs, depending on the data used, as well as the type of damage that is under investigation. Due to this fact, simple CIs can be used when evaluating different measurement techniques as these CIs require less time to calculate. A direct comparison of the input data to the CI is under investigation and not the CIs themselves. The complexity and accuracy of different CIs has been investigated to a great extent by various researchers. Based on this, complex CIs will not be used for comparative purposes.

Because of the complexity and practical problems involved in vibration monitoring of epicyclic gearboxes, the planet separation technique is used to simplify fault diagnostics on these complex gearboxes. During the literature study and research, no reference was found which either confirms or denies the accuracy of the technique by making use of practical measurements. This is due to the fact that there is currently no method by which valid vibration data can be directly recorded from the outside of an epicyclic gearbox. No data is thus available to directly compare the calculated planet separation data with. The largest problem limiting the direct comparison is the fact that the centre of the planet gear is rotating relative to any transducer placed externally on the gearbox, thus nullifying externally measured vibration signals.

A comparison of data obtained from the use of the planet separation technique with directly measured data is thus warranted, and is to be investigated. There are a number of practical problems that must be overcome before a direct comparison is possible. Were it possible to remove the relative motion between the planet gears and an accelerometer used to measure the vibration, while at the same time calculating the signal by means of the planet separation technique, direct comparison of the data becomes viable. This would provide an acceptable method to directly and consistently measure vibration data from an epicyclic gearbox.

The value of such an investigation is that the accuracy of the method will be qualified or shown to be incorrect. The comparison of the planet separation technique to real data will require implementation of the technique. No commercial software could be found that makes use of the planet separation technique, which could be used for further research purposes. The algorithm is to be developed and tested, in house before any comparison is possible.

Another aspect that does not seem to be addressed sufficiently in the literature is the evaluation of the planet separation technique in terms of a single planet gear on the carrier. This method of testing can only be used if the gearbox under investigation can be modified to make use of a single planet gear. The use of a single planet gear would not be a method that could be used in commercial vibration monitoring techniques. It is beneficial to evaluate the data obtained from a single planet gear.

There is currently limited experience with practical vibration measurement of epicyclic gearboxes. A study into the data obtained from a single planet gear would expand the practical base that is required for further development of suitable commercial vibration monitoring techniques. By removing the vibration caused by multiple planet gears, and focusing on the vibration from a single

gear in mesh, a greater understanding of the manner in which the rotation of the planet gear in the gearbox effects the vibration data can be obtained. This is required before a full understanding of a complete epicyclic gearbox can be reached.

The following aspects will receive direct investigation in this research work:

- A technique to enable direct vibration measurement of an epicyclic gearbox will be investigated and implemented. This forms the main contribution of this work. The results obtained from this technique will be compared to data obtained by means of the planet separation technique which is an accepted method for vibration analysis of epicyclic gearboxes.
- A brief comparison between the difference in signals measured from an epicyclic gearbox with a single planet gear and the same gearbox with multiple epicyclic gears is made. This is done to assist in the global understanding of an epicyclic gearbox and the development of this work.

The issues listed above are to be addressed in the research work. Direct vibration measurements on an epicyclic gearbox will require measurement on the planet carrier itself as this is the only component that does not rotate relative to the planet gears. An expansion on the methods employed to obtain the required data is included to ensure that the complexities and issues involved with such measurements are fully documented, and can serve as a basis for further research work. Development of the methods will focus on the practical implementation and measurement of data from the gearbox. The interpretation and explanation of the data is included.

1.6. Document overview

To assist in the understanding of this document, a brief overview is provided. This document is divided into seven main chapters. Each chapter is discussed briefly.

Chapter one presents an introduction to epicyclic gearboxes in general. The different manners in which the gearbox can be operated are discussed. The method of vibration monitoring of gearboxes is introduced and discussed. The application of epicyclic gearboxes in the aeronautical environment is discussed and the complexity of epicyclic gearboxes is illustrated with the findings

from a case study. This is followed by a literature study which expands on the current position of research work involving epicyclic gearboxes.

In chapter two the requirements of an epicyclic gearbox for experimental investigations as part of this research project is discussed. The background to the selection of such a gearbox is included with the layout as well as the reasoning resulting in the selection of the gearbox for the research. This is followed by a theoretical expansion, as well as a practical investigation into the selected gearbox. The test bench facility used during testing is discussed and illustrated.

Chapter three describes the implementation of the planet separation technique or epicyclic time synchronous averaging process on the selected gearbox. A number of areas of caution found during the development of the method and the issues relating thereto are discussed. There are a number of practical implementation problems that are solved during the implementation development and these issues are discussed in detail. The signal processing that is required is evaluated to give the reader a clear understanding of the methodology used during the implementation. The results obtained from the technique are discussed and the validity of the results are proven. Interesting averaging abnormalities were seen and these are discussed to present a clear picture of the results obtained from application.

The development of the method of planet carrier vibration monitoring is discussed in chapter four. Some serious implementation problems are discussed together with the solutions for such problems. The signal processing that might be required to solve some of the issues related to planet carrier vibration monitoring is discussed.

Chapter five provides a platform for data interpretation and review. The results from different configurations and data measurement methods are compared and evaluated. This chapter provides a basis for critical evaluation of the different techniques and configurations. The findings and conclusions that can be drawn from evaluating the data are discussed in chapter six.

There are a number of further research possibilities that lead on from the research work under discussion in this dissertation. These possibilities are discussed in chapter seven.

Appendix A containing the MATLAB® programs, with a brief discussion of each program is attached.

Chapter 2 - Bonfiglioli epicyclic gearbox test bench

A gearbox is required for use in obtaining experimental data. Initially the use of an Oryx helicopter gearbox was envisaged. Preliminary testing was performed on such a gearbox that was being tested during acceptance testing after a major overhaul as shown in figure 2.1.

Figure 2.1 - Oryx gearbox during testing on test bench

During this testing a number of issues relating to the use of a gearbox for testing purposes became apparent.

a. The cost of running the test rig must be reasonable. To make use of the test bench shown in figure 2.1 is so costly that dedicated testing could not be performed. Thus no testing was possible beyond acceptance tests that were to be conducted irrespective of research requirements. This implied that no damage could be introduced to the gearbox for

measurement purposes. It is clear that it should be relatively cheap to run the test rig in order to conduct extensive testing.

b. The data obtained during the above testing illustrated that the separation of the vibration signal originating from the epicyclic sets from the measured data would be extremely difficult. This was due to the fact that there are many gears in the helicopter gearbox. In addition, the test rig has its own gearbox which also contributes to the measured vibration signal. This results in a highly complex vibration signal. Any gearbox that is to be used for research purposes should be as simple as possible to make sure that vibration signals obtained from such a gearbox have as little interference as possible.

c. A helicopter gearbox must be tested at a pre-set speed. Thus, no variation on this speed was possible for testing purposes. The ability to adjust speeds during research work is imperative to suit different testing conditions and methods.

d. No damage could be introduced due to the cost of the components of a helicopter gearbox. Components that had been damaged while in service are the only method of damage induction open to research using this gearbox.

Taking the above factors into consideration, it was decided that testing on a helicopter gearbox is not currently a viable option. A more controlled environment is required. Such an environment is available at the University of Pretoria's, Sasol laboratory. The limitation at this facility is the size of the equipment that can be used. It is impractical to introduce a large gearbox with a high load requirement to this facility. It is thus clear that a small, inexpensive epicyclic gearbox with a variable speed controller is required. A gearbox suitable for research purposes which is supplied by Bonfiglioli was consequently selected. This gearbox will be discussed in greater detail in the following sections of this chapter.

No test bench at the University of Pretoria could be modified to accommodate the epicyclic gearbox as an additional component into an existing system. The design of a new test bench was required and enabled the incorporation of a number of features for the testing of the epicyclic gearbox into the test bench. The test bench itself will be discussed in greater detail in the course of this chapter.

2.1 Basic layout of a Bonfiglioli epicyclic gearbox

The 300 series epicyclic gearbox from Bonfiglioli has a gear ratio of 5.77:1. The gearbox was selected with input and output shafts of the same diameter to enable integration of the gearbox with other systems. Figure 2.2 shows the assembled gearbox. The left hand shaft is the output shaft with the right hand shaft being the input shaft. Figure 2.3 shows the gears from the gearbox.

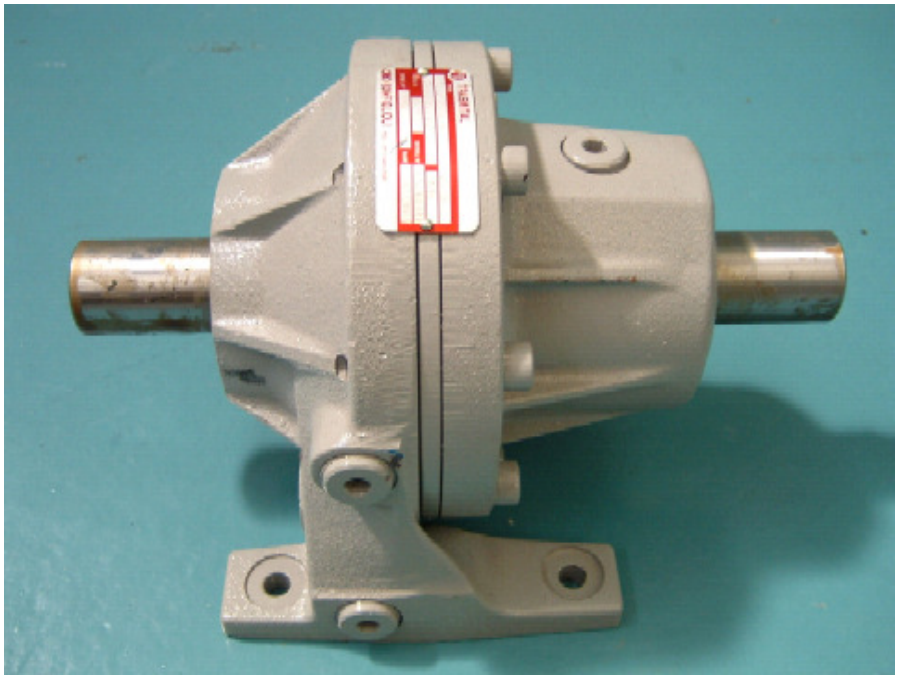

Figure 2.2 - Bonfiglioli 300-L1-5.77-PC-V01B-E

The Bonfiglioli epicyclic gearbox as can be seen in figure 2.2 consists of 3 planet gears. The number of teeth of the gears in the gearbox is given in table 2.1.

Table 2.1 - Number of teeth of gears

Gear	#Teeth
Ring / Annulus	62
3 x Planets	24
Sun	13

The planet carrier is floating which means that is affixed to the output shaft by means of splines which allow it to move axially as required. There is a wear plate that prevents the carrier from moving further than the sun gear in one direction and it cannot move further on the splines than there is engagement space. The planet gears are hardened and use the inside of the planet gear

as the inner bearing race. Loose needle bearings are then inserted between the planet gear and the planet gear shaft with the shaft itself being the other race of the bearing. There is thus no replaceable bearing as such. According to Bonfiglioli this was done as it requires less space and thus allows for a thicker shaft and larger needle bearings which effectively provides a larger bearing, increasing the load ability as well as reliability of the gearbox.

Figure 2.3 - Gears of the gearbox

The gearbox is easy to open and maintain, making it especially suited to this research as planet gears can be easily changed by opening the gearbox and removing the retaining cir-clips. This is ideal as the planet carrier does not need to be removed to do this.

2.2 Theoretical analysis of Bonfiglioli gearbox

McFadden and Smith (1985) develop a method to calculate the gear mesh frequencies and sidebands using equation 2.1 which states that the phase angle of any contribution, Q_{ims}, to the spectrum is determined only by the initial position of the planet gear with respect to the transducer, the number of teeth on the ring gear, as well as the meshing harmonic, m and sideband number, s. It is assumed that the time delay caused by the propagation of the vibration around the annulus is small.

$$Q_{ims} = P_i\left(mN_r + s\right) \qquad \textbf{(2.1)}$$

The phase contributions to the spectrum can then be summated to obtain a list of the observable frequencies. Using McFadden's technique, the observable frequencies for the Bonfiglioli gearbox are calculated and given in table 2.2:

Table 2.2 - Table of observable frequencies

	$\lvert Q_{mn}\rvert/N$		
s	**m=1**	**m=2**	**m=3**
8	0	**1**	0
7	**1**	0	0
6	0	0	**1**
5	0	**1**	0
4	**1**	0	0
3	0	0	**1**
2	0	**1**	0
1	**1**	0	0
0	0	0	**1**
-1	0	**1**	0
-2	**1**	0	0
-3	0	0	**1**
-4	0	**1**	0
-5	**1**	0	0
-6	0	0	**1**
-7	0	**1**	0

From table 2.2 it is seen that at s = 0, the GMF, as well as two times the GMF, will be suppressed due to phase interference. The upper side band at the GMF is expected to be present on the frequency spectrum with two times the lower side band visible. At two times the GMF, the lower side band, as well as two times the upper side band, will be accentuated. Three times the GMF will be accentuated according to table 2.2.

This information is used when evaluating the spectrum of the signal obtained from the epicyclic gearbox. The fact that the GMF will be suppressed implies that the GMF cannot be used for evaluation purposes, and that other methods of comparison between increasing damage levels are required. The spectrum obtained from vibration measurements was investigated and it is clear that GMF suppression occurs. The C-130 gearbox was evaluated in a similar fashion and GMF suppression was also calculated to occur. This was confirmed when actual vibration measurements were evaluated and the GMF found to be suppressed as seen in figure 2.4.

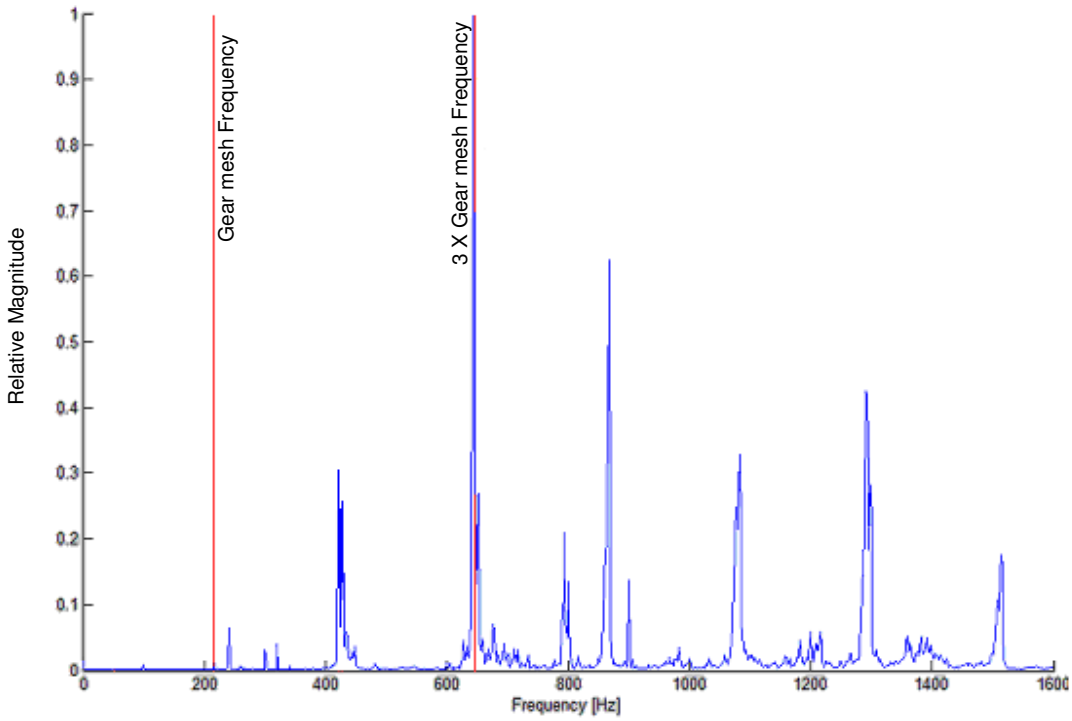

Figure 2.4 - Power spectrum for the undamaged Bonfiglioli epicyclic gearbox

To fully understand the Bonfiglioli gearbox, the number of rotations that occur before the identical set of gear teeth are again in mesh must be determined. Furthermore ,the tooth meshing sequence is of utmost importance in developing the full understanding of the meshing pattern of the specific gearbox. Both reset rotations and gear mesh sequence must be calculated and verified before further development of the gearbox is possible.

Using the equation listed by Samuel, Conroy and Pines (2004:11) the number of rotations before reset are calculated using the lowest common multiple in equation 2.2:

$$n_{\mathrm{Re}set,g} = \frac{lcm(N_g, N_r)}{N_r} \qquad \textbf{(2.2)}$$

From equation 2.2 it can be calculated that $n_{Reset,p}$=12 and $n_{Reset,s}$=13. For every 12 carrier revolutions the same planet/ring teeth will be in mesh, and for every 13 carrier revolutions the same planet/sun gear teeth will be in mesh. After 12 carrier revolutions a single compiled data signal will be available for each planet gear, with contributions for each planet gear tooth. The same is applicable after 13 carrier revolutions for the sun gear, with contributions for each sun gear tooth.

The gear mesh sequence is now calculated using equation 2.3

$$P_{n,g} = \mathrm{mod}(nNr, Ng) + 1 \qquad \textbf{(2.3)}$$

The gear mesh sequence is given in table 2.3:

Table 2.3 - Planet gear mesh sequence

Gear Tooth	Carrier Rev
1	0
15	1
5	2
19	3
9	4
23	5
13	6
3	7
17	8
7	9
21	10
11	11
1	12

If the data from table 2.3 is displayed for each planet gear tooth as done in table 2.4, it is seen that at a single ring gear tooth only every second planet gear tooth is engaged. Any sensor that is mounted on the gearbox directly opposite a ring gear tooth will only be able to measure every second plant gear tooth directly, as only every second planet gear tooth will mesh with any given ring gear tooth.

Table 2.4 - Planet gear tooth engagement

Tooth #	1	2	3	4	5	6	7	8	9	10	11	12	13	14	15	16	17	18	19	20	21	22	23	24
Engagement																								

It is thus clear from the theoretical analysis that the gear meshing pattern must be incorporated in any programming that is done for gearbox evaluation. Alternatively, more than one sensor will be required to fully capture the vibration information from this epicyclic gearbox.

The number of reset rotations, as well as the planet gear tooth engagement, was verified on the Bonfiglioli gearbox by opening the gearbox and numbering the teeth of the ring, sun and planet gears. The ring gear was fixed while the sun gear was rotated by hand and the meshing pattern verified for each tooth as well as the number of reset rotations. Thus the validity of the calculation was confirmed and further development using these values is credible.

Taylor (1994), Crawford and Crawford (1992) and Flender Bocholt (n.d.) develop the equations governing the frequencies displayed by the gearbox in detail. The expected frequencies can be calculated from these equations. This is implemented in a MATLAB® program and used during the development of this dissertation.

The focus of this dissertation is not on the frequencies themselves and they are not discussed in further detail. The calculations are attached in appendix B together with a program used to calculate the frequencies expected for a T-56 C-130 Hercules epicyclic gearbox. This was done as verification of the programs, as well as for fault diagnosis on aircraft that are monitored at the SAAF VCC (Vibration Control Centre).

2.3 Practical development of Bonfiglioli gearbox

The epicyclic gearbox required modification to enable the vibration monitoring techniques to be applied. The exact position of the centers of the planet gears is required to simplify the windowing procedures. This modification was very easy to perform. A capping plug illustrated in figure 2.5 was removed from the side of the gearbox and replaced with the white adaptor that is seen in figure 2.6. A magnetic pickup could then be installed in the adaptor and secured. The planet carrier was modified to enable three triggering pins to be installed. This modification can be seen in figure 2.7 where the magnetic pickup is aligned with a triggering pin installed on the back of the planet carrier.

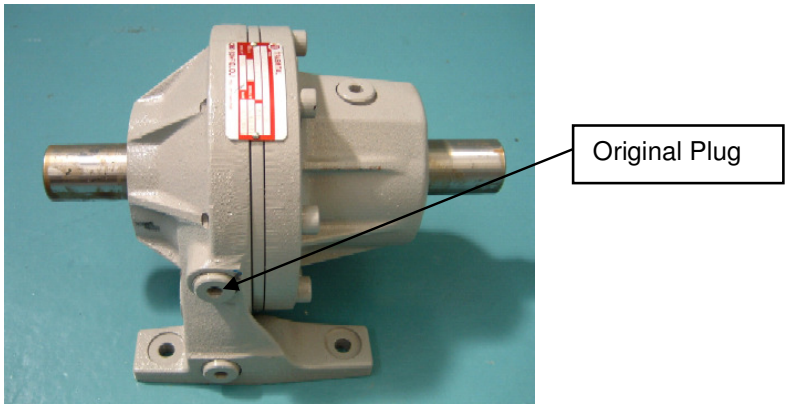

Figure 2.5 - Plug to be replaced on gearbox

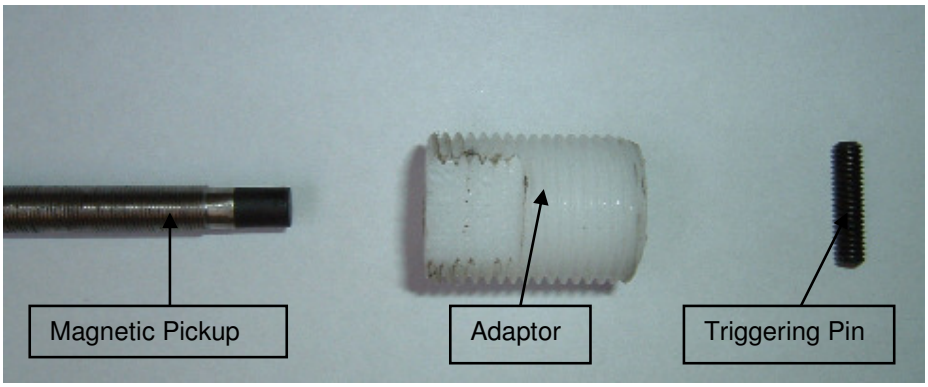

Figure 2.6 - Magnetic pickup with adaptor and trigger

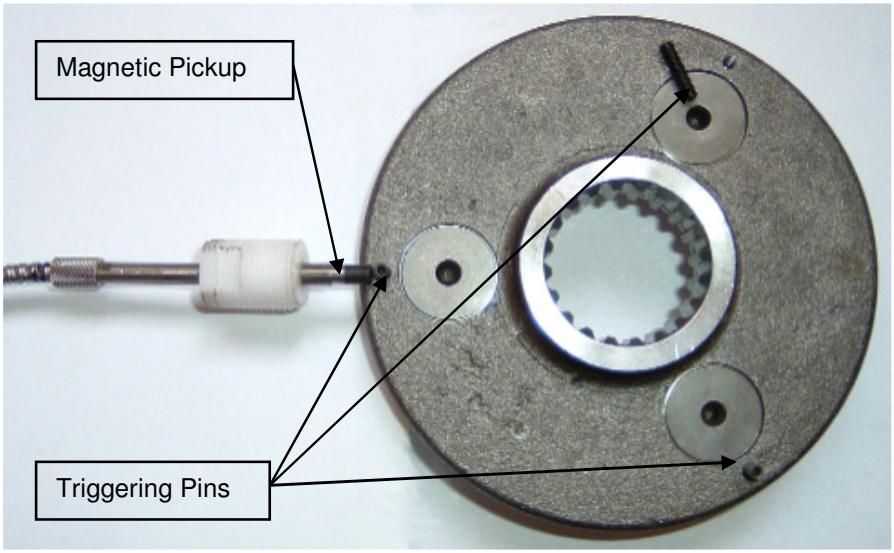

Figure 2.7 - Modified planet carrier with magnetic pickup

2.4 Epicyclic gearbox test bench

A test bench for the testing of the Bonfiglioli epicyclic gearbox was designed and commissioned at the University of Pretoria, Sasol Laboratory as discussed earlier in this chapter. The test bench is configured in a speed down, speed up configuration as can be seen in figure 2.8.

Figure 2.8 - University of Pretoria epicyclic gearbox test rig

A direct current electric motor seen in figure 2.9 is used to supply torque to the gearboxes. This motor manufactured by Brook Crompton is rated at 3 kW @ 3 000 rpm. The motor speed is controlled using a speed controller supplied by U & S Power Electronics. This speed controller allows bi-rotational direction of the motor as well as speed control over the operational range of the motor.

Figure 2.9 - DC electrical motor

Torque is applied to the gearboxes by means of a throttled hydraulic pump. A hydraulic load was selected due to the fact that load applied by means of an electric alternator or generator was seen to adversely affect the signal measured from an accelerometer in the area close to such a generator or alternator. The hydraulic system was designed by Hytec and is seen in figure 2.10 with the hydraulic pump seen in figure 2.11.

The system is capable of running continually under a 3 kW load. This means that the test bench can be run for long periods of time should such testing be required. The system is capable of supplying a load for both rotational directions. Load is supplied by means of a proportional pressure relief valve that can be controlled either by a signal generator or constant voltage source. Thus, the load on the system can easily and quickly be varied depending on the requirements of a test procedure.

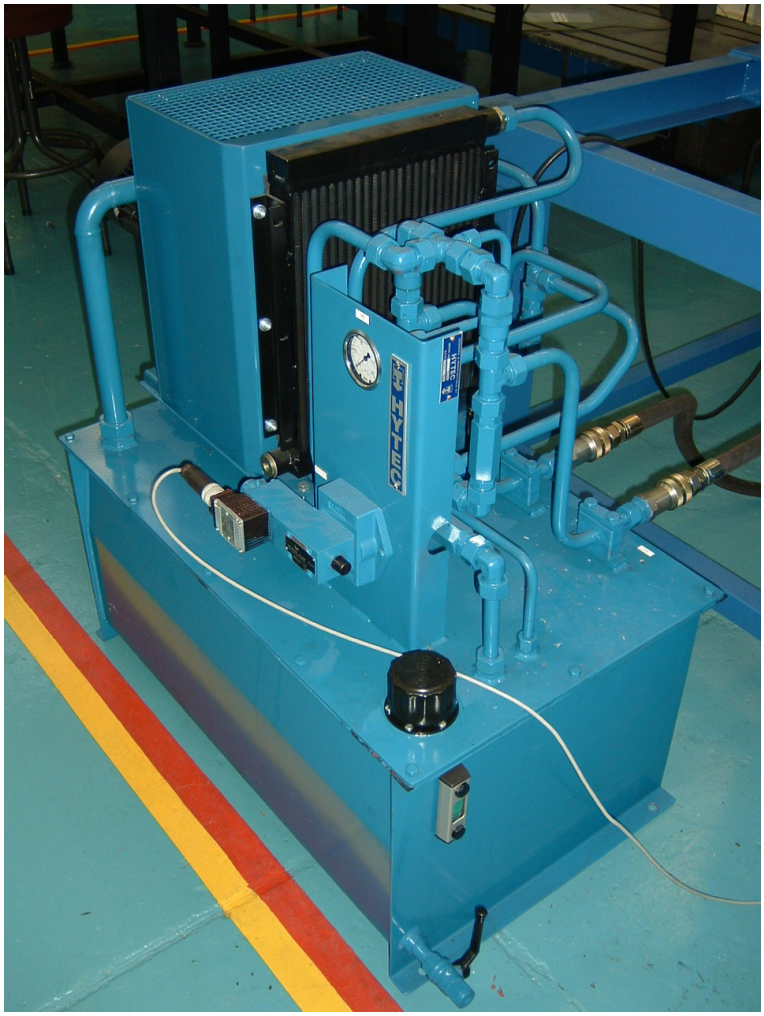

Figure 2.10 - Hydraulic system for test bench

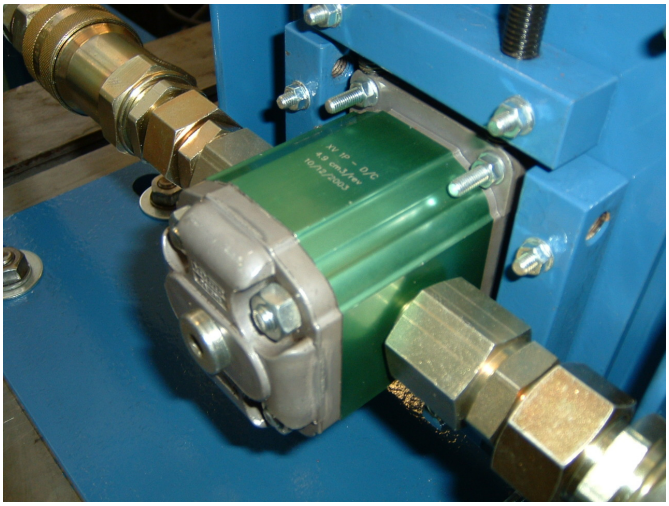

Figure 2.11 - Hydraulic pump used to apply load

The gearboxes are connected with the first gearbox reducing the rotational speed from the electric motor, while the second gearbox is connected to allow the rotational speed to be increased. The output speed from the electric motor is thus the same as the output speed of the second gearboxes.

Further details regarding the design and development of the test bench is discussed in detail by Schőn (2004).

All couplings on the test bench were aligned using the in house Easy-Laser, laser alignment equipment as seen in figure 2.12. This was done to ensure that vibration caused by misalignment was reduced to well within acceptable levels, during vibration measurement from the gearboxes.

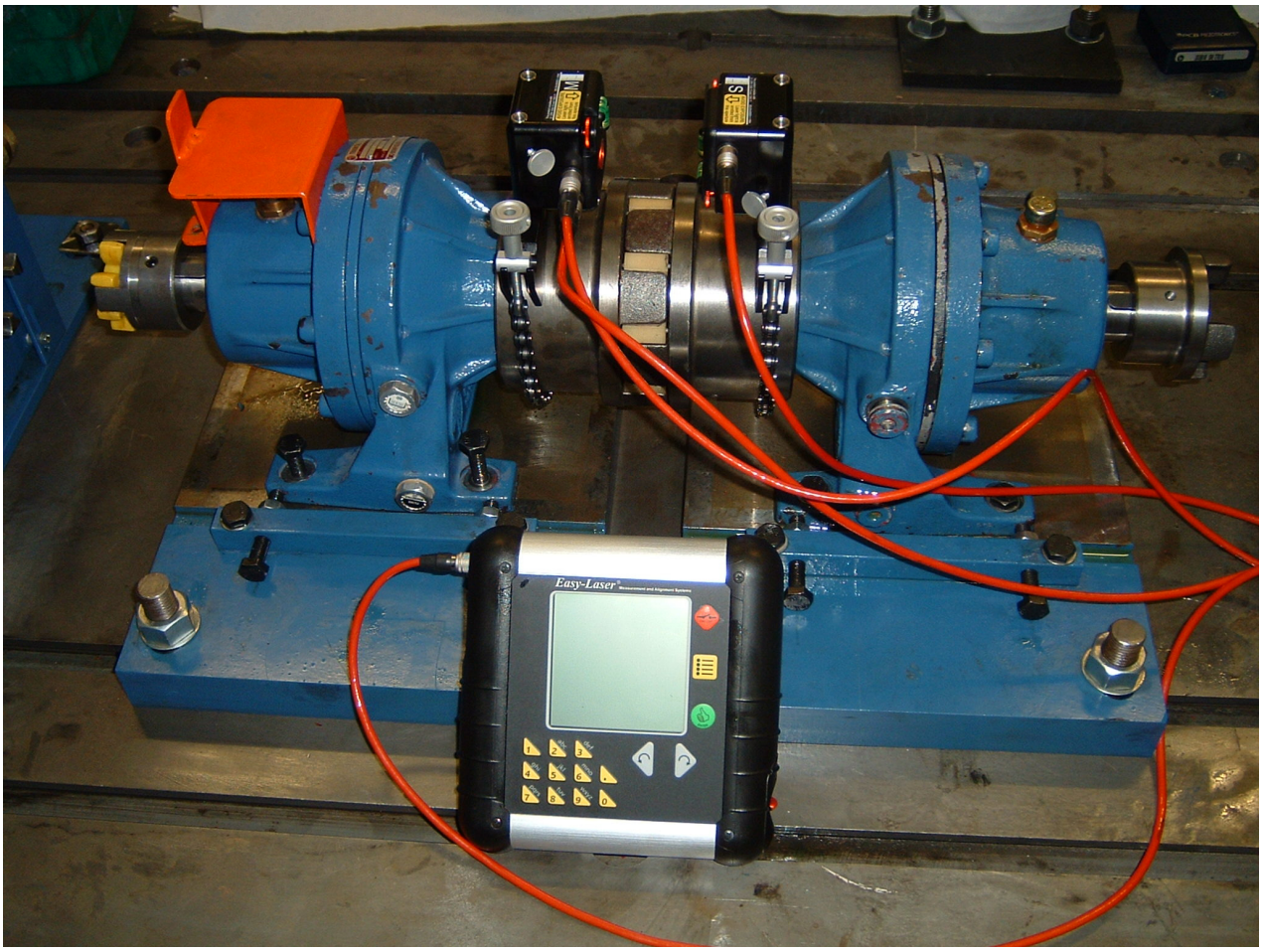

Figure 2.12 - Laser alignment of shafts

To determine what components of the frequency spectrum were connected to rotational speed and which were from external sources, a number of waterfall plots were created during run up, run down

cycles. An example of such a plot is given in figure 2.13. It is clear from figure 2.13 that there is vibration present as orders of gearbox revolution speed. It is also clear that there is vibration present that is not related to shaft speed but related to external fixed frequencies.

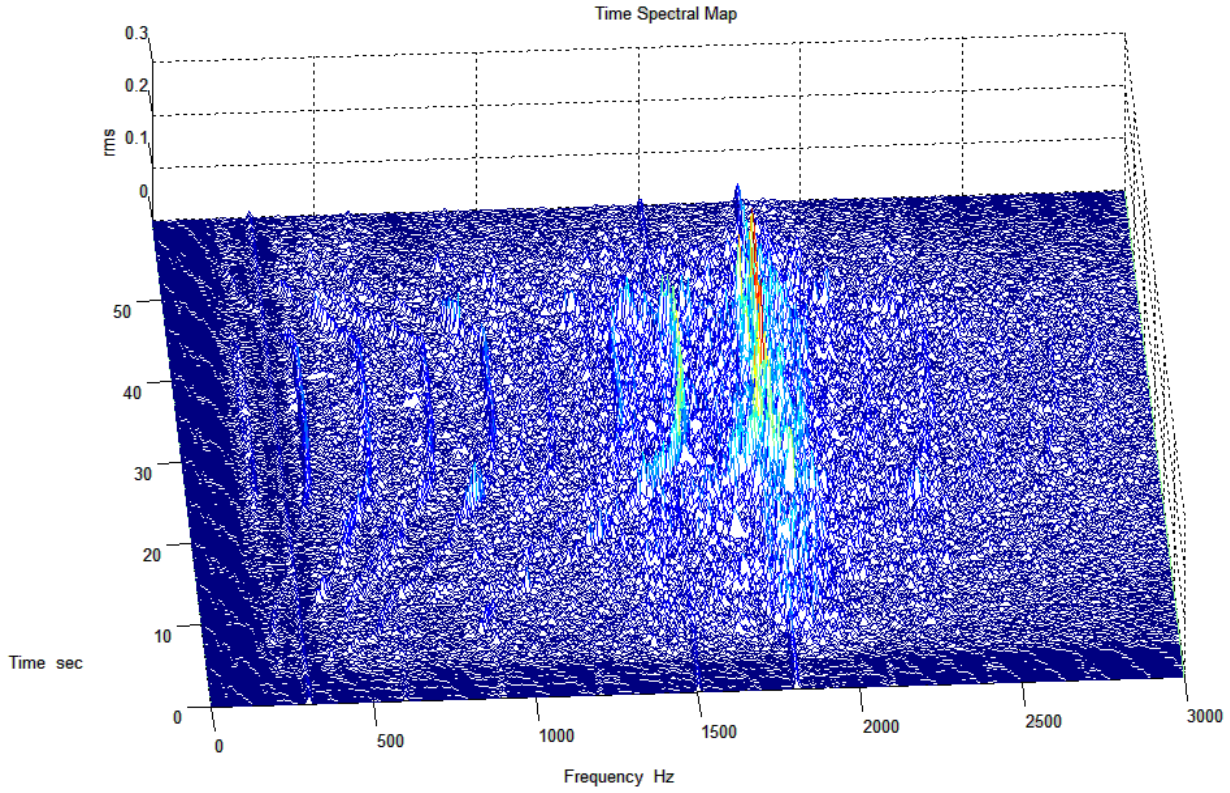

Figure 2.13 - Waterfall plot 0 - 3 kHz, 0 - 1080 - 0 rpm

This is more clearly seen in figure 2.14 where vibration from unrelated sources can clearly be seen at 300Hz as well as 600Hz. Unrelated source vibration is also clear below 100Hz. The frequency of external sources must be known when the spectrum of the vibration from the epicyclic gearbox is evaluated to determine important spectrum peaks from those originating from fixed vibration sources. This is of critical importance when evaluating the final data obtained from measurements.

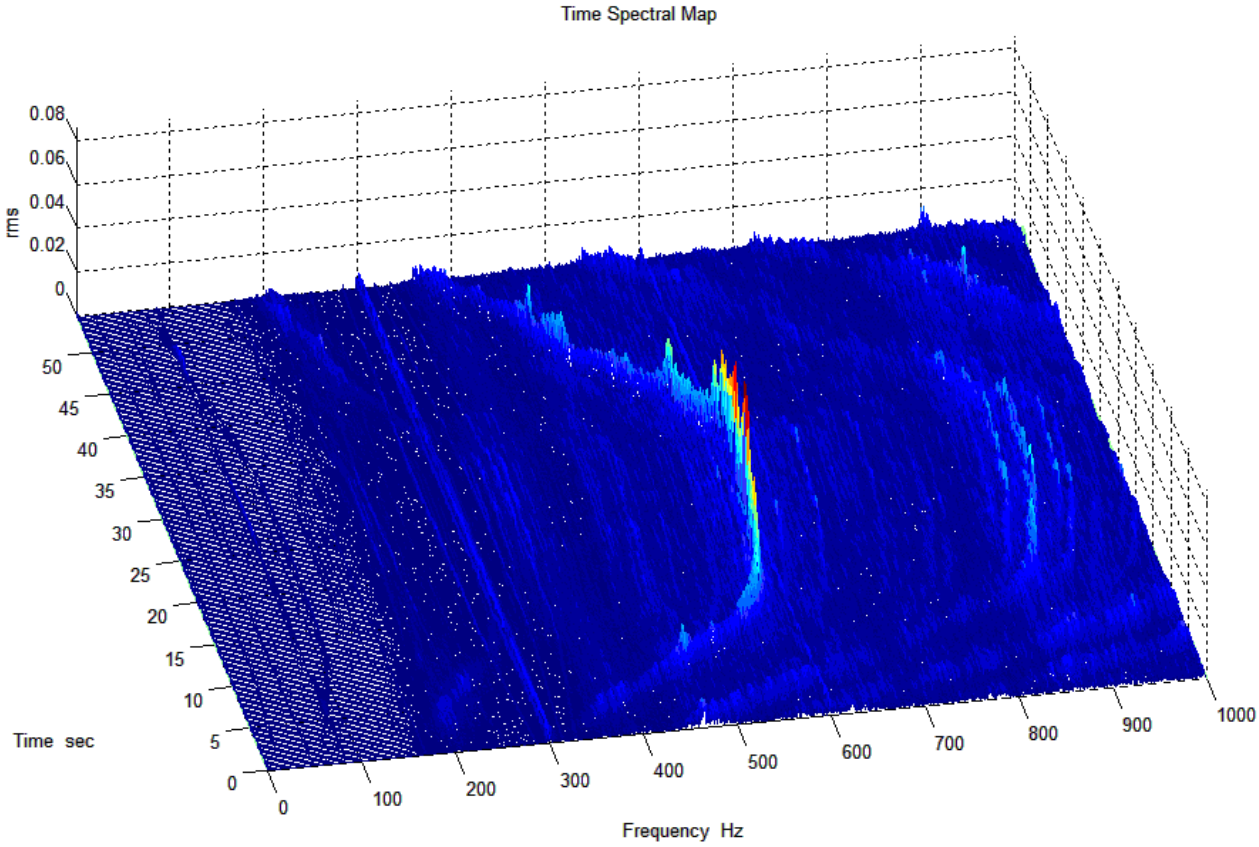

Figure 2.14 - Waterfall plot 0 - 1 kHz, 800 - 1700 - 1000rpm

The gearbox speeds should be carefully selected to ensure that frequencies of interest do not lie at the same frequency as external vibration. This would result in incorrect deductions of the vibration spectrum. The waterfall plot was thus used to evaluate different operating regimes.

Chapter 3 - Implementation of epicyclic time synchronous averaging

3.1. Implementation reasoning

From the evaluation of the literature considered in chapter 1, it is apparent that the most robust method of fault identification for an epicyclic gearbox would currently be the so called planet separation technique often referred to as the "Australian patent" technique. This method is a TSA (Time Synchronous Averaging) method specifically modified for epicyclic gearboxes. For the purpose of this dissertation the method of epicyclic gearbox time synchronous averaging will be referred to as EpiTSA (Epicyclic Time Synchronous Averaging). This method gives an indication of a fault on a planet gear and seems to be fairly robust. The implementation of this method is thus proposed and will serve as a basis of comparison for the research described further in this dissertation. There are, however, a number of variations in which the technique can be applied as was discussed by Samuel, Paul and Conroy (2004). In general, the approach is the same but there are small differences depending on which variables are used. Different variables include the single or multiple accelerometer approach, the number of teeth used per window, different types of windows that can be used, overlap size and storage methods. These variables are directly determined by the program implementer and will have a slight effect on the results obtained through application of the method. As there is no single or specific approach available at present, all that can be defined is the basic application that has been discussed in previous chapters. The specific implementation of the technique will thus vary from individual to individual.

3.2. Areas of caution

During the implementation of the EpiTSA a number of problems were identified that required specific attention. Some of these problems could easily be solved. There are also a number of issues that require caution during the implementation thereof. Each of these problems is discussed individually.

3.2.1 Tooth mesh sequence

It would appear that in most epicyclic gearboxes all planet gear teeth mesh with all ring gear teeth. Thus, an accelerometer placed directly above any ring gear tooth will be capable of recording all planet gear teeth meshing with the ring. As described in paragraph 2.2, a single ring gear tooth on the Bonfiglioli gearbox will only mesh with either even or odd planet gear teeth. To implement the EpiTSA technique, data from all planet teeth must be obtained. There are thus two options to solve this problem:

a. The window width must be adjusted to enable data from two teeth to be captured under the 1:1 transfer ratio of the Tukey window. To make this possible, data from six teeth must be recorded so as to ensure that the taper part of the window overlap to a 1:1 ratio, as stipulated by McFadden (1994), as a condition for the use of a window. The issue with applying the technique in this manner, is that the initial assumption, that the transfer path between the gear mesh point and the transducer remains constant during the rotation of the planet gear, may no longer be valid. This results in the classic problem of epicyclic gearboxes being repeated. The six teeth correspond to a quarter rotation of a planet gear, and using this data as representative of a meshing pattern may invalidate data and is thus not ideal.

b. Two or more accelerometers may be used to obtain a composite vibration signal as discussed by Samuel, Conroy and Pines (2004). By making use of two accelerometers, one mounted directly opposite a ring gear tooth engaging even planet gear teeth and the second mounted opposite a ring gear tooth engaging odd planet gear teeth, a composite signal can be created by using the data obtained from both. This option seems attractive as two gear meshes are measured during each planet rotation, thus decreasing the time length of signal required as discussed by Samuel et al.

It was decided to implement the dual accelerometer method. This option is a modification of the Samuel et al. method and provides a method of implementation that will not invalidate vibration data.

3.2.2 Window size

A number of problems were encountered with the selection of a window size. Equation 1.1 describes the TMP of a gear. Samuel et al. state that a minimum of 26.8 samples per tooth mesh is required to fully define the tooth mesh vibration of a tooth. The direct application of this equation to an epicyclic gearbox is questioned. The following velocity diagram describes the tooth speeds across a rotating planet gear:

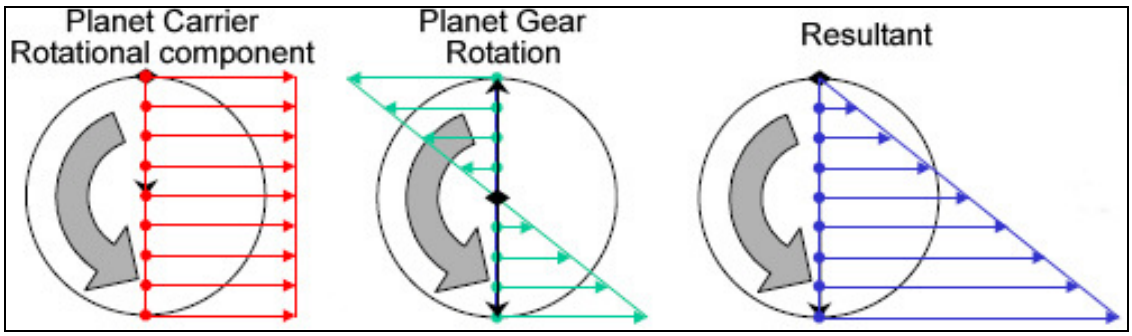

Figure 3.1 - Planet gear velocity diagram

If one were to use the rotational speed of only the planet gear itself, the tooth mesh period would give a false indication of the meshing period as the centre of the planet gear moves with time and this is not accounted for in equation 1.1. An alternative method is thus required to determine the TMP of the planet gear. A simple solution was found to this problem. Using the tacho pulse which marks the centre point of each planet as it passes the accelerometer, the number of samples between tacho points was determined. There are 14 planet gear teeth that mesh between each tacho point. This was determined by counting the number of teeth that mesh between planet gears during manual rotation of the open gearbox. The samples per tooth were obtained by simply dividing the number of samples between tacho points by the number of teeth which passed the accelerometer during the same time period. This method was found to be highly accurate and was more reliable than any method of calculation. The TMP is obtained from the data that is being processed and not from theoretical values, thus resulting in a TMP that accurately represents the measured data.

There are a number of ways to apply the window position. The simplest method would be to make use of the starting point of the window as a reference. If the TMP is not exactly correct, the window data would be skewed to one side of the center point of the mesh period i.e. the window data will be too early or too late. It was decided in conjunction with other factors such as speed fluctuation and

window length, that the centre point of the window must be used to determine the position of the data. This being the case, any error on the window size will cause a fault where the taper section of the windows goes to zero, thus minimizing a fault. This necessitates a window size with an odd number of points.

3.2.3 Speed fluctuation

The TSA process requires rotational speed to be fairly constant and then interpolation is used to ensure that sampling points align, thus making averaging possible. If the windows applied to the epicyclic vibration signal were defined using the starting or end points, the averaging process would be sensitive to speed fluctuations. By defining the windows using a centre point and a tacho pulse, the exact centre of each window is known, independent of the speed. This provides a measure of robustness built in to improve speed fluctuation resistance. The window is then extracted according to the number of data points around the centre. By physically extracting data points around a centre point, small speed variations do not have a large effect. Thus, a fair amount of robustness is built into the system.

The rotational speed during testing is determined from the tacho pulse recorded. A maximum speed deviation is determined from this data. The user can set a maximum allowable speed deviation. Should the preset deviation be exceeded, the program warns the user. This feature is used to restrict the program from using data obtained when there are large speed fluctuations which may cause errors, and thus protects from medium to large speed fluctuations.

3.2.4 Tukey window taper steepness

McFadden states that the window applied to the vibration data must always summate to unity. This is only possible with a limited number of window types. In paragraph 2.2 the problem of the tooth mesh sequence is discussed and a two accelerometer composite signal is suggested. The problem with this approach is that the number of data points on the taper section of the signal must correspond exactly to the number of points on the 1:1 ratio section of the signal. If the number of points are defined, the α value must be adjusted to ensure that the number of points on the taper section equal the number of points over the tooth mesh. To correctly determine the most suitable α value, an optimization process is required. Many of the standard optimization techniques require

the derivative of the function that must be optimized, to be known. The problem with determining the optimum α value is that no function exists to be optimized. There are a number of conditions that must be met in which an optimum solution exists. Furthermore, the number of data points can be adjusted slightly to obtain a better result is available within a few points.

A suitable optimization algorithm was found in the particle swarm optimization algorithm (PSOA). The details on the PSOA were obtained from Wilke, Kok and Groenwold (2005). The PSOA is ideally suited to this type of optimization as it does not require a fixed function or derivative thereof, and can be performed for any number of variables. This can be seen in the MATLAB® program OptimFun which is a subprogram of the PSOA TukeyOptim, both of which are attached in Appendix A. It is clear that if the result of the points where a particle is, are unwanted, the function value at that point is simply penalized as seen in line 91 of the program, thus making those points undesirable. The swarm activity can be seen in figure 3.2.

The top left block shows the random starting points for the swarm. Each point is the position of an individual of the swarm. The attractiveness of the individuals point is then fed back to the swarm as a whole. The following iteration (It# 1) uses a percentage of the most attractive result obtained from the swarm in totality, as well as the most attractive point obtained by the individual, together with a random variation to determine the next position of the individuals of the swarm.

The reasoning is that each individual will be drawn to its own most attractive point, while at the same time attracting other individuals of the swarm to that same point. Thus, the most attractive point will be the point where all individuals, as well as the swarm itself, congregate. As the number of iterations increase, the swarm can be seen moving towards the most attractive point. Individuals can also be seen to be identifying other points that might be more attractive.

After the PSOA has been allowed to run, the values obtained will be the optimal point that the swarm can find. In this case the α are values given on the Y-axis, with the number of points given on the X-axis. Each member of the swarm will test different α values for different numbers of points. The optimum will then be found by the swarm after a number of iterations.

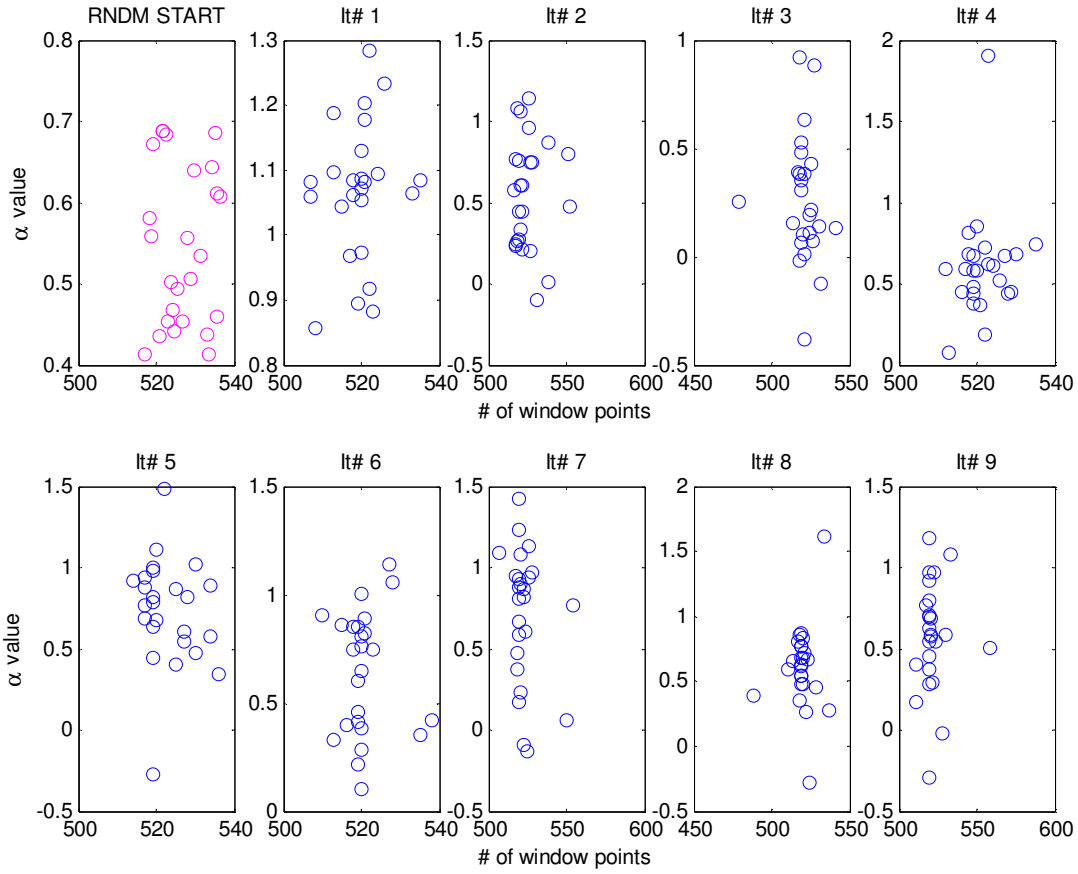

Figure 3.2 - Particle swarm activity during optimization

3.3 Practical implementation problems encountered

3.3.1 Magnetic pickup probe contact

The application of TSA requires a tacho signal to enable averaging to be implemented. With EpiTSA a tacho signal is not necessarily required, as the modulation of the signal can sometimes be used to determine the position of the planet carrier. The modulation of the Bonfigliogli gearbox was seen to be unreliable to be used for the determination of planet gear position. This can be seen in figure 3.3 where a section of signal obtained from the gearbox is given with a tacho pulse marking the planet as it passes the accelerometer. The large peaks seen in the vibration signal are caused by induced damage on a single gear tooth. This will be discussed at a later stage.

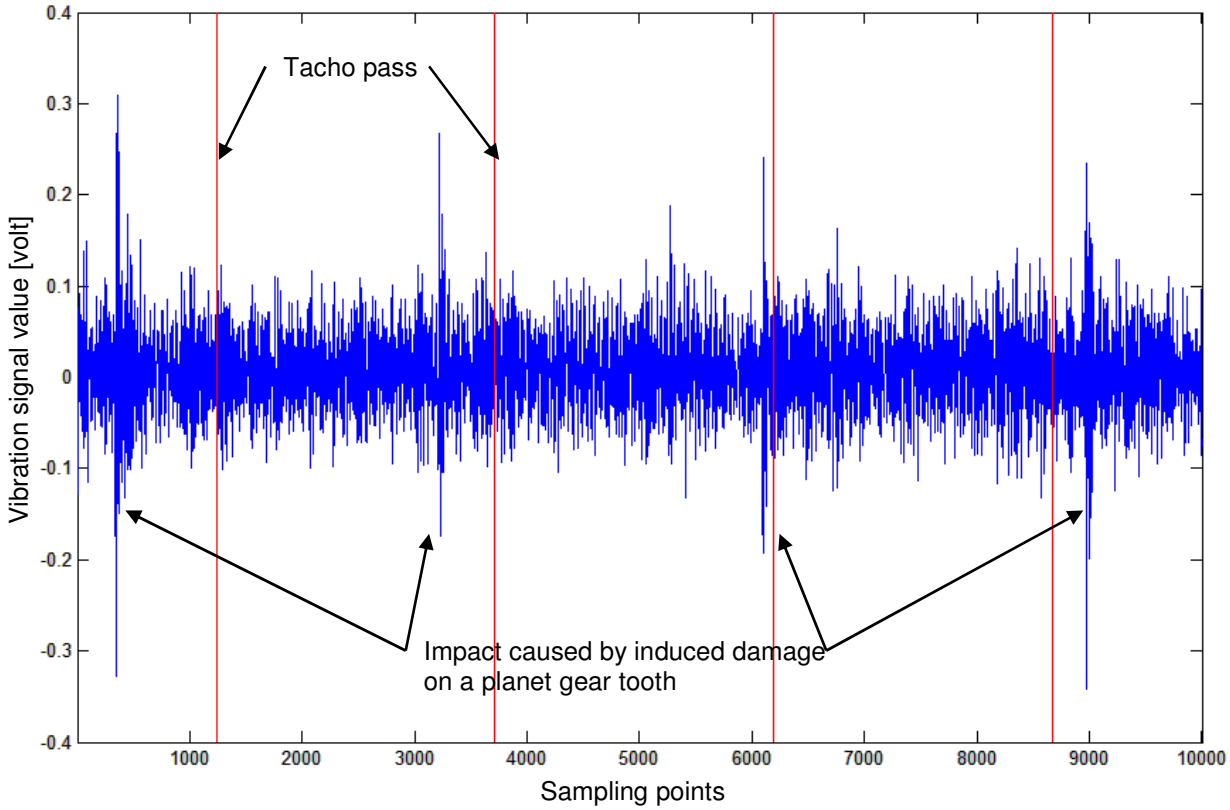

Figure 3.3 - Raw vibration signal with planet pass marked

It is thus clear from figure 3.3 that the passing of the planet must be recorded by external means. As described in paragraph 2.3, modifications to the gearbox were made to insert a probe with a trigger, thus recording the exact centre point of each planet as it passes the measurement point. When the modifications were tested, the eddy current probe that was used was damaged due to contact with the planet carrier. The planet carrier is floating and can move freely in an axial direction. It was therefore decided to shim the carrier to stop the rearward floating of the carrier. Due to the design of the gearbox it was not possible to measure the tolerances without specialized equipment. To determine the thickness, a 1mm thick shim was inserted between the output shaft and the carrier. This was too large and caused the input shaft to be forced against the wear plate with such force that the gearbox could not be rotated by hand. The shim was then reduced to 0.5mm thickness which was sufficient to prevent axial motion of the planet carrier without causing severe contact between wear plates. The eddy current probes were, however, still making contact with the carrier. The adaptor seen in figure 2.6 was modified by moving the probe hole 2mm to one side away from the carrier. This modification proved successful and no contact between the carrier and probe could be found even under severe loading conditions.

3.3.2 Accelerometer mounting

The accelerometer mounting location is determined by the exact location of the planet gear tooth that is to be monitored. This requires accurate positioning of the accelerometer on the outside of the gearbox. During initial gearbox evaluation, accelerometers were mounted to the epicyclic gearbox housing by means of magnetic mounts. Although this type of mounting is sufficient for general vibration mounting it is insufficient for the measurement of highly accurate data.

Stud mounting of the accelerometer to the gearbox housing is required. To determine the exact mounting location of the accelerometer, the ring gear was removed from the gearbox. The ring gear teeth were numbered and the teeth under investigation were selected. Stud mounting holes were drilled and tapped at the required location on the outside of the ring gear. This ensured that the correct locations were used during all vibration measurements.

3.4 Signal processing

3.4.1 Tacho signal manipulation

The tacho signal is to be used for two purposes. The first use for the tacho signal is an accurate display of rotational speed for the gearbox. The easiest way to perform this is by using a 1 pulse per revolution impulse from a magnetic pickup located on the shaft keyway. This was done by manufacturing a bracket to mount the probe just above the keyway. The probe and keyway is seen on the left in figure 3.4 while on the right hand side of the photo is the display unit indicating true input speed. The speed displayed was verified using two different hand-held tachometers which had been calibrated. No signal manipulation is required for this signal as all manipulation is done by the speed display unit.

Figure 3.4 - One pulse per revolution speed display system

The second use for a tacho signal is for the determination of the exact position of the planet gears as they pass the accelerometer mounted on the ring gear. This requires signal manipulation to extract useful timing data from the signal. The modifications done to the gearbox are described in paragraph 2.3. A section of the raw tacho signal obtained from a magnetic pickup is given in figure 3.5. The MATLAB® program [TriggerPoints] which is attached in appendix A2 is used to calculate the centre point of each impulse and this point is illustrated using circles. The centre point is defined as the middle point between the points on the tacho signal which are above a user-defined trigger level. This program is used to determine the centre points of each planet gear as it passes the accelerometer and is shown by red circles, as well as the determining the planet gear number using a higher trigger level on one planet gear that has an increased voltage reading and is illustrated using green circles. This information can then be used in other MATLAB® programs.

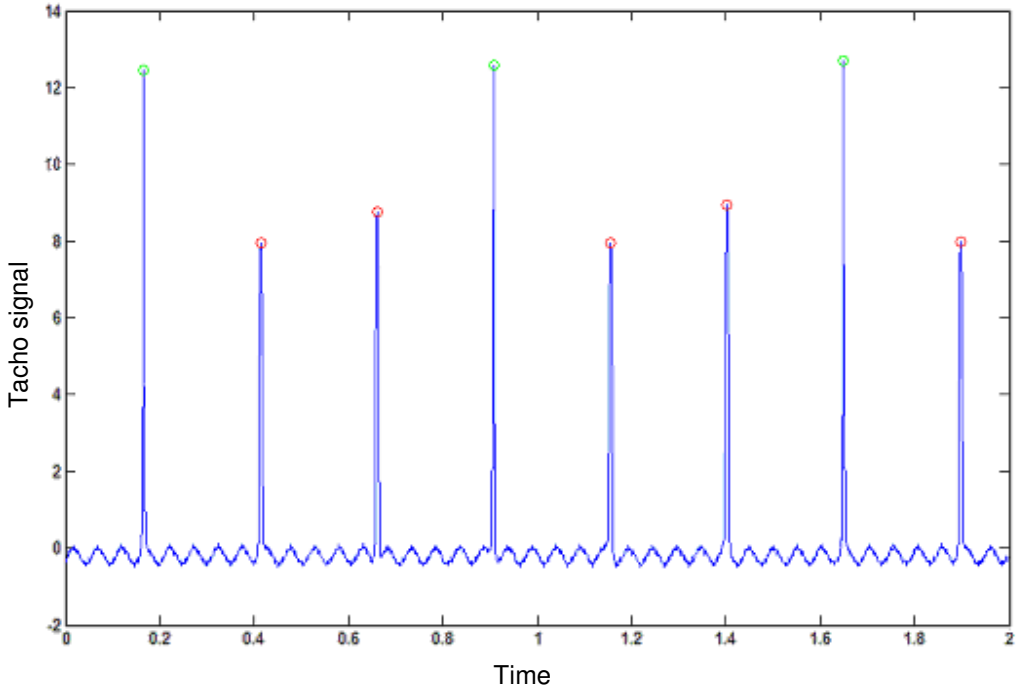

Figure 3.5 - Tacho signal with calculated centre points

3.4.2 Extraction of a window of data

A window of data must be extracted from a signal obtained from an accelerometer. To enable data extraction, the centre points of the window must be described, as well as the window length. These are the two variables that are required together with acceleration signal. The MATLAB® program [WindowExtract] is attached in appendix A3. The program gives as output a vector containing a window of data at each centre point. This vector can then be used by other programs as required.

3.4.3 Determination of tooth numbers

As each planet gear passes an accelerometer mounted on the outside of the ring gear, the tooth in mesh must be known. This can be calculated using equation 2.3. The tooth mesh sequence is determined using the MATLAB® program [ToothLookup]. This program has been written specifically for the Bonfiglioli gearbox and is attached in appendix A4. The output of this program is a vector containing the revolution number, planet gear in mesh and tooth in mesh, at two points on the ring gear.

3.4.4 Assimilation of planet gear signal

The assimilated planet gear signal is created using the MATLAB® program [EpiTSA]. This program makes use of different subroutines as described above to generate the assimilated planet gear signal. The program was tested during each step using different methods. The final test was performed using a unit vector on one input while a zero input was given on the other input. The result from this was a stable value of 0.5 over the entire generated planet gear signal. When both inputs were set to unit value, a stable value of 1 was achieved over the entire assimilated tooth signal. This tooth signal was calculated using a real tacho signal obtained from the test bench and two unit inputs of the same length as the tacho signal resulting in 8 averages.

3.5. Results of epicyclic time synchronous averaging

Damage was induced on a single planet gear tooth by grinding away approximately 30% of a single tooth as well as grinding the tooth flanks. The damaged planet gear is seen in figure 3.6.

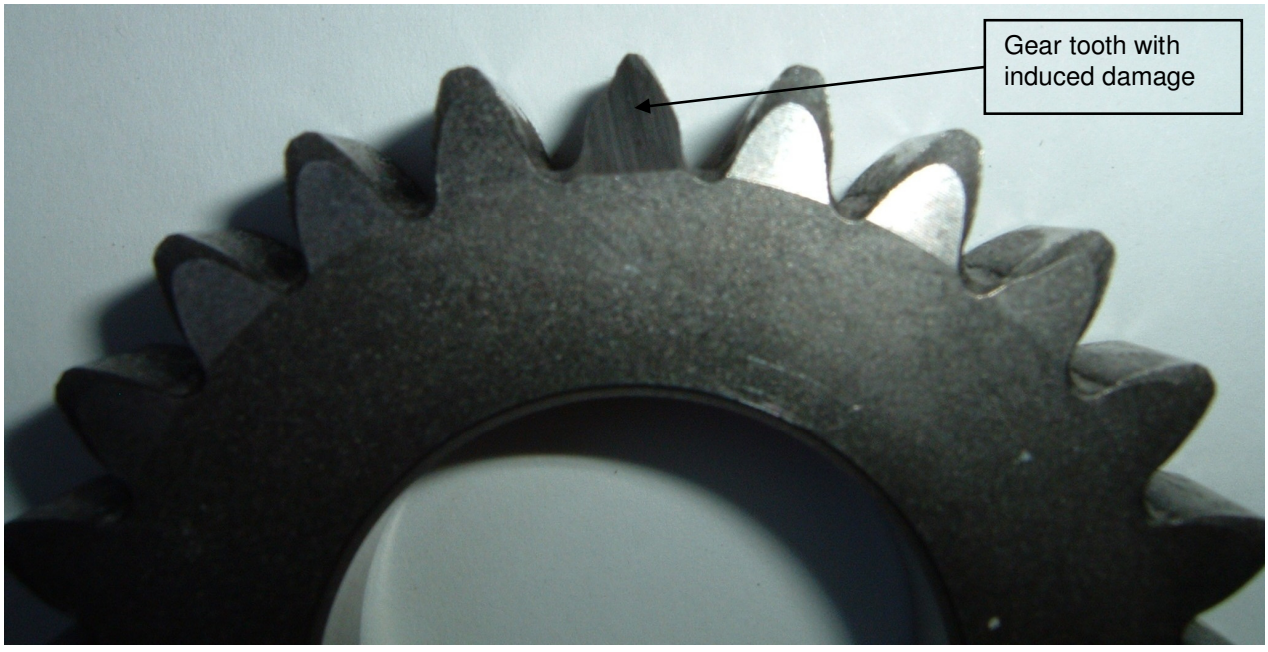

Figure 3.6 - Induced damage on a planet gear tooth

Data was taken from the epicyclic test bench at a constant speed. A bandwidth of 10kHz was used which resulted in a sampling period of 25 600 samples per second. This was done to obtain a standard number of samples per tooth, enabling comparison between different levels of damage

and different accelerometer locations. The number of samples per tooth as determined in paragraph 1.4 conforms to the minimum number of samples as specified by Samuel, Conroy and Pines (2004). The data was then processed and the kurtosis value calculated with the speed verified using a MATLAB® function at 1 187 rpm under a maximum load for the data illustrated here. The damaged tooth is clearly seen when compared to an undamaged gear as seen in figure 3.7 below:

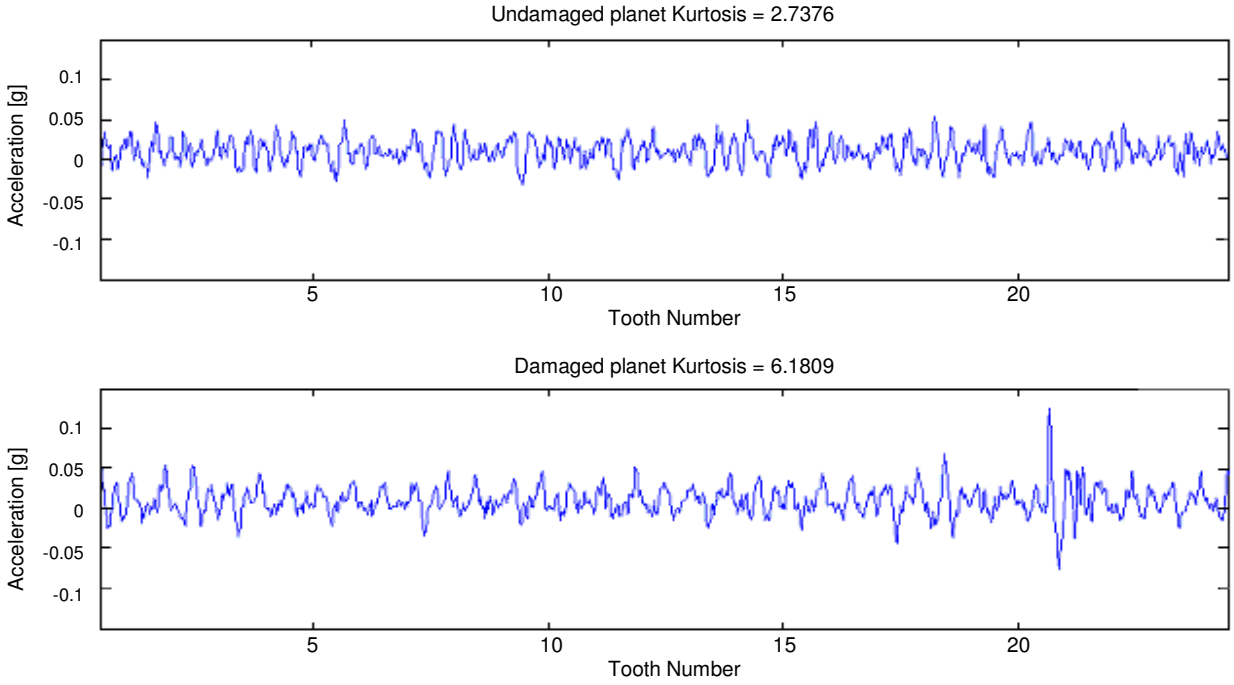

Figure 3.7 - EpiTSA Signal for damaged vs undamaged condition

Decker (2002) points out that the kurtosis value of Gaussian noise is very close to 3 which should be featured by a gear in good condition. The undamaged planet gear in figure 3.7 has a kurtosis value of 2.7 while the damaged gear has a value of 6.2. Thus the severe damage induced on the planet gear was clearly detected by the EpiTSA technique.

3.6. Epicyclic time synchronous averaging abnormalities

During testing, a single damaged planet gear was used. It was expected that a fault would be seen on planet gear 1, which was the position that the gear was mounted on the planet gear, when the EipTSA method was applied. The results given in figure 3.8 are obtained from the severely damaged planet gear discussed in paragraph 3.5. As seen with P1 (Planet Gear 1) the damage is

very clear in the compiled time signal. This can be verified with both the kurtosis at 9.2 and crest factor of 8.6. Both these values give clear indication of damage.

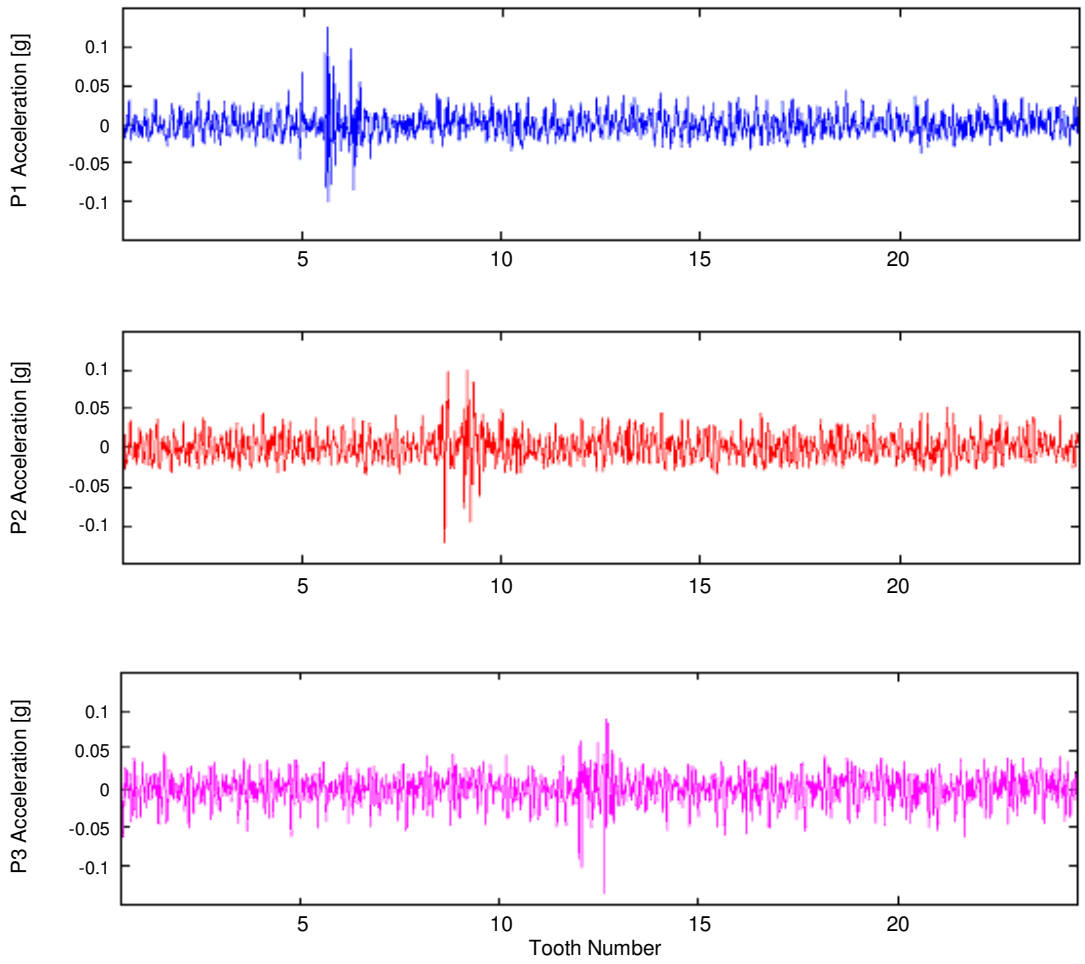

Figure 3.8 - Epicyclic time synchronous averaging result

The signals for P2 and P3 are not expected to show any damage and be very close to zero. As is seen in figure 3.8, this is not the case. Initially it was thought that that there may be some form of damage on the undamaged gear teeth. To ascertain that this was not the case, all planet gears were examined under a microscope to ensure that there was no damage present. It could thus be verified that there was no damage on the other planet gears. Another problem that could affect the output of the EpiTSA, was an incorrect window size selection. The same data was re-evaluated using a number of different window sizes but the effect was seen with all window sizes. The program used to generate the EpiTSA was then re-checked step by step for the entire program. New testing methods were used to verify the accuracy of the program. These methods included a

pause in the program as each window was extracted and inserted into position on the compiled signal. The program was then further modified to insert a unit impulse at each step thus creating a stepped output. These compiled signals were then visually evaluated at each step of insertion in the final compiled signal. The program was seen to be working as designed and no faults were detected. Finally, the planet carrier with gears, as well as the sun and ring gears, were removed and set up as in the gearbox. The sun gear was rotated by hand as it would be in the gearbox. Using this method, it became apparent that there is a relationship between the tooth that is faulty and the other teeth on the other planet gears. This tooth offset corresponds to 3 teeth when counted on the gears.

All teeth are referenced from the point where they engage with a marked tooth on the ring gear which is directly opposite accelerometer 1, with the tooth engaged marked as tooth 1. Thus with P1 T1 engaged P2 T4 and P3 T7 will be engaged with the ring gear. To explain the phantom damage phenomenon seen in figure 3.8, assume that tooth number 6 on P1 is damaged. This tooth will be in mesh a number of times during a single rotation of the planet carrier. What is clearly seen as the planet gears rotate is that P1 T6, P2 T9 and P3 T12 will be engaged simultaneously. This occurs at both the ring and sun gears. This explains the phantom damage seen in figure 3.8 that was not expected.

If one follows the steps of the EpiTSA program given in appendix A, and using the above information, it can be shown that if P1 with a damaged tooth is at position 1 in figure 3.9, a window with the damage is extracted from accelerometer 1. However, the vibration caused by the damaged tooth on the ring gear will also be measured at accelerometer 2 which will be applied to the tooth of P2 in mesh at that point.

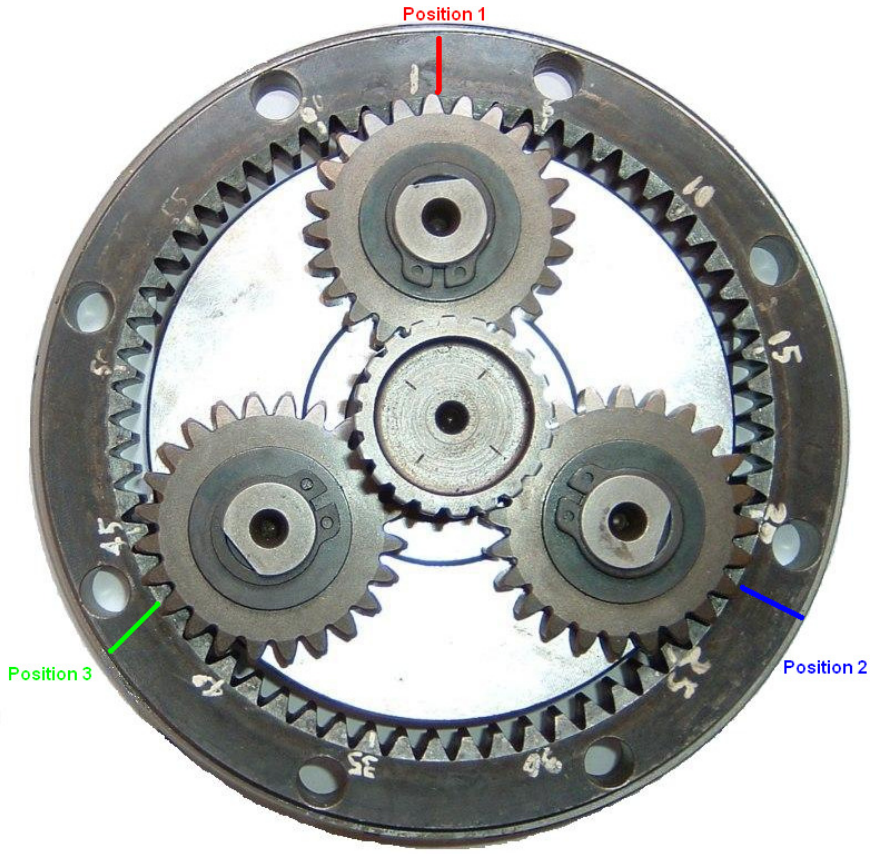

Figure 3.9 - Epicyclic gears in mesh

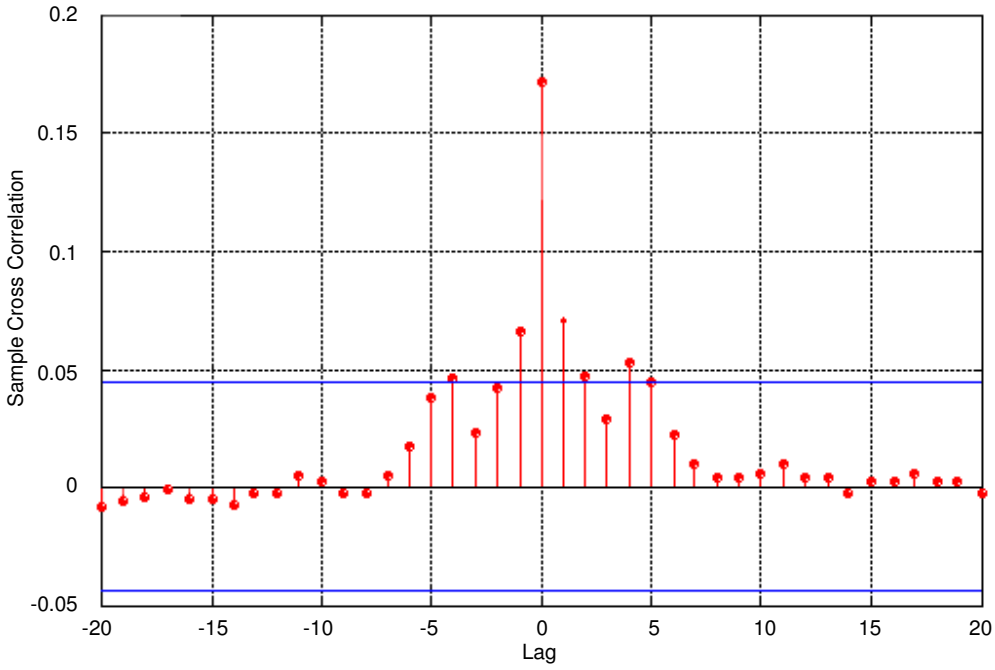

Figure 3.10 - Cross-correlation between acc1 and acc 2

From figure 3.10 it is seen that there is a very small component of the two signals, which have a distinct relationship between them. This means that the two signals obtained from the externally mounted accelerometers on the ring gear contain small amounts of similar properties. There is, however, a large component of the signals that does not hold a relationship with each other and originates from the planet gear that is to be measured, thus enabling the planet separation technique to be applied successfully. The data used in figure 3.10 was measured using a single planet gear. This confirms that a section of the vibration caused by the damaged planet gear can be transferred to the signal measured at the undamaged tooth in mesh, causing phantom damage. The transfer effect is clearly seen in the time domain signal in figure 3.11 which shows time domain data measured simultaneously from two accelerometers mounted at two different locations.

There are 3 different rotational positions that will affect the output signal. Individual adjustment in the phantom damage effect will occur depending on which tooth is damaged. As discussed in paragraph 2.2, each ring gear tooth will only be in mesh with either odd or even planet gear teeth. Thus, depending on which tooth is damaged (even or odd), there will be a small amplification of the phantom damage on either P2 or P3.

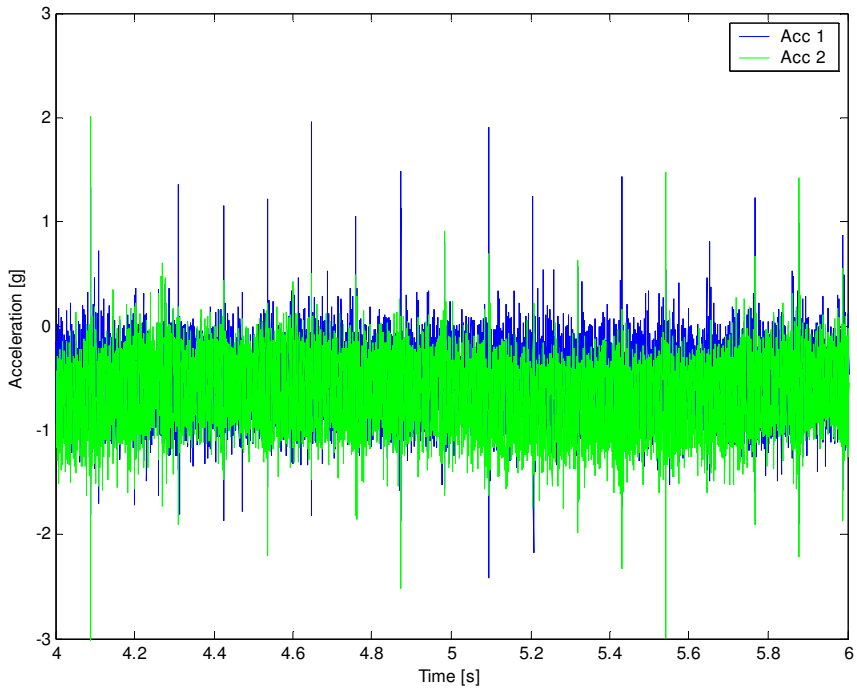

Figure 3.11 - Raw time signals from accelerometers 1 and 2

Each position that causes phantom damage is discussed individually with the effects of each position summated.

a. P1 at position 1 with P2 at position 2

Due to the damage, there will be associated acceleration as the tooth passes through mesh. This acceleration will be detected with the accelerometer mounted at position 1. The accelerometer at position 2 will also detect this vibration as it is attached to the same structure as the first accelerometer. When the EpiTSA method is applied, the vibration detected at position 2 will be applied to the tooth in mesh although it is not produced by the tooth in mesh. The level of vibration will however be slightly lower than at the point of origin due to the transfer path.

b. P1 at position 2 with P3 at position 1

The reverse of what happens above will take place. This involves the damaged tooth vibration being transferred to P3 through the common ring gear. The vibration from the damaged tooth will be detected by the EpiTSA method and applied to P3.

c. P1 at position 3 with P2 at position 1 and P3 at position 2

Vibration caused by damage will be transferred to both planet gears.

The effects described above will be summated with the resulting phantom damage seen in figure 3.8.

Chapter 4 - Planet carrier vibration monitoring

4.1 Implementation reasoning

From the literature that was reviewed, it is apparent that there have been no or very few attempts at measurements obtained from the inside of an epicyclic gearbox. These measurements, although impractical to implement on a commercial basis, are ideal for comparison to existing separation techniques as the transfer path between the accelerometer and the planet gear remains constant when the accelerometer is attached to the planet carrier. The successful measurement of this data will provide an alternative approach to the planet separation technique.

4.2 Implementation problems

Before monitoring on the planet carrier was possible, there were certain issues that had to be addressed. These issues are discussed briefly to ensure that the problems involved with this type of measurement are understood.

4.2.1 Planet carrier accelerometer mounting

The installation of accelerometers on the planet carrier presented a number of problems. The main concern for installation of accelerometers in the gearbox is the possibility that the accelerometers and cables become entangled in the gears during operation. This would cause damage to the sensors which are costly to replace. After careful investigation, it was decided to cut slots in the carrier and place the accelerometers in recesses. This would prevent the accelerometers falling into the gears should their attachment fail for any reason. The cables are placed under a ring that is bolted into place. This prevents the cable from catching in the gears and being torn from the accelerometers. These modifications can be seen in figure 4.1

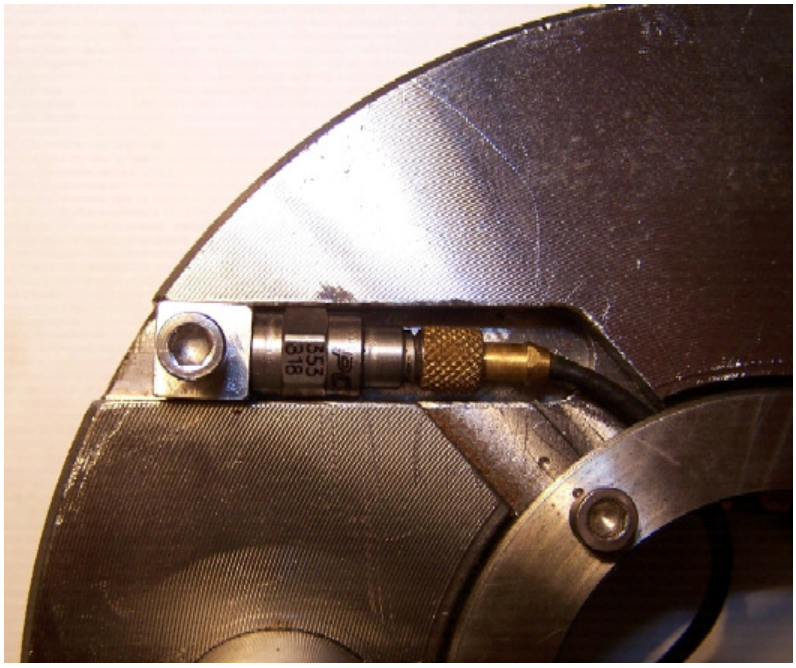

Figure 4.1 - Modifications to mount accelerometers on planet carrier

4.2.2 Slip ring usage

It was decided to make use of slip rings to transfer the signal from the rotating shaft to the stationary data acquisition equipment. There were a number of problems that were encountered which had to be solved before the slip rings could be used. The slip-rings were supplied by M-Tek in Pretoria. The manufacturer specified that the maximum surface speed should not exceed 1.2 [m/s]. This means that the maximum revolution speed of the slip ring should not exceed 345 [rpm]. It was pointed out that the slower the revolution speed, the better the signal quality as well as the longer the life of the slip-ring. Being gold plated, the wear rate is very high. The slip rings could thus not be used on the input shaft but only on the output shaft of the gearbox. This suited the mounting of the accelerometers on the planet carrier which fits on the output shaft by means of splines.

The brushes that run on the surface of the ring must be exactly positioned and pre-loaded. This required the design of a mounting that was suitable for both the test rig as well as mounting of the brushes. The design was confirmed with M-Tek before manufacture. The final mounting with the slip rings can be seen in figure 4.2.

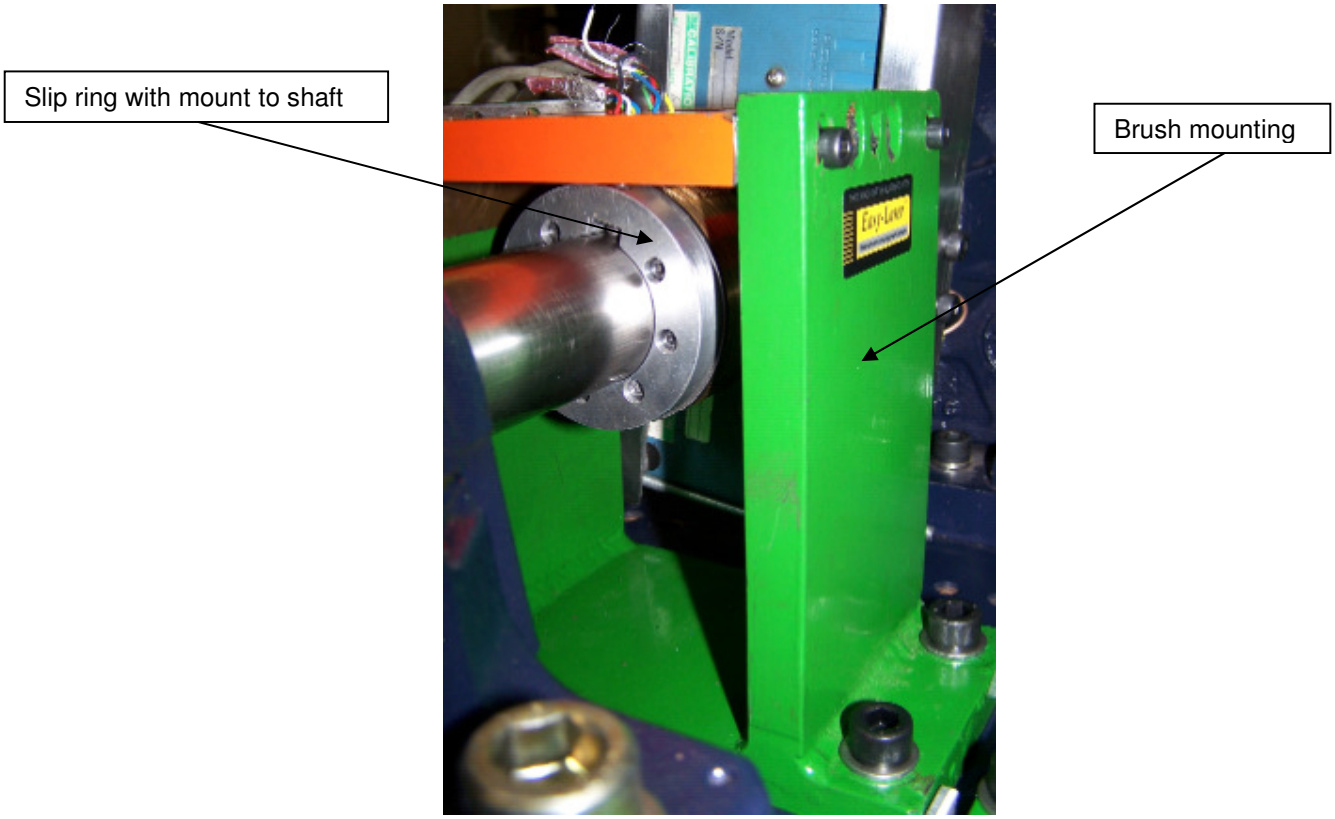

Figure 4.2 - Slip ring with mounting

The mounting provides for course as well as fine adjustment in all 3 axis. This ensured that exact adjustment was possible to fully align the grove and brush. To increase the consistency of the data transferred through the slip ring, 3 rings were used to transmit each channel.

4.2.3 Gearbox output shaft modification

The accelerometer cables had to run through the inside of the shaft. To make this possible, the shaft centre was drilled out and modified to allow a hole to be drilled normal to the shaft axis, through the centre of the shaft. This made it possible to run the cable through the shaft, and once outside the gearbox, the cables emerged from the shaft to be connected to the slip rings.

The output shaft had to be lengthened to enable the hole to be drilled for the cables to exit the shaft. Furthermore, space had to be allowed for the slip rings, as well as the power supply for the accelerometers. Design of shafts is discussed in detail by Bonfiglioli Riduttori (1995). Material specifications were obtained for the original shaft which was manufactured from 20MnCr5. This

material was not available locally. A suitable replacement material was found in AISI 5120. The shaft was case hardened to 57-61HRC to a depth of 0.4 to 0.6mm. This material and hardness specification was obtained from the original equipment manufacturer for the gearbox and was verified at the South African Air Force laboratory to ensure that the replacement shaft was manufactured to the same standard as the original shaft. This was done as the shaft was a safety critical item and should the shaft have failed under operation, serious injury and damage to equipment could occur.

The length of the new shaft, together with the weight of the shaft coupling, caused a moment on the output shaft that increased the risk of damage to the gearbox bearings on the output side. Furthermore, the slip rings required that the shaft had to have virtually no bending or variation in rotational path. It was therefore necessary to place a support bearing at the end of the shaft just before the coupling. This bearing is seen in figure 4.3.

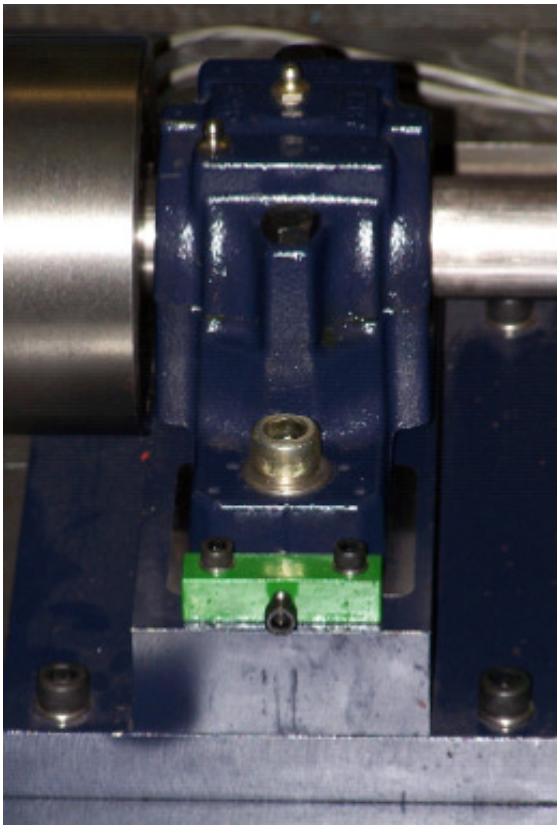

Figure 4.3 - Output shaft support bearing

4.2.4 Accelerometer power supply

The PCB accelerometers require power to enable the circuitry to function. After discussion with a number of consultants, including Andy Lobato of Helitune Limited who had made use of slip rings in the past, it became clear that signal conditioning should occur before the signal was put through the slip rings. This was verified with laboratory testing prior to the actual use of the slip rings. High quality signals were required for comparison purposes and it was decided to make use of the PCB battery powered power supplies which are commercially available. The problem with the use of the boxes is that the signal must be passed through power supplies before passing through the slip rings. The power supply boxes were required to rotate together with the output shaft. A bracket was built which was firmly clamped to the output shaft. The power supply boxes were clamped into the bracket as seen in figure 4.4.

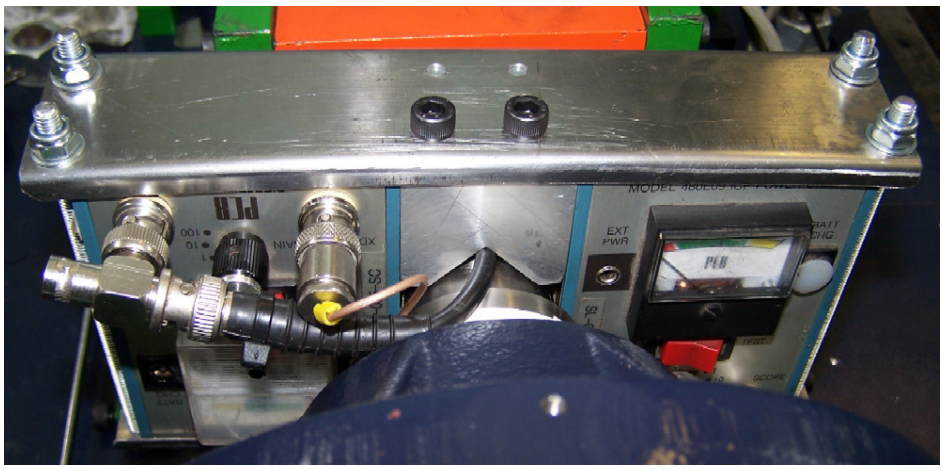

Figure 4.4 - PCB battery powered power supplies

4.3 Signal processing

The raw signal obtained from the accelerometers mounted on the planet carrier is given in figure 4.5 where the two signals obtained from the planet carrier can be seen. The signal is clearly seen to be superimposed on a sine carrier wave. Initially this was thought to be caused by faulty equipment. It can be deducted that the sine wave carrier seen in figure 4.5 is caused by the accelerometer rotating through gravity.

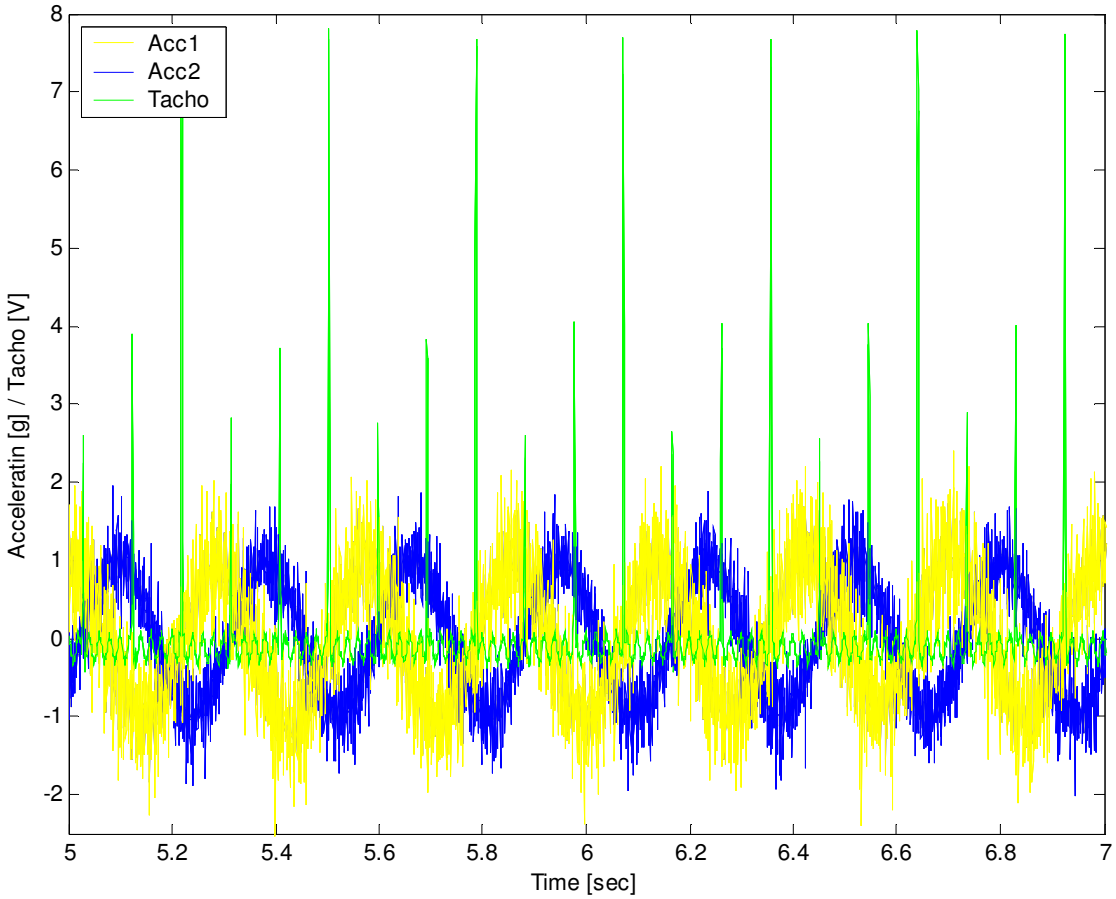

Figure 4.5 - Raw signal from planet carrier

The sine carrier wave can be ascribed to the accelerometers rotating through gravity as follows:

a. The magnitude of the sinusoidal acceleration oscillates between ±1g which is gravitational acceleration with direction changed from positive to negative.
b. A FFT of the raw signal above shows a large frequency component in the bandwidth of 3.4 to 3.6 Hz. This corresponds to the rotational frequency of the carrier.
c. The signals are out of phase by exactly 120°. This corresponds to the positioning of the accelerometers on the planet carrier.
d. Every third tacho pulse shown in figure 4.5 is from the same planet carrier. It is clear that the signal follows the exact position of the accelerometer as it moves through 360°

The effect of gravity can be removed through filtering before the vibration signal is used. Different filters were evaluated and the Butterworth filter was found to be the most effective for the removal of the sine wave carrier. Using the forward and reverse filtering method of MATLAB®, there is very little phase shift due to the filtering. It is however, not necessary to remove the carrier frequency if the data is used in the frequency domain where the frequency at 3.5 hertz will be large due to the above mentioned effect.

Chapter 5 - Data interpretation and review

In figure 5.1 the Power Spectrum for the undamaged epicyclic gearbox as measured on the outside of the gearbox is seen. As calculated in paragraph 2.2 and seen in figure 5.1, using the theory of McFadden and Smith (1985) it is clear that the Power Spectrum is not dominated by the GMF but by 3 x GMF.

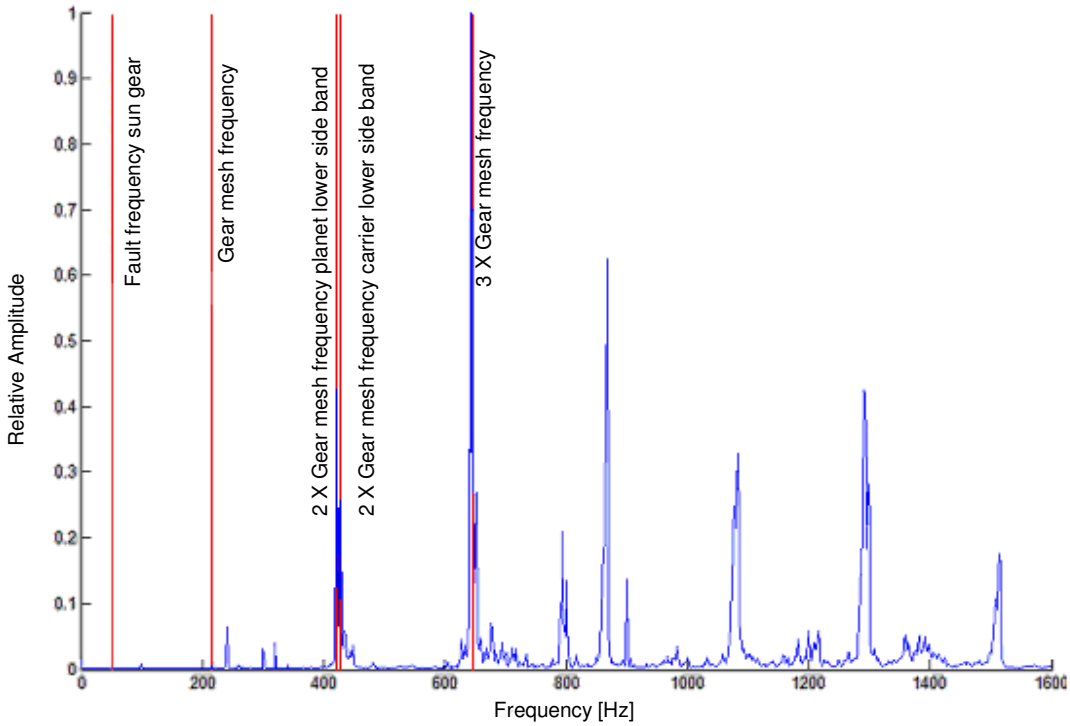

Figure 5.1 - Power spectrum for undamaged epicyclic gearbox

5.1 Single planet gear versus complete planet set

A comparison between a complete set of planet gears and a single planet gear could not be found in the available literature. A comparison between the complete set of three planet gears and a single planet gear will provide an indication of the manner in which multiple planet gears affect the measured vibration signal.

A single tooth was damaged and the damaged gear mounted on P1. Four different damaged conditions were considered. These are as follows:

a. (UD) Undamaged. An undamaged planet gear was used where there was no damage induced on any teeth.
b. (SD) Slight damage. The tooth surface was sanded using a belt sander. Due to the fact that the gear material is very hard only a slight roughness could be seen on the tooth meshing surface
c. (MD) Moderate damage. The tooth surface was touched against a grinding wheel. This caused a slight deformation of the gear shape, however, this effect was not severe.
d. (ED) Extreme damage. The gear surface was ground heavily and a part of the side of the gear tooth was removed. The ED tooth is visible in figure 3.7.

When a single planet gear is compared to the complete planet set, the effect of the damage can be identified more clearly. This observation is valid for both the planet separation technique as well as for frequency domain techniques. McFadden and Smith (1985) state that for a single planet gear, symmetric sidebands are expected around the gear mesh frequency. The PSD obtained from data measured when only a single planet gear is present does not illustrate this. As has been discussed previously, data measured at a single point on the outside of the gearbox contains phase information for all planet gears at their respective positions. If the data from multiple planet gears is used to calculate the PSD, the effect of planet phasing is introduced and sidebands become visible in the PSD. Although not possible to replicate this situation in practical use of an epicyclic gearbox, this observation confirms the theory behind the epicyclic gearbox. This may also provide a method of verification for the planet separation technique, as only the damaged planet gear is evaluated without cross-talk from the other planet gears. The verification of the planet separation technique is discussed in the following chapter.

5.1.1 Externally measured vibration data

This comparison will be made on the data obtained from the externally mounted accelerometers. Externally measured data for increasing levels of damage on a planetary gearbox with a full set of planet gears is given in figures 5.2, 5.3, 5.4 and 5.5.

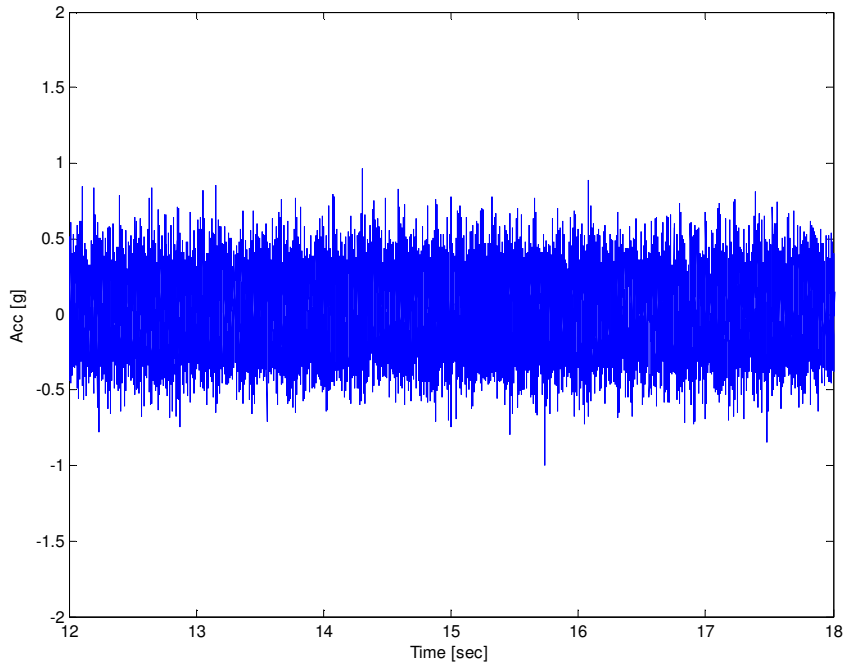

Figure 5.2 - Externally measured time signal – UD gear full planet set

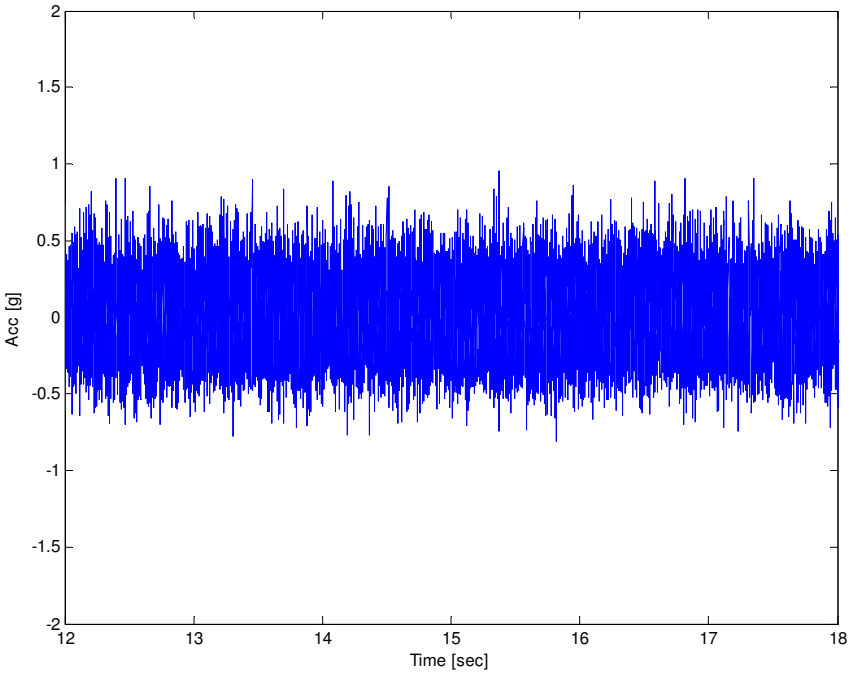

Figure 5.3 - Externally measured time signal – SD gear, full planet set

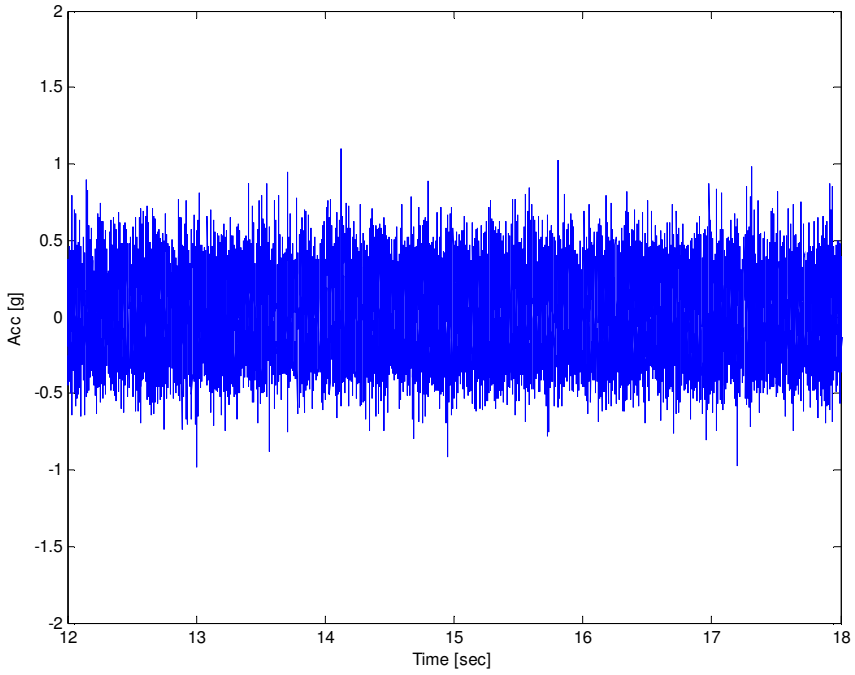

Figure 5.4 - Externally measured time signal – MD gear, full planet set

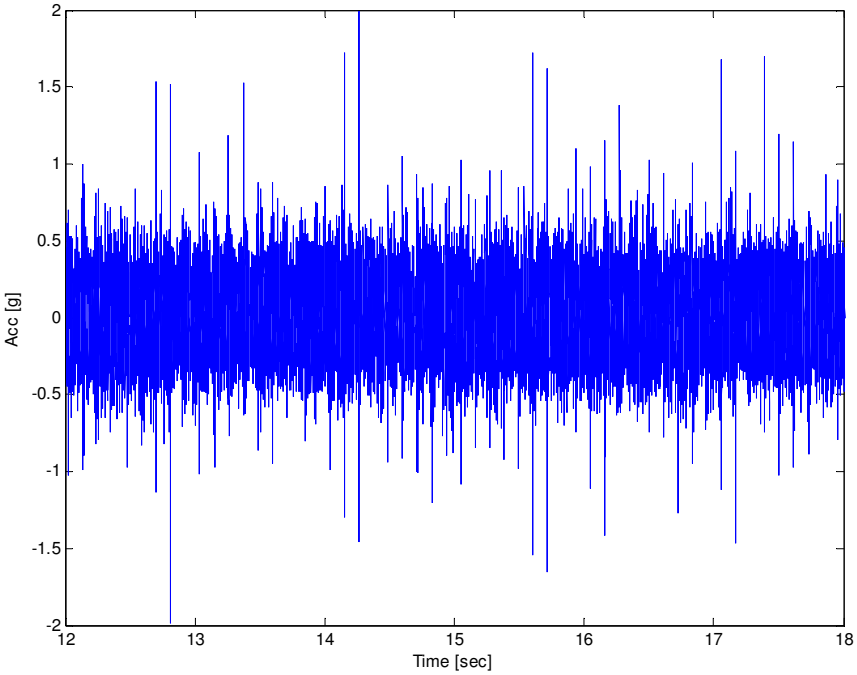

Figure 5.5 - Externally measured time signal – ED gear, full planet set

Data measured for increasing levels of damage with only a single, damaged planet gear present is shown in figures 5.6, 5.7, 5.8 and 5.9

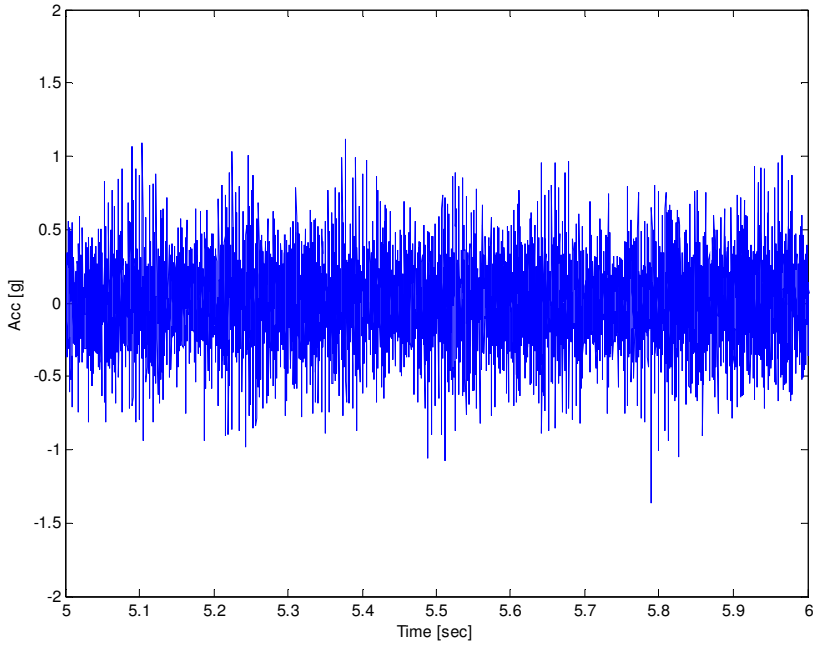

Figure 5.6 - Externally measured time signal – UD gear, single planet

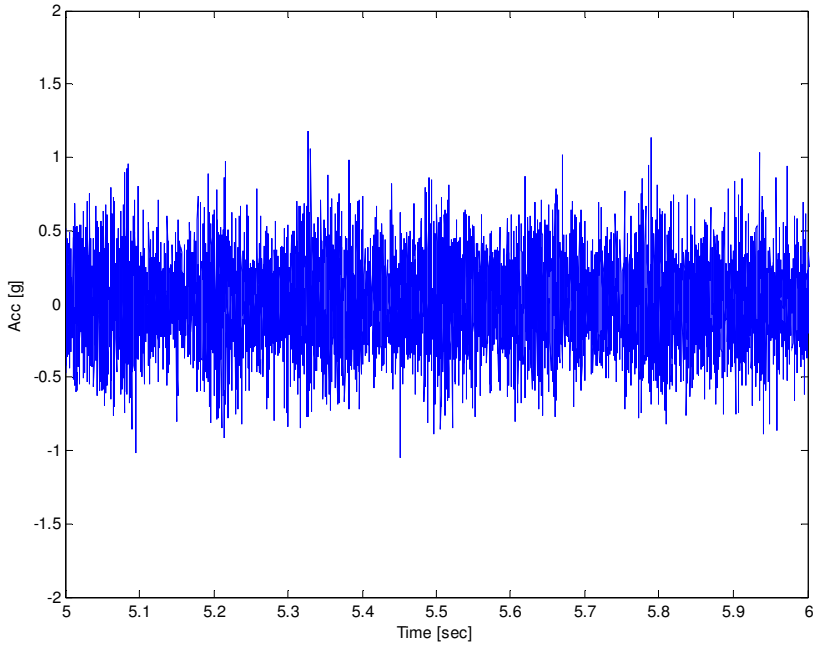

Figure 5.7 - Externally measured time signal – SD gear, single planet

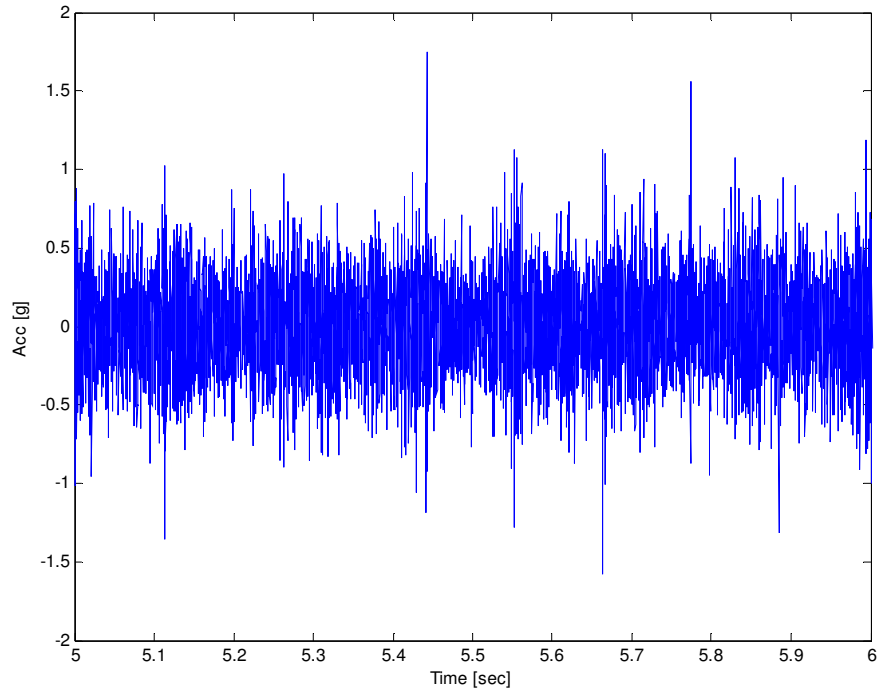

Figure 5.8 - Externally measured time signal – MD gear, single planet

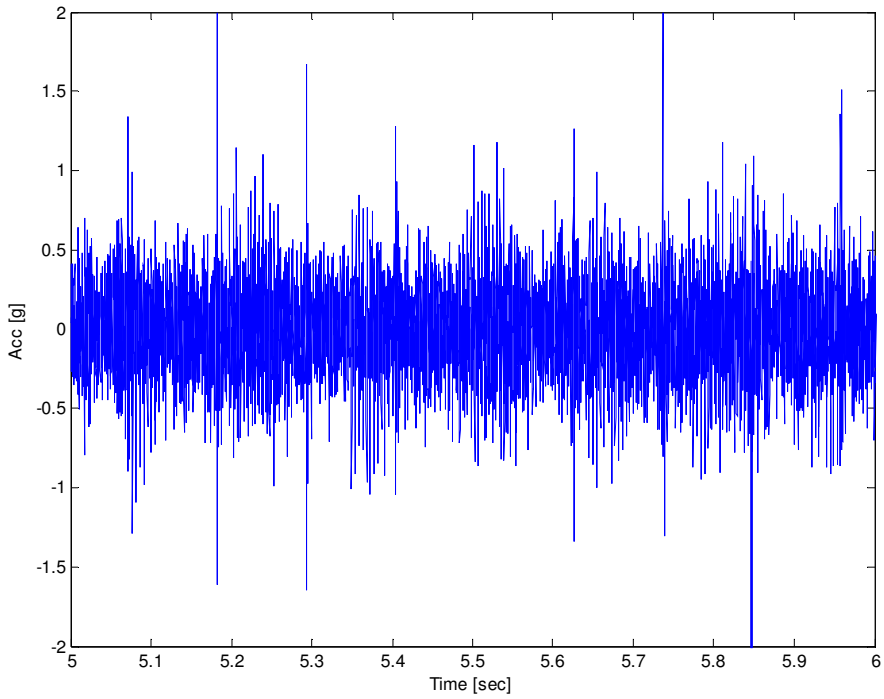

Figure 5.9 - Externally measured time signal – ED gear, single planet

For a first evaluation, the data is examined in the frequency domain. This is done by means of the power spectrum and a comparison made between the single planet gear and the complete planet gear set for each level of damage. It must be noted that the damage introduced on the gear tooth was not identical. There were variations in the angle at which damage on the gear tooth was introduced. This was for the case for slight damage and relative damage. The damaged caused for the extreme damage included tooth face damage as well as removal of a section of the tooth. If the damage was introduced by means of wear or by means of progressive material removal, the frequency domain data is expected to retain the wear signature. In this case the wear signature is expected to vary slightly across the different levels of damage.

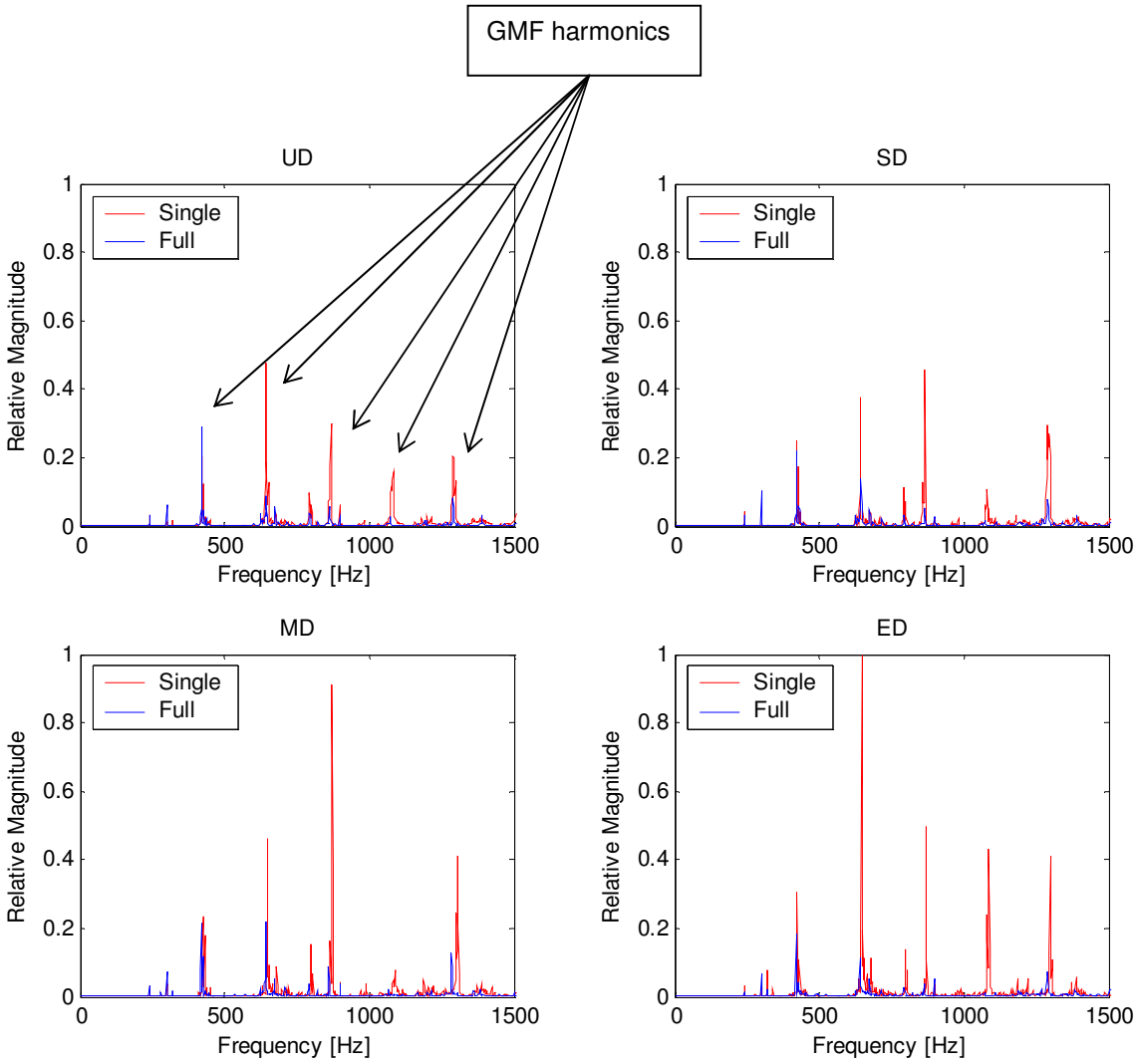

Figure 5.10 - PSD for single and multiple planet Gears

From figure 5.10 it is quite clear that there is a significant difference in the amount of energy that is seen when only a single planet gear is present as the level of damage increases. Furthermore, the harmonics of the GMF frequency are more clearly defined when there is only a single planet gear present. The harmonics for the single planet gear are clearly seen in the PSD at the indicated points. It must be recalled that direct signal averaging of epicyclic gearboxes is limited by the fact that there is relative motion between the different planets and their gear mesh points, and the accelerometer used to measure the vibration (McFadden and Howard, 1990). This causes the reduced sensitivity of the measured, multiple planet gear data, to a gear fault. Direct use of the frequency domain data is thus insufficient if used on its own. Other methods of data comparison are therefore required.

For further investigation, the planet separation technique is used on the data and the damage indicators plotted against increasing levels of damage as seen in figure 5.11. The damage indication ability of a CI is increased when a single planet gear is compared to a full planet set. This increased damage detection ability can be seen in figure 5.11. The kurtosis value for MD with a single planet gear is 36% higher than for a full set of planet gears. The single planet gear scenario yields a 99% higher value of kurtosis in comparison to the full set of planet gears when ED is evaluated. In terms of the crest factor, an increase of 37% for the MD and 32% for the ED is seen.

It is interesting to note that for a single planet gear, the effect of tooth fault transmission to the other planet gears, as discussed in paragraph 3.6, is very small. The crest factor for a full set of planet gears shows an increased sensitivity to this phenomenon. If a CI is calculated for all planet gears, from a signal measured with only a single planet gear present, no fault indication is expected on the second and third planet gear. There is a limited amount of phantom damage that can be seen in the actual data. This effect is minimal for a single planet gear with CIs showing only a small increase. For the full set of planet gears, the phantom damage effect is seen to be much higher with phantom damage clearly visible on the undamaged planet gears. Both damage indicators can be used to identify the planet gear on which a fault is located. The phenomenon of phantom damage makes identification of the damaged planet gear more complex for the crest factor than for the kurtosis value.

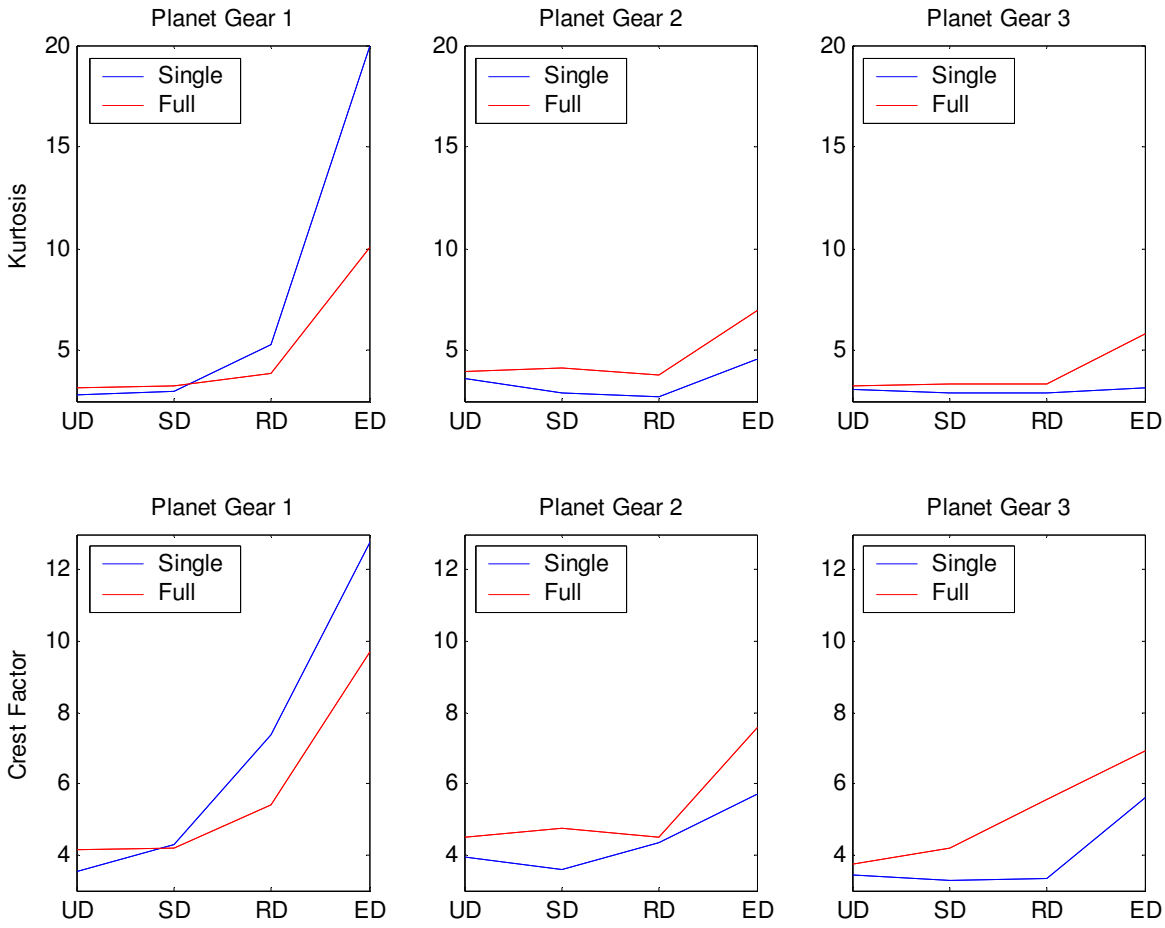

Figure 5.11 - Damage indicators for increasing levels of damage

5.1.2 Internally measured data

The cross-correlation for the two internally mounted accelerometers is given for the ED case with the full set of planet gears in figure 5.12. From this figure it is clearly seen that the data obtained from the two internally mounted accelerometers is virtually identical. The position of the accelerometer on the planet carrier is thus irrelevant, as the signal measured at any point will be the same. Figures 5.13, 5.14, 5.15 and 5.16 show the vibration signals measured internally for increasing levels of damage with a full planet set. This data was measured simultaneously with the data given in figures 5.2, 5.3, 5.4 and 5.5. The frequency content of the data measured internally is compared for single and multiple planet gears in figure 5.17. Once again it is clear that the energy associated with multiple planet gear is much higher than that of a single planet gear, as is expected.

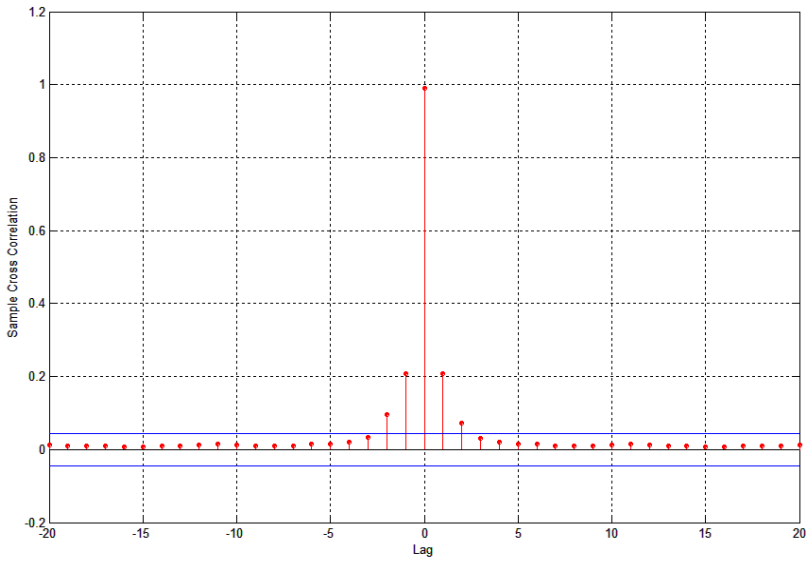

Figure 5.12 - Cross-correlation for internally mounted accelerometers

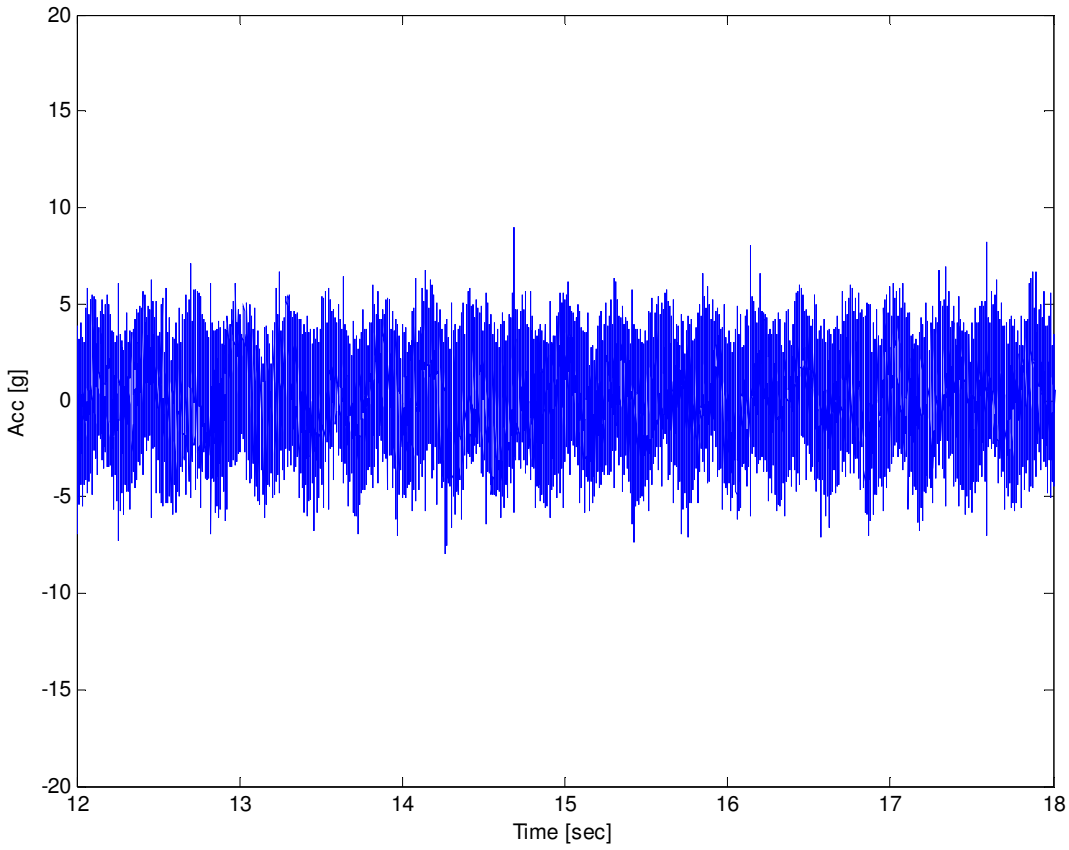

Figure 5.13 - Internally measured time signal – MD gear, full planet set

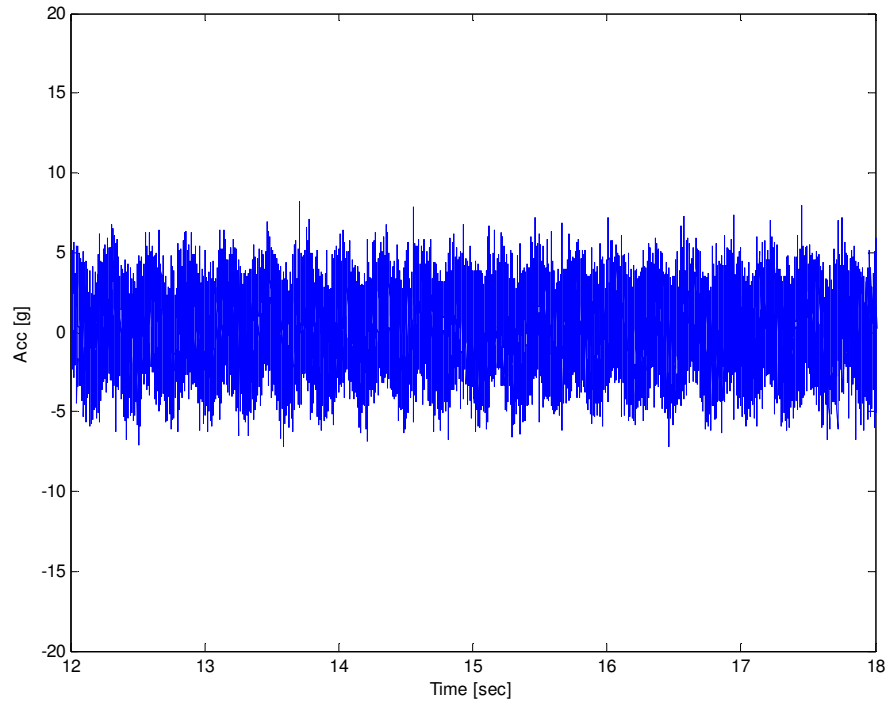

Figure 5.14 - Internally measured time signal – SD gear, full planet set

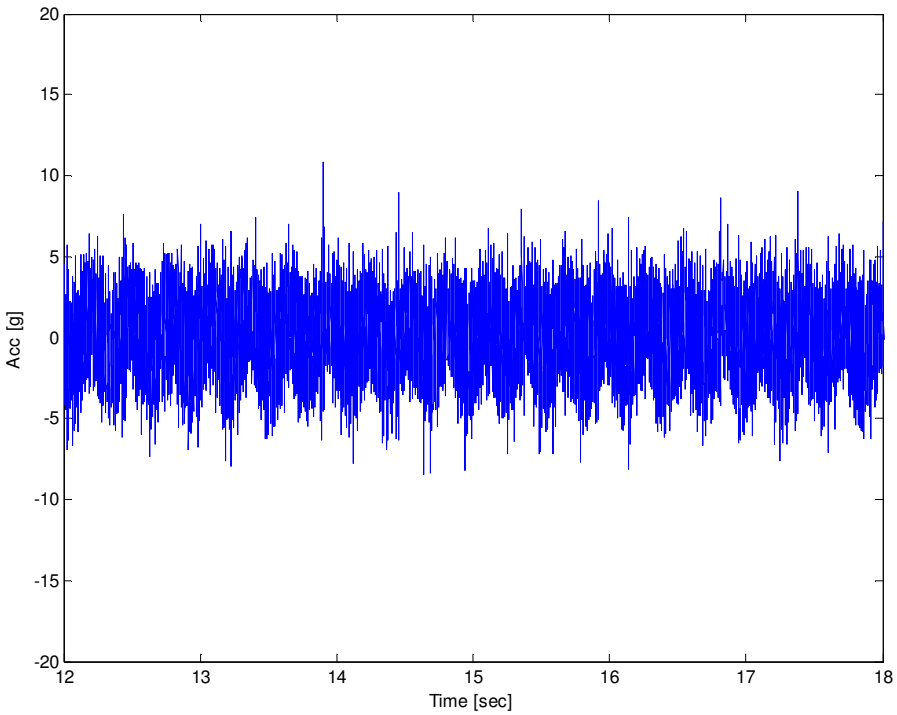

Figure 5.15 - Internally measured time signal – MD gear, full planet set

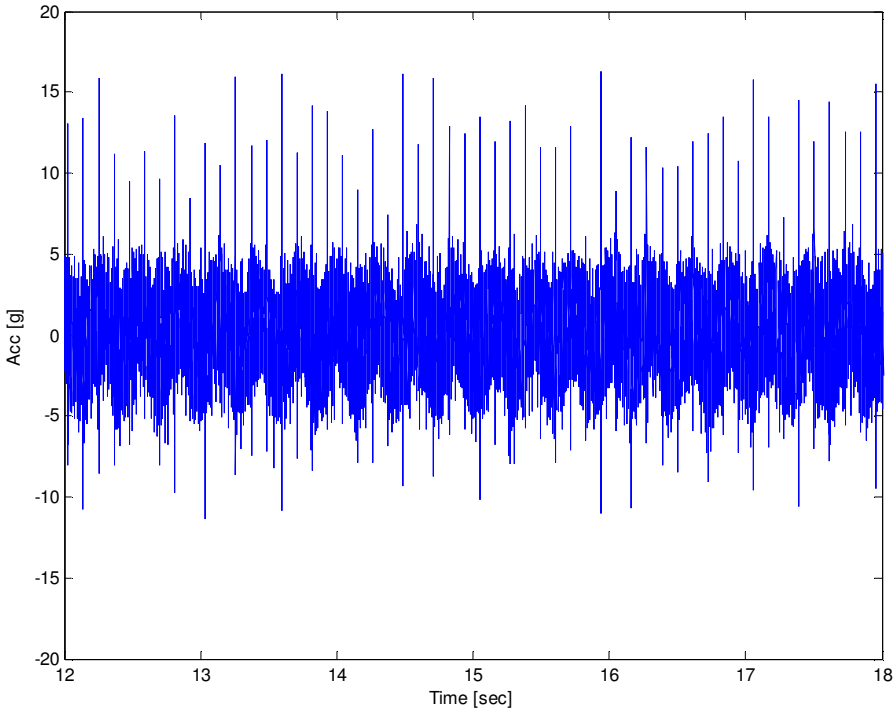

Figure 5.16 - Internally measured time signal – ED gear, full planet set

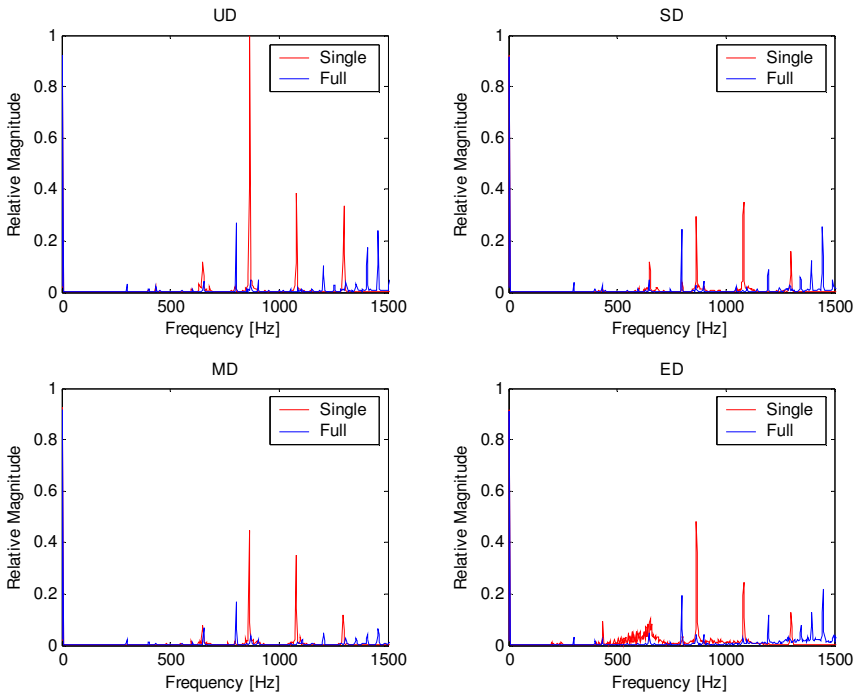

Figure 5.17 - Single and multiple planet gears for different levels of damage

5.2 Comparison of externally measured data to internally measured data

The data for the internally and externally mounted accelerometers are compared with a cross-correlation given in figure 5.18 below:

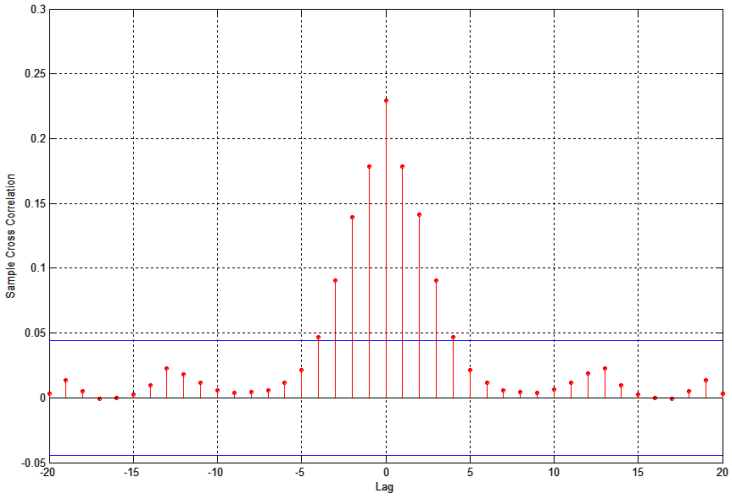

Figure 5.18 - Cross-correlation for internally and externally mounted accelerometers

The above figure shows that there is a limited amount of repeated data, in the measured data. The repeated data is limited in its contribution to the total vibration signal. Energy levels from the two sets of data are compared in terms of the RMS of the signal in figure 5.19. The RMS value of the internally measured signal is 406% larger than the RMS of the externally measured vibration signal.

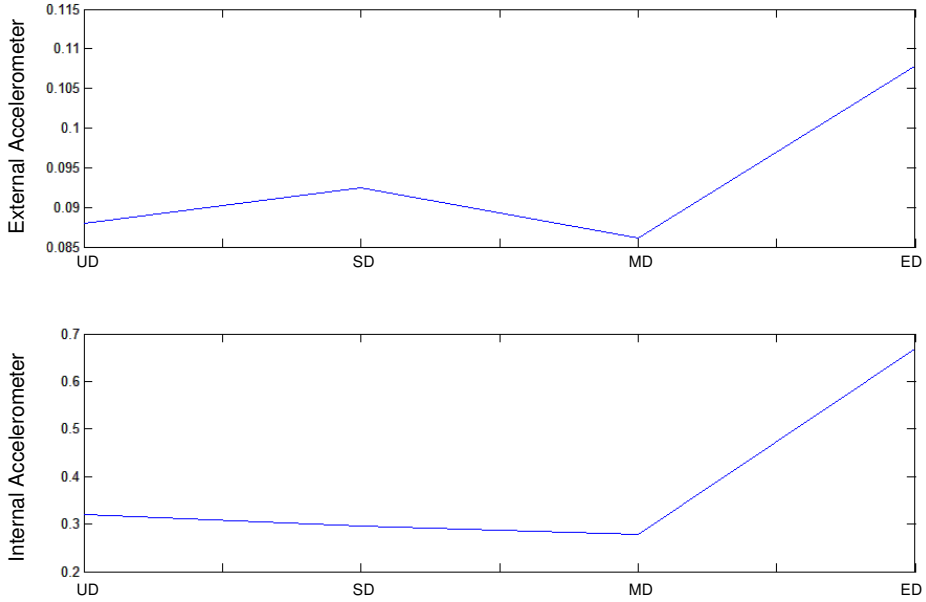

Figure 5.19 - RMS values of raw vibration data for different levels of damage

It is clear, as discussed by Heyns (2003), that the RMS is not sensitive to early faults as there is large variation in the RMS values for low levels of damage. The time signals obtained internally and externally for a full planet set with ED is shown in figure 5.20. It is clear that the externally measured data is of much lower magnitude than the internally measured data. It is also clearly seen that the impact caused by the damaged tooth is visible in both signals. This also confirms the fact that vibration caused by damage is transmitted through the entire ring gear.

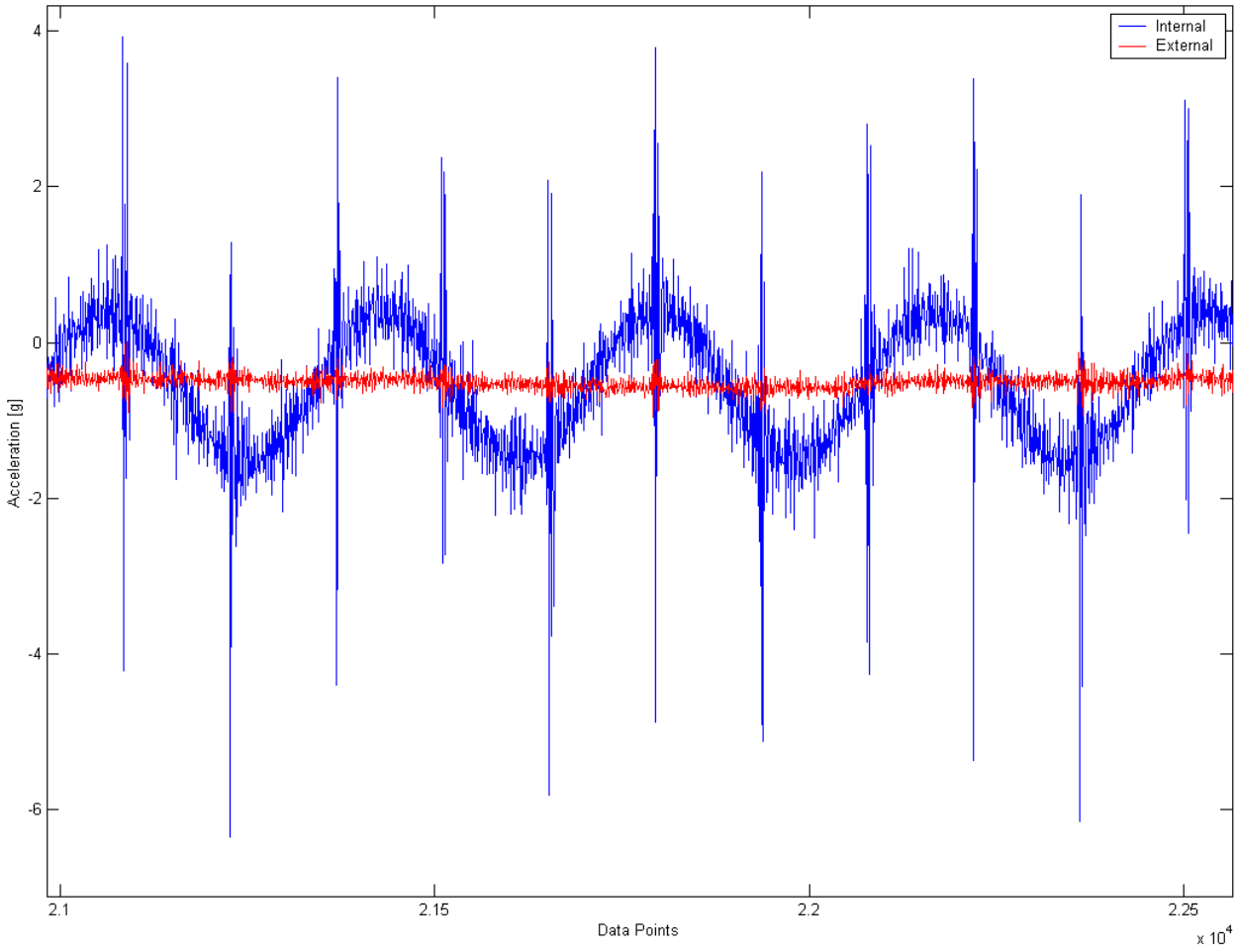

Figure 5.20 - Internally and externally measured raw vibration signal

5.3 Comparison of vibration separation algorithm to internal measurement

Before the internally measured vibration data can be directly compared to the signal generated by means of the vibration separation algorithm, the internally measured signal requires averaging. If one considers the fact the every 13th revolution of the planet carrier is a reset revolution, the

obvious point for averaging is the beginning of the reset revolution. At this point, the identical gear teeth are in mesh thus providing a repeatable signal. Furthermore, the number of averages possible is then identical to the number of averages obtained through the EpiTSA averaging technique.

Initially, a MATLAB® program was written to implement the averaging. There were however, a number of problems involved in implementing this averaging technique. The largest factor affecting the averaging was found to be very small speed variations. Small speed variation caused data indicating a fault to be offset by five to fifteen data points. One must bear in mind that a sample rate of 25 600 samples per second was used. The data extracted from the internally measured signal is shown for 4 periods which cover an entire planet gear tooth mesh sequence. The same set of gear teeth are in mesh at point 0 of each window of data. A window of data seen in figure 5.21 can also be described as a reset revolution. This is the period that it takes for identical gears to re-mesh.

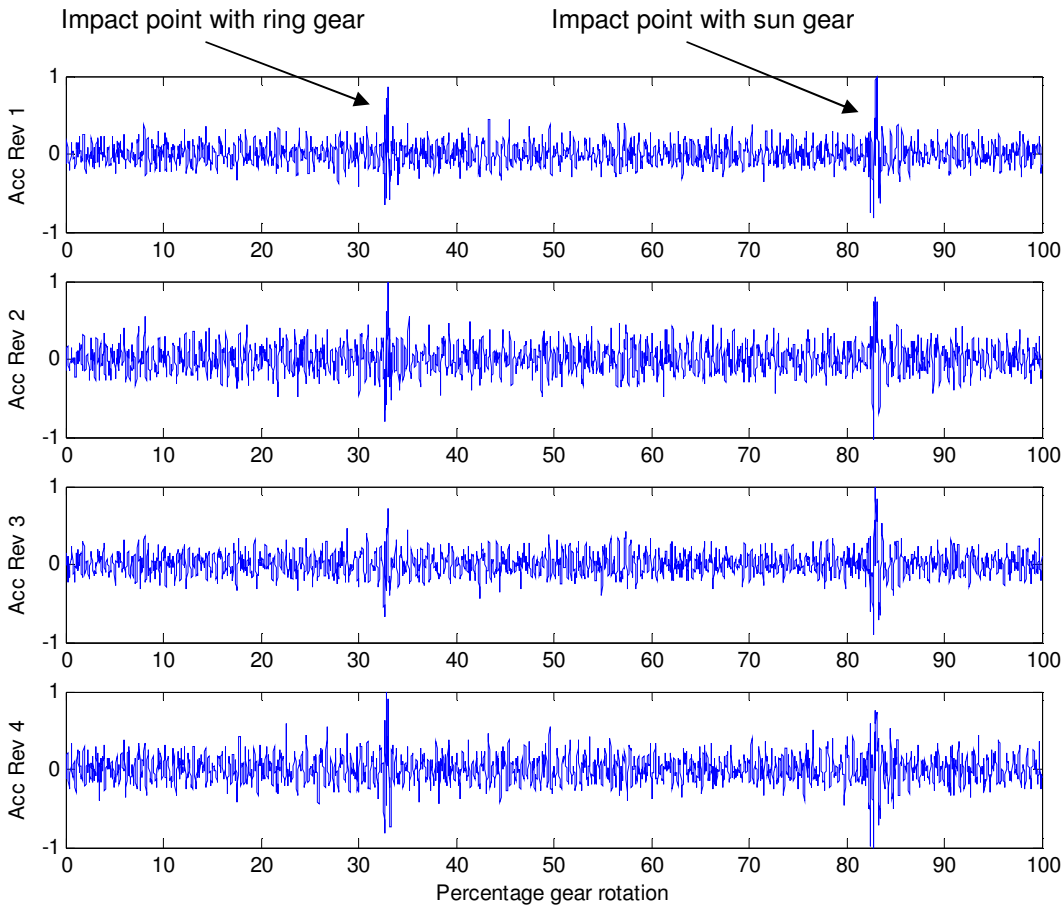

Figure 5.21 - Internally measured data for 4 reset revolutions with MD

The data was measured for a single planet gear with MD. The impact damage can be clearly seen for both the ring and sun gear. This is expected to be seen from the planet gear as the mesh from both these mesh points will be recorded as an impact in the recorded vibration signal. If the position of each peak is carefully noted by determining the exact signal point at which the peak is located, it becomes clear that there is slight movement of the peak by a few data points. The result of averaging 8 averages using the above data is seen in figure 5.22. The impact points are still visible but the amplitude thereof relative to that of the meshing floor amplitude is much lower. An adaptive modification algorithm was designed and implemented to align the peaks caused by damage. This filter was seen to work well on data that had clear damage such as that used to generate figure 5.23, and signal refinement was possible. The algorithm was unable to adjust data that was obtained from slight or no damage as it could not detect an impact point with any measure of accuracy. The algorithm would often determine the incorrect point to be the impact point. Thus, data was adjusted around an incorrect point causing corruption of the averaged data. The algorithm was discarded, as one of the fundamental issues regarding such an algorithm is its reliability in all circumstances. For direct data comparison the same signal processing must be applied to all data as this eliminates the use of the adaptive algorithm.

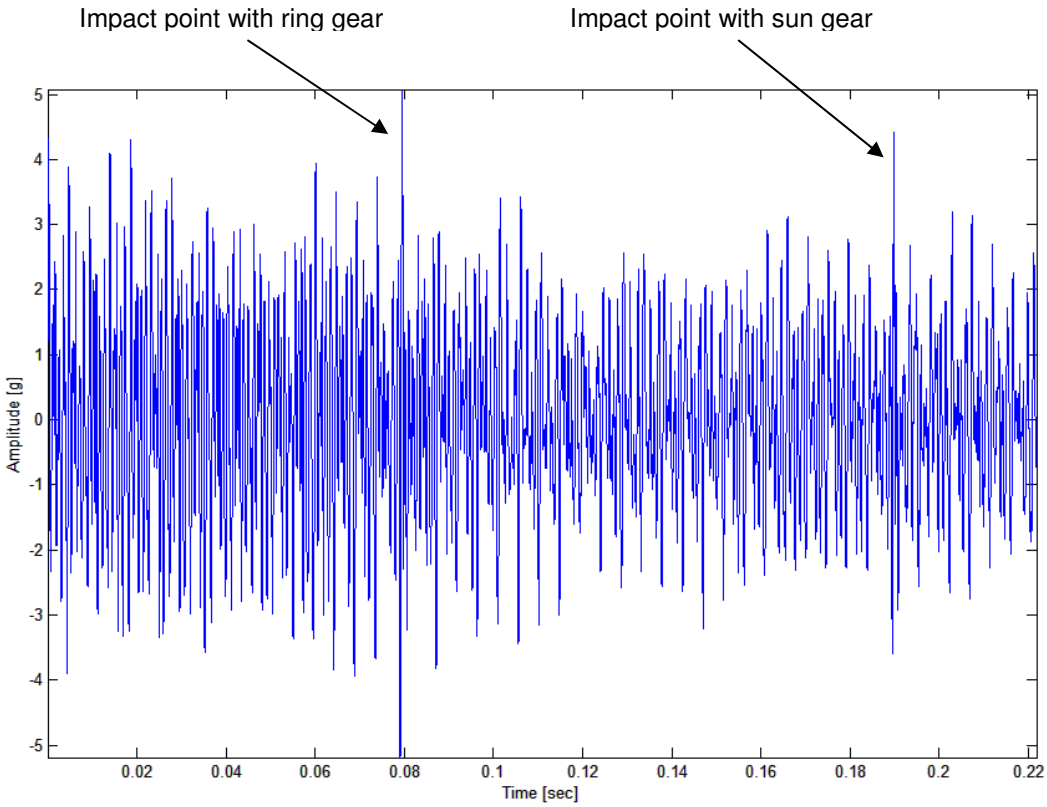

Figure 5.22 - Internally measured data for 8 averages

It was seen that the internal vibration measurements could be used to identify faults in the case of ED. This is illustrated in figure 5.23. The two peaks which indicate damage in the top plot and bottom plot are not aligned. This is due to the tooth numbering of the EpiTSA method which adjusts the data to be filled in a fixed tooth matrix while the time data is obtained directly from the accelerometer in the time domain. The data in the top plot is time domain vibration level while the data in the bottom plot is tooth domain vibration level.

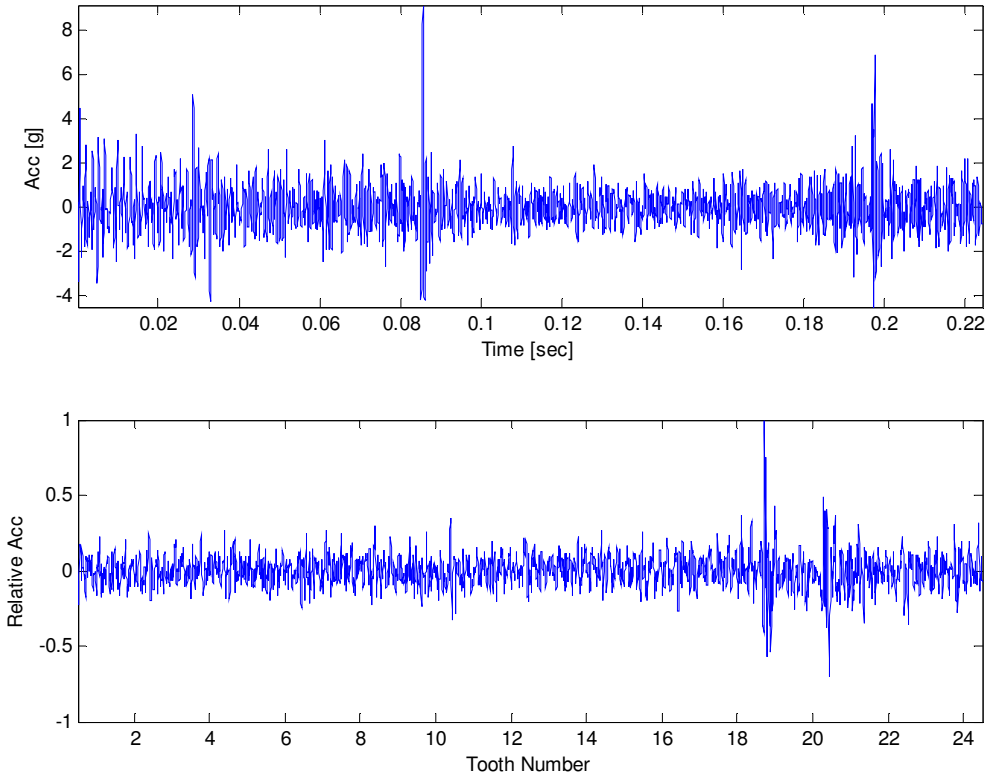

Figure 5.23 - Internally measured time signal and EpiTSA signal for ED

Internally measured vibration data for a full planet set is compared for increasing levels of damage in figure 5.24, while figure 5.25 compares increasing levels of damage for the EpiTSA method. Both figures illustrate the limited damage detection ability of vibration measurement on epicyclic gearboxes. When the signals obtained using the planet gear that had slight damage is compared, both the internal as well as the EpiTSA method fail to clearly illustrate the damage. The reduced detection ability of both methods is also evident when the CI's are compared to each other. In the case of moderate damage both methods illustrate the damage. The internal measurement gives a clearer indication of the damage than the data obtained from the EpiTSA method.

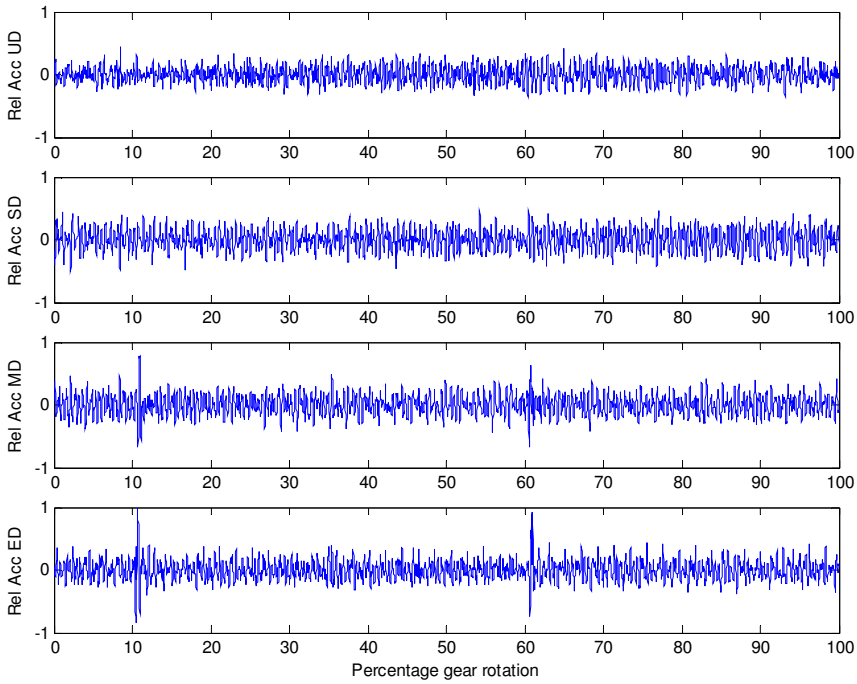

Figure 5.24 - Internally measured signal for increasing levels of damage

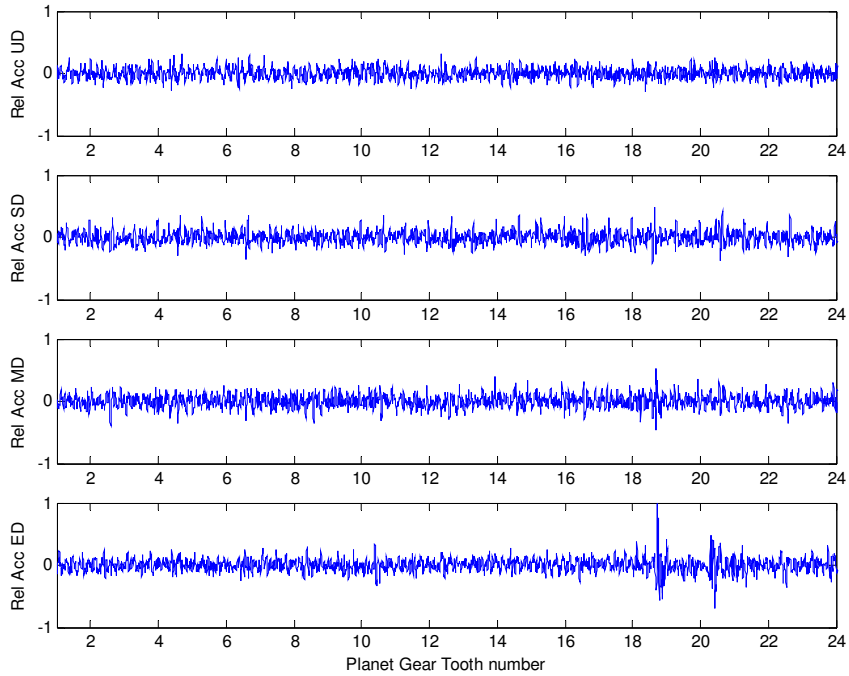

Figure 5.25 - EpiTSA for increasing levels of damage

An alternative to calculating the CIs for the averaged vibration data obtained from the internal vibration measurement involves the determination of the CI for each rotational period of the epicyclic gear. These CIs are then stored and can then be used for further processing. This method has the advantage of obtaining CIs from data with minimal raw data processing. The CIs obtained from each window give a true reflection of the level of damage from the small segment of vibration signal. As discussed and shown in figure 5.22, the level of impulsivity of the raw signal is reduced during the averaging process. Thus, a CI obtained from this data will show a reduced sensitivity to damage. The optimum approach involves the recording of the CI for each window of data obtained during the averaging process.

Once the CIs for each window of data have been determined, different approaches can again be followed to obtain an overall CI which is to be evaluated as representative of the condition of the gearbox under investigation. There are two methods that can be employed to calculate the CIs required for a comparison between the internally measured data and the EpiTSA signal. As discussed earlier, the CIs are determined and recorded for each window of data under investigation. The recorded CI values can then either be averaged across the entire range of determined values or the maximum indicator value obtained during the period under investigation can be used. The results of both methods are compared to the EpiTSA values for the same data set in figure 5.26. The RMS values were not used for comparison purposes. This is due to the fact that the RMS values for the internally mounted accelerometers are in the region of 20 times higher than the EpiTSA signal. Direct comparison is highly complex due to the fact that the RMS values remain fairly constant, thus decreasing the fault identification ability of this indicator. When this is combined with a large deviation in energy levels between the internal and externally measured data, direct comparison is not advisable.

When the data from the planetary gearbox measurements is evaluated for the single gear case as in figure 5.26, it must be noted that the single planetary gear is a special case and cannot be used in a fully operational gearbox. If the kurtosis value for the single gear case is evaluated it is clear that the EpiTSA method is effective in determining increasing levels of damage. Both the average and maximum kurtosis value are in order levels of the same magnitude, but show decreased sensitivity to increasing damage, thus neither approach has a significant advantage over the other. The EpiTSA method values for ED are in the region of 330% higher than for the internally measured kurtosis value. This phenomenon is only for the single planet gear situation. Once a full planet gear is evaluated, the EpiTSA method is equaled and slightly outperformed by the internal measurement method.

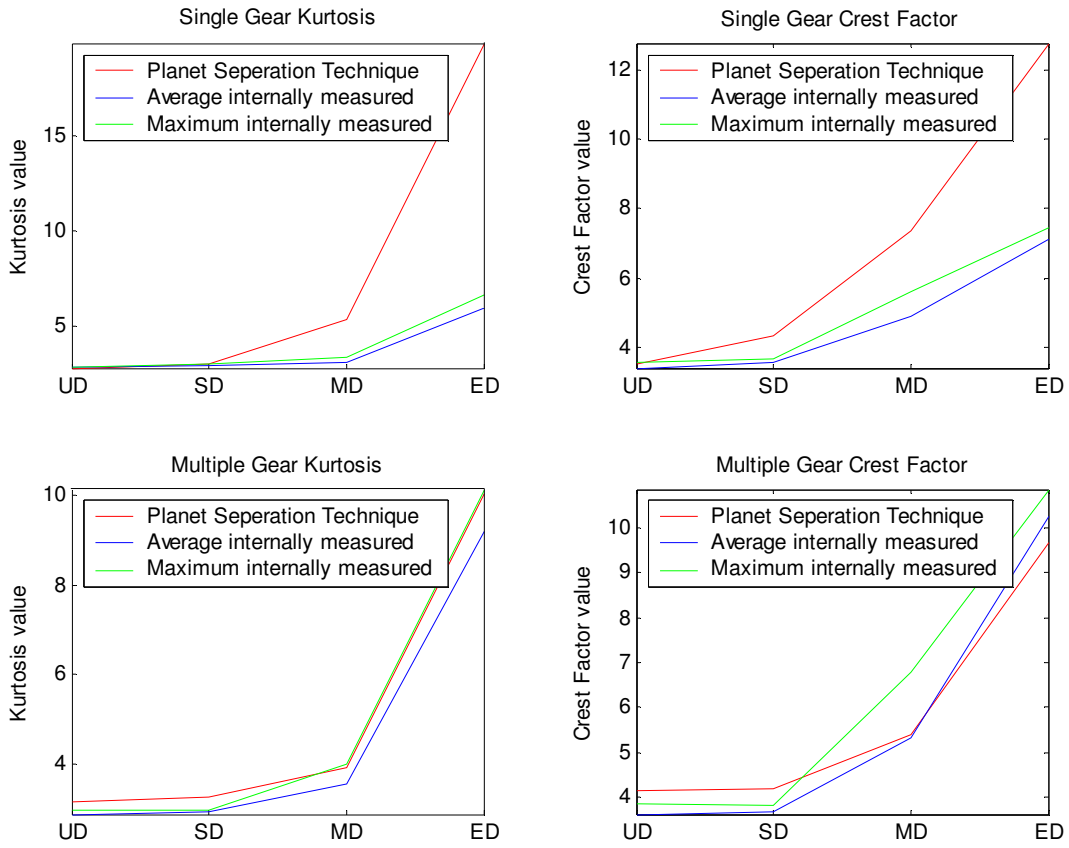

Figure 5.26 - DI comparison for EpiTSA signal and internally measured data

The crest factor for the single gear shows again that the EpiTSA method is more effective at determining increasing levels of damage. It must be noted that the margin of variation is much lower than for the kurtosis value. The crest factor obtained from the internally measured data by both averaging, as well as for the maximum value, is able to predict increasing levels of damage. Thus, the internally measured data, as well as the EpiTSA, can be used to determine increasing damage for the single planet gear.

The evaluation of the CIs for multiple planet gears is of more interest to this work than the single planet gear application. This method most accurately reflects the case of an operational gearbox. From figure 5.26 for the multiple gear kurtosis, it is immediately apparent that the damage indication from the maximum kurtosis value for the internally measured data is on par with the measurements obtained by the EpiTSA method. The average kurtosis value gives a similar indication of damage as the other two methods. A clear indication of increasing levels of damage can be seen, making

this approach suitable for damage determination. The evaluation of the multiple gear crest factor illustrates an interesting situation. The maximum crest factor is seen to supersede the EpiTSA method for fault determination with the average crest factor giving a higher indication of extreme damage than the EpiTSA.

It is thus clear from the evaluation of the results that the method of internal vibration measurement is as successful in determining damage in an epicyclic gearbox as the EpiTSA method. The EpiTSA method is a well-known and widely used method for applying vibration measurement to determine the damage level of an epicyclic gearbox. This confirms that the internal measurement of vibration data on an epicyclic gearbox is able to accurately predict damage levels on such a gearbox. It is also clear that the internally measured vibration data is more effective at determining damage for an entire planet gear set than for a single planet gear. Although the single planet gear application is not likely to arise in operational use of an epicyclic gearbox, it is an important observation from a research perspective.

Chapter 6 - Conclusions

6.1 Internal vibration measurement of epicyclic gearboxes

A new method to directly measure vibration data of an epicyclic gearbox is suggested. This method was successful implemented by means of accelerometers internally mounted on the planet carrier. One of the major issues restricting direct vibration monitoring of epicyclic gearboxes is the relative movement of the planet gear to the transducer. The internal measurement technique eliminates this issue by allowing the transducer to rotate on the planet carrier itself. This means that there is no relative motion between the transducer and the planet gear.

This technique can successfully be used as a method to directly measure vibration levels on epicyclic gearboxes. This method provides an alternative technique that does not require complex data extraction. Implementation of this technique using current sensor technology is intricate and limits operation of the gearbox. It is clear that as sensor technology improves this measurement technique can become an attractive alternative to epicyclic gearbox vibration monitoring.

6.2 Planet separation technique versus internally measured vibration data

As illustrated, the internal measurement of vibration data and the associated processing of the data is able to accurately capture degradation of an epicyclic gearbox. The condition indicators of the epicyclic gearbox obtained from internal measurement were compared to condition indicators calculated using recognized techniques on data obtained from the same gearbox under the same damage conditions. The internal measurement method was therefore verified as an acceptable method to determine degradation of an epicyclic gearbox. Although one would intuitively expect this result, this method has not been explored before.

The greatest advantage of an internal measurement approach is that the conversion of the raw data to useful damage indicators is simplified and does not require complex post-processing of the data, as is the case for the EpiTSA method.

There are a number of restrictions on the use of internal measurement on epicyclic gearboxes. The most important of these is the specialized modification of the gearbox itself as well as the shaft that

is required to install accelerometers internally. These modifications necessitate the modification of the shaft, thus reducing the strength of the shaft itself, as well as generating the possibility of leakage of the gearbox lubricant. The planet carrier requires modification which reduces the strength of the carrier. Slip rings and accelerometer amplification devices have to be installed which restrict the use of the gearbox to low rotational speed. Accelerometers and associated cabling rotate internally in the gearbox, thus risking damage to the accelerometers and gearbox. The averaging process of internally measured data is extremely susceptible to even the slightest speed fluctuation. This problem can be overcome by means of data processing. The effort, time and money required to modify the gearbox makes it a very unattractive option for practical implementation.

Taking all these factors into consideration, it is clear that internal vibration measurements can be used to determine increasing damage of an epicyclic gearbox. The technique was shown to equal, and in certain circumstances, supersede the effectiveness of recognized vibration monitoring techniques in determining levels of damage by means of condition indicators.

The fields of wireless communication and telemetry are continually developing. It is quite reasonable that the combination of sensors and wireless transmitters will be launched in the near future. As soon as this occurs, the internal measurement of epicyclic gearboxes in practical applications can become a reality. A wireless accelerometer can be mounted in an operational epicyclic gearbox. Direct measurement within the gearbox is then possible. The technique has been shown to yield accurate results and data obtained by this means requires minimal post processing.

6.3 Single planet gear measurements

Damage indicators for a gearbox containing only a single planet gear have a far greater ability to detect a fault on a planet gear. All damage indicators show is a clear, increasing trend, as damage levels increase. This is evident when even the most simple of damage indicators is evaluated. The monitoring of a single planet gear simplifies the complexity of a planetary gearbox. This is due to one of the factors complicating the measurement of the gearbox, this being the identical gear mesh vibration caused by multiple planet gears in mesh simultaneously, is removed from the measurement. Vibration measured by a transducer, originates from the single planet gear in mesh. This measurement may be useful for individual planet gear testing, to determine the quality of the

gear or if there is damage present. This could only be applied in a specialized situation where gear quality is critical to the application, for example aircraft planetary gearboxes. The vibration level from a single gear can be measured in a dedicated single planet gear test bench. A CI can be allocated to the measured gear. If the CI is over a predetermined limit, the gear can be rejected. Alternatively, planet gears from the same planetary set can be compared using CIs to evaluate if one of the gears in the set is damaged. This method can be used extensively in the aeronautical industry.

6.4 Phantom damage

Phantom damage was visible on the planet gear signal developed for the undamaged planet gears. This phantom damage was visible even when no planet gear was present. In their research work, Samuel, Joseph and Pines (2004), detect this phantom damage and report it as corruption on the vibration signal of the undamaged planet, which they said, requires further study. It became clear during investigation of the gearbox and comparison of raw time domain signals that there is a distinct transfer of high vibration levels associated with damage to the undamaged planet gear. This serves as an explanation of the finding of Samuel et al. and the phantom damage phenomenon is thus confirmed as one of the potential dangers of implementation of the planet separation technique.

6.5 Torque sensitivity

During the initial investigation of the epicyclic gearbox, torque sensitivity of the gearbox was repeatedly raised as an important issue with planetary gearboxes. Mike Hoeper from Flender commented on this issue during personal discussions regarding epicyclic gearboxes. Keller and Grabill (2003), in their research work, confirmed that the vibration levels of an epicyclic gearbox are extremely load sensitive. The effectivity of the different fault diagnostic techniques was clearly seen to increase as loads increase. Keller and Grabill point out that the CIs used could only identify faults at high torque loads. This was clearly seen in the levels of indicators used in this research. This is an important point when one evaluates epicyclic gearboxes. Low torque levels can easily conceal gear faults.

6.6 Suppression of the gear mesh frequency

McFadden and Smith (1985) as well as McNames (2002) show that for multiple planet gears there will, under certain circumstances, be suppression of the GMF with asymmetry of the sidebands. These findings are easily confirmed when the data from the gearbox is evaluated. McNames continues to state that the PPF will be the fundamental frequency in frequency spectrum should GMF suppression occur. This would confirm the assumption of Raithby and Baillie (2004) regarding the findings of their investigation. The PPF of the gearbox under investigation could, however, not be seen in the frequency domain. The calibration certificate for the accelerometers used in this investigation give the error percentage at 10Hz as -0.3%. The PPF is thus expected to be seen in the frequency domain. The third harmonic of the GMF frequency is evident for all measurements even where there is no damage present. This is another acceptable frequency that should be measurable according to McFadden and Smith.

McFadden and Smith state that for a single planetary gear, symmetrical sidebands around the tooth mesh frequency occur. In the gearbox under investigation, the GMF was not visible as a clear peak when only a single planet gear was present. It seems to be possible that due to vibration being transmitted through the ring gear and then averaged, the effect of GMF suppression will still be evident even when only a single planet gear is present. This effect will require further investigation before it can be stated with any authority. No literature was found relating to practical investigation regarding measurement of data from a single planet gear mounted on a planet carrier.

Chapter 7 - Further Research Possibilities

7.1 Investigation of single planet condition monitoring

The use of a specialized test rig to quantify damage or verify non-damage of individual planet gears has interesting applications. Certain applications of epicyclic gearboxes, such as the aeronautical industry, cannot allow the use of suspect or damaged gears due to the criticality of the gears. In such applications it would be desirable if individual gears could be tested, especially if the gearbox has sustained damage in other areas and where there is the possibility of damage to the epicyclic gearbox. The gears can then be qualified as undamaged and returned to service or withdrawn from service.

Alternatively, quantification of levels of damage of an epicyclic gearbox may be required during research activities. A dedicated test rig can be used to evaluate individual planet gears and assign degradation levels to individual gears. In this way, the effect that a damaged planet gear has on the remaining planet gears can be investigated. This information is important as no indication of the interdependence and transmission of damage for planet gears could be found in the literature.

Discussions with interested parties in the aeronautical industry have suggested that a testing method for individual planet gears would increase the reliability of gearboxes which have been repaired or re-built, as gears could be tested and certified before installation. This would be of special importance in the aeronautical industry where validation of components is required prior to them being installed in an aircraft.

This specific application for individual gear testing would not be used in an operational gearbox but for specific testing.

7.2 Use of EpiTSA under varying speed and load conditions

The EpiTSA algorithm developed and used for this research is limited to constant speed conditions. As this algorithm makes use of synchronous averaging, it can be expanded to varying speed conditions. Expansion of this algorithm is made more complex by that fact that there are multiple gears in mesh that must be monitored simultaneously. The ability to use the EpiTSA algorithm under varying speed conditions would prove very useful in the industrial environment where speed cannot always be held constant.

7.3 Other possible measurement methods

The measurement used for the current research is based on the use of accelerometers as sensors for the detection of vibration. Alternative methods of vibration monitoring can be investigated. Some of the methods were evaluated, but due to complexities involved, it was decided not to pursue the investigation further. These methods may however, provide better results for internal measurement than the accelerometer used with slip rings if the implementation thereof can be simplified or made possible.

As accelerometer and Bluetooth technology improve, the production of an accelerometer connected to a Bluetooth transmitter, using kinetic energy as a power source, is becoming increasingly more likely. This would provide an ideal solution to this problem of internal monitoring but is currently not a viable solution as no such sensor exists. As soon as this technology becomes available, internal measurement of an epicyclic gearbox immediately becomes an excellent tool for gearbox monitoring even in industrial applications.

A possible alternative to an accelerometer is a laser velocimeter which can be used through a window in the gearbox. The problem with this approach on an epicyclic gearbox is that the laser will have to rotate with the shaft or make use of a mirror to rotate. The rotation of the laser head with the shaft is not advisable as the chance of damage to the equipment is very high. It is for this reason that a laser velocimeter was not used for the current research. The use of a mirror with a laser beam is possible under limited situations. To make it possible to use the laser a hollow shaft with end access is required. This has a number of problems including the fact that the lubricating oil cannot be retained in the gearbox but would simply run out of the hollow shaft. Furthermore, a hollow shaft may affect the maximum torque transmission of the shaft as has been discussed. The final drive to the load source can also not be placed over the end of the hollow shaft. Thus a belt, chain or similar drive is required to attach the load to the gearbox. Under laboratory conditions the use of a laser beam with mirrors can be investigated.

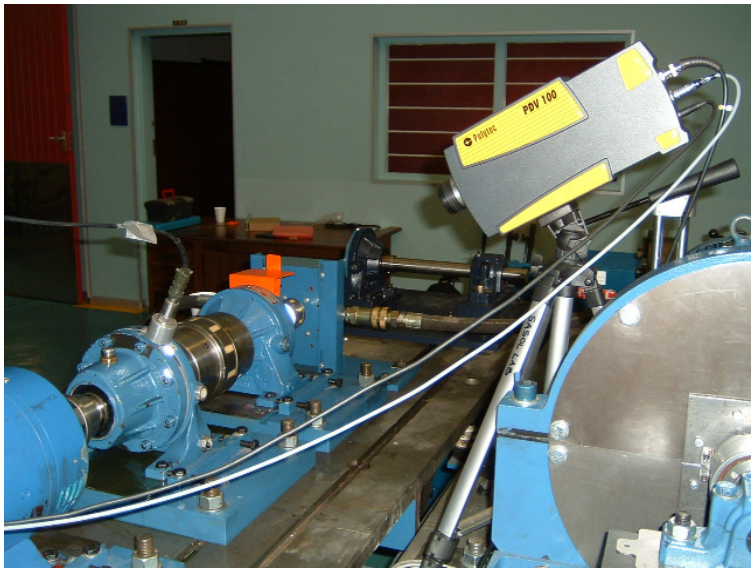

Figure 7.1 - Laser velocimeter usage

Testing on the epicyclic gearbox using a laser was performed as seen in figure 7.1. The laser velocimeter was used and data compared to data obtained from an accelerometer. It became clear that at low frequencies the laser velocimeter gave far superior results to accelerometers. Due to the fact that many of the frequencies expected to be found on the Bonfiglioli gearbox are at very low frequencies, the increased frequency resolution at low frequencies would provide a distinct advantage. The problem with the application of laser measurement is that two laser velocimeters are required to accurately measure the vibration data from the gearbox. This poses two problems.

a. The cost of a laser velocimeter is very high. Two units are required which simply doubles the costs involved in monitoring a gearbox. This method can thus be investigated if suitable funding is available.

b. The use of a laser raises repeatability issues. The accelerometers used during this investigation were stud mounted at positions that were pre-determined. The positions could not be altered or moved in any way. As seen in figure 7.1 the laser head is mounted on a tri-pod. This means that the exact positions of measurement can vary. This problem can be managed if care is taken to always ensure the positioning of the lasers is exact and the same positions used during each measurement.

Chapter 8 - References

Bonfiglioli Riduttori S.p.A (Eds) (1995). Gear Motor Handbook. *Springer-Verlag Berlin Heidelberg*

Buyukataman K. & Kazerounian K. (1994) Critical Vibration of Aircraft Epicyclic Gear Systems. *30th AIAA/ASME/SAE/ASEE Joint Propulsion Conference, Indianapolis, IN, 27-29 June 1994*

Crawford A.R. & Crawford S. (1992). *The Simplified Handbook of Vibration Analysis – Volume 1.* Computational Systems, Incorporated (CSI) Knoxville, TN 37932

Decker H.J. (2002). Crack Detection for Aerospace Quality Spur Gears. *Report ARL-TR-2682 and NASA/TM-2002-211492 April 2002*

Decker H.J. & Lewicki D.G. (2003). Spiral Bevel Pinion Crack Detection in a Helicopter Gearbox. *Report ARL-TR-2958 and NASA/TM-2003-212327 June 2003*

Flender Bocholt. (n.d.) Planetengetriebe. [Planetary Gears] *Bocholt*

Forrester D. & Blunt D. (2003). Analysis of Epicyclic Gearbox Vibration. *HUMS2003 CD-ROM* [CD]

Goldman S. (1999). Vibration Spectrum Analysis 2nd edition. *New York: Industrial Press Inc.*

Heyns P.S. (2003). Mechanical Vibration Measurement and Analysis. Vibrations MEV732. *University of Pretoria*

Howard I.M. (1990). Epicyclic Transmission Fault Detection by Vibration Analysis. *Australian vibration and noise conference 1990 : Vibration and noise – measurement, prediction and control ; Melbourne, 18-20 September*

Howard I. (1995). Vibration signal processing using MATLAB®. *Acoustics Australia, Journal of the Australian Acoustical Society, April 1995, Vol 23, No. 1, pp 9 -13*

Kahraman A. (2001). Free torsional vibration characteristics of compound planetary gear sets. *Mechanism and Machine Theory 36*

Keller J.A. & Grabill P. (2003). Vibration Monitoring of UH-60A Main Transmission Planetary Carrier Fault. *Proceedings of the American Helicopter Society, 59th Annual Forum, Phoenix, Arizona, May 6 – 8, 2003*

Lai E. (2004). Practical Digital Signal Processing for Engineers and Technicians. *Great Britain: Newnes*

Lobato A. (27 March 2004). Personal discussion. Director Helitune Limited. Hatchmoor Industrial Estate, Torrington Devon

McAdams D.A. & Tumer I.Y. (2002). Towards Failure Modeling in Complex Dynamic Systems: Impact of Design and Manufacturing Variations. *Proceedings of 2002 ASME Design Engineering Technical Conferences; Montreal, Quebec, Canada, 29 September – 2 October*

McFadden P.D. (1987). Examination of a Technique for the Early Detection of Failure in Gears by Signal Processing of the Time Domain Average of the Meshing Vibration. *Mechanical Systems and Signal Processing, 1987, 1(2), pp 173-183*

McFadden P.D. (1990). Time Frequency Domain Analysis of Vibration Signatures for Machinery Diagnostics. *Department of Engineering Science Oxford University, 1990*

McFadden P.D. (1994). Window Functions for the Calculation of the Time Domain Averages of the Vibration of the Individual Planet Gears and Sun Gear in an Epicyclic Gearbox. *Journal of Vibration and Acoustics, April 1994, Vol. 116 / 179*

McFadden P.D. & Howard I.M. (1990). The detection of seeded faults in an epicyclic gearbox by signal averaging of the vibration. *Propulsion Report 183, Defence Science and Technology Organisation, Aeronautical Research Laboratory*

McFadden P.D. & Smith J.D. (1985). An explanation for the asymmetry of the modulation sidebands about the tooth meshing frequency in epicyclic gear vibration. *Proceedings of the Institute of Mechanical Engineers. 1985, Volume 199, pp 65-70*

McInerny S.A., Hardman B., Keller, J.A. & Bednarczyk R. (2003). Detection of a Cracked-Planet Carrier. *Proceedings of the 10th International Congress on Sound and Vibration, Stockholm, Sweden, July 7 – 10 July 2003*

McNames J. (2002). Fourier Series Analysis of Epicyclic Gearbox Vibration. *Journal of Vibration and Acoustics, Technical Briefs. January 2002, Vol 124 pp 150-152*

Meltzer G. & Ivanov Y.Y. (2003). Fault Detection in Gear Drives with Non-Stationary Rotational Speed – Part 1 The Time-Frequency Approach. *Mechanical Systems and Signal Processing (2003) 17(5) pg 1033-1047*

Meltzer G. & Ivanov Y.Y. (2003). Fault Detection in Gear Drives with Non-Stationary Rotational Speed – Part 2 The Time-Quefrency Approach. *Mechanical Systems and Signal Processing (2003) 17(2) pg 273-283*

Mosher M., Pryor A.H. & Huff E.M. (2002). Evaluation of Standard Gear Metrics in Helicopter Flight Operations. *Proceedings of the 56th Mechanical Failure Prevention Technology Conference, Virginia Beach, VA, April 15 – 19, 2002*

Parker R.G. (2000). A Physical Explanation for the Effectiveness of Planet Phasing to Suppress Planetary Gear Vibration. *Journal of Sound and Vibration, 236(4), pp 561-573*

Polyshchuk V.V., Choy F.K. & Braun (2002). Gear Fault Detection with Time-Frequency Based Parameter NP4. *International Journal of Rotating Machinery, 8(1): 57-70*

Raithby S.D. & Baillie A.S. (2004). Vibration Analysis Diagnostics Reduction Gearbox S/N AGO25440. *Integrated health monitoring Vibration Analysis Diagnostic Report, Report # 05/04, 7 June 2004*

Samuel P.D., Conroy J.K. & Pines D.J. (2004). Planetary Transmission Diagnostics. *Report E-14544 and Nasa/CR-2004-213068 May 2004*

Samuel P.D. & Pines D.J. (2001). Classifying Helicopter Gearbox Faults using a Normalized Energy Metric. *Smart Materials and Structures – Institute of Physics Publishing 10 (2001) pg 145 – 153*

Samuel P.D. & Pines D.J. (2004). A review of vibration-based techniques for helicopter transmission diagnostics. *Journal of Sound and Vibration (in press)*
Samuel P.D. & Pines D.J. (2003). A Planetary Gearbox Diagnostic Technique using Constrained Adaptive Lifting. Proceedings of the HUMS2003 – DSTO International Conference on Health and Usage Monitoring, Melbourne, Australia, 17-18 February 2003

Schőn P.P. (2004). Unconditionally convergent time domain adaptive and time-frequency techniques for epicyclic gearbox vibration. *Unpublished dissertation. Pretoria: University of Pretoria*

Stander, C.J., Heyns P.S. & Schoombie W. (2002). Using vibration monitoring for local fault detection on gears operating under fluctuating load conditions. *Mechanical Systems and Signal Processing,* 16(6)

Taylor J.I. (1994). *The Vibration Analysis Handbook*. Vibration Consultants, Inc. Tampa, FL 33611

Wilke D.N., Kok S. & Groenwold A.A. (2005). Particle Swarm Optimization Part I: Notes on diversity *Article submitted November 2005*

Wu B., Saxena A., Khawaja T.S., Patrick R. & Vachtsevanos G. (2004) An Approach to Fault Diagnosis of Helicopter Planetary Gears. *School of Electrical & Computer Engineering, Georgia Institute of Technology, Atlanta, Georgia 30332-0250, 404-894-4132*

Wu B., Saxena A., Patrick R. & Vachtsevanos G. (2005). Vibration Monitoring for Fault Diagnosis of Helicopter Planetary Gears. *School of Electrical & Computer Engineering, Georgia Institute of Technology, Atlanta, Georgia 30332-0250, 404-894-4132*

Appendix A

MATLAB® Programs

A1 MATLAB® Program – TukeyOptim

As discussed in paragraph 3.2.4, an optimization algorithm is required to ensure that the number of points on the taper section of a tukey window equal the number of points over the tooth mesh section of the window by adjusting α value of the tukey window. This necessitated the development of an optimization algorithm that will adjust the desired number of points, within a given boundary, to obtain the optimum number of points as well as the corresponding α value, within the boundary. As discussed, this optimization algorithm makes use of the particle swarm principle which allows a number of particles to be randomly released in the optimization space. Each particle finds a solution at that random point in the optimization space. The swarm then communicates the suitability of the points with all members. Using the most suitable point that the particle itself has found, together with the most suitable point that the swarm as a whole has found, as well as adding a random deviation, a new point is selected to which the particle moves. The particle then evaluates the new point against its previous most optimum point. The swarm then communicates with all members and the optimum point found by the swarm is again communicated to all members of the swarm. This process is repeated until either, the entire swarms optimum remains a single point or a given number of iterations are completed. This optimization algorithm can be used with any number of particles and can be used to solve for any number of variables, making it a multi-dimensional optimization algorithm.

Minor modifications to the basic optimization algorithm have been made to increase the programs suitability to the solution of the Tukey window optimization and as such the algorithm has been renamed to “TukeyOptim”. The program makes use of an initial number of points which is required as input to the program. The program uses a weight of 2 for the personal best value and a weight of 0.4 for the random addition. Upper and lower boundaries are set to ensure that the solution obtained is within a useable range. The program is then set to look for a maximum or minimum value when evaluating how suitable a specific point is. The function “OptimFun” is used to determine the suitability of a specific point. The number of particles, as well as the maximum number of iterations are set and can be adjusted.

```
function[GX] = TukeyOptim(DesNP);
%TUKEYOPTIM       Program to determine the optimum number of points and alpha
%                 value for a tukey window to be used in EpiTSA;
%
%INPUTS
%     DesNp       Desired Window Size;
%OUTPUTS
%     GX          Optimal output points
%
%     EAMPLE:     (NumberOfPoints, Alpha) = TukeyOptim;
%     SEE ALSO:   OPTIMFUN, EPITSA
%     REFERENCES: Particle swarm optimization Part I:  Notes on diversity
%                 D.N. Wilke, S. Kok & A. Groenwold
%WRITTEN BY:      M.R. de Smidt
%DATE:            2005-10-14
%MODIFIED:

clc; close all;
%--------I N I T I A L I Z A T I O N--------
c1 = 2;                             %Weight Personal to Group best
c2 = 2;                             %Weight Personal to Group best
w = .4;                             %Weight new velocity to old velocity
var = 2;                            %Number of variables
    %[Theta,A]
ub = [175;0.7];                     %Upper bound
lb = [125;0.4];                     %Lower bound
Ext = -1;                           %Extreme direction 1 for max, -1 for min;
%vfac = 1;
ipop = 20;                          %Population size
imax = 1135;                        %Max number of iterations

%--------R A N D O M   S T A R T I N G--------
%Inital random X values
for a = 1:var;
      X(a,:) = unifrnd(lb(a),ub(a),1,ipop);
end
X(1,:)=DesNP;                       %Start all with desired NP
                                    %ONLY FOR TUKEY OPTIM
%Initial blank velocity vector
V = ones(var,ipop);

%Determine function values at points
for a = 1:ipop;
      F(1,a) = OptimFun(X(:,a),var);
```

```
end

%Disp flock behaviour
figure(6);
subplot(2,5,1);
plot(X(1,:),X(2,:),'mo');
%Determine best points
if Ext == 1;
      [GBest,GPos] = max(F);        %Determine group max value
elseif Ext == -1;
      [GBest,GPos] = min(F);        %Determine group min value
end
%Allocate best points
GX = X(:,GPos);                     %Assign group best
PX = X;                             %Assign personal X points
PBest = F;                          %Assign personal best
f = 1;

%-----------------O P T I M I Z A T I O N   L O O P-------------
for a = 1:1:imax
      %disp(['Iteration #',num2str(a)]);        %Display iteration #
      r1 = rand(var,ipop);                      %Random direction var 1
      r2 = rand(var,ipop);                      %Random direction var 2
      for b = 1:ipop
            v=c1*r1(1:var,b).*(PX(1:var,b)-X(1:var,b))+...
            c2*r2(1:var,b).*(GX(1:var,1)-X(1:var,b));
            V(1:var,b)=w*V(1:var,b) + v(1:var,1);  %Determine new velocity vec
      end
      X = V + X;                                %New X points
      X(1,:)=ceil(X(1,:));
      Fc = zeros(1,ipop);                       %Blank function value
      for c = 1:ipop
            Fc(1,c) = OptimFun(X(:,c),var);     %Determine function value
            switch Ext
            case 1
                  for e = 1:var
                        if X(e,c) > ub(e,1) |  X(e,c) < lb(e,1);
                              if Fc(c) > 0;
                                    Fc(c) = Fc(c)*-1;
                              elseif Fc(c) == 0;
                                    Fc(c) = -1;
                              end;
                              Fc(c)=Fc(c)*100000;     %Penalization - exceedence
                        end
                  end
```

```
      case -1
            for e = 1:var
                  if X(e,c) > ub(e,1) |  X(e,c) < lb(e,1);
                        if Fc(c) < 0;
                              Fc(c) = Fc(c)*-1;
                        elseif Fc(c) == 0;
                              Fc(c) = 1;
                        end;
                        Fc(c)=Fc(c)*100000;     %Penalization - exceedence
                  end
            end
      end
end

switch Ext
case 1
for d = 1:length(F)
      if Fc(d) > F(d)                     %Find individual best
            PX(:,d)=X(:,d);               %Record indiv best position
            F(d) = Fc(d);                 %Record individual best value
            end
end
[tGBest,GPos]=max(F);                     %Determine group max value
if tGBest >= GBest;
      GX = X(:,GPos);                     %Determine group best position
end
GBest = tGBest;

case -1
      for d =1:length(F)
            if Fc(d) < F(d)               %Find individual best
            PX(:,d) = X(:,d);             %Record individual best position
            F(d) = Fc(d);                 %Record individual best value
      end
end
[tGBest,GPos]=min(F);                     %Determine group min value
if tGBest <= GBest;
      GX = X(:,GPos);                     %Determine group best position
end
GBest = tGBest;
end

if a <= 9
      figure(6);
```

```
            subplot(2,5,(a+1));
            plot(X(1,:),X(2,:),'bo')
            title(['It# ',num2str(a)]);
      elseif a >=(imax-9)
            figure(7)
            subplot(2,5,f);
            plot(X(1,:),X(2,:),'bo')
            title(['It# ',num2str(a)]);
            %axis([146.5 147.5 0.655 0.659]);
            hold on;
            f = f+1;
      end
      hold on;
end



function[F] = OptimFun(Val,Var);
%OTIMFUN    Program to determine function value at given points
%
%INPUTS
%     Val   Vector of X values at point
%     Var   Number of variables
%
%OUTPUTS
%     F     Function value
%
%     EXAMPLE:    (FunctionValue)=OptimFun([Var1 Var2 Var3],3);
%     SEE ALSO:   TUKEYOPTIM, EPITSA
%     REFERENCES:
%WRITTEN BY:      Capt M.R. de Smidt
%DATE:            2005-10-17
%MODIFIED:

F=1;
if rem((Val(1,1)),3) ~= 0;                %Penalize if not divisible by 3
      F = 1e10;
      break;
end
TapN=Val(1,1)/3;                          %Number of points in taper
if rem((TapN-1),2) ~= 0;                  %Penalize if no centre point
      F = 1e10;
      break;
end
```

```
if Val(1,1)<=0|Val(2,1)<=0
      F = 1e10;
      break;
end
Win = tukeywin(Val(1,1),Val(2,1));        %Determine tukey window

for b = 1:TapN;                           %Extract increasing taper
      TUp(b)=Win(b);
end
c = 1;
for d = ((2*TapN)+1):length(Win);         %Extract decreasing taper
      TDn(c) = Win(d);
      c = c+1;
end
Fault = 0;
for e = 1:length(TUp);                    %Determine variation from 1
      S(e) = abs(TUp(e) + TDn(e));
      Fault(e)= S(e) - 1;
end
Fac = sum(Fault);                         %Determine fault due to variation
F=F*(Fac*100);                            %Penalize by the fault
```

A2 MATLAB® Program – TriggerPoints

Due to the high sampling rate that is required during data capture from the epicyclic gearbox, combined with the large size of the trigger that is used, the tacho signal indicates a large square trigger point similar to a square wave. In addition, the rotational speed of the rotating planet carrier varies with time. It is imperative that the point at which the centre of the planet gear tooth signal under investigation be known to allow accurate averaging.

The function "TriggerPoints" evaluates a given tacho signal. All points above a given trigger value are recorded. The centre point is then determined from the points above the trigger level. This enables the averaging function used in other programs to adapt to small variations in speed as well as ensuring that the correct data points are used during the averaging process.

The signal that is under investigation, as well as the trigger value, is required as inputs to the program with outputs being a vector of trigger points and the number of centre points that the program has determined.

```
function[TP,NCP] = TriggerPoints(SIG,TV);
%TRIGGERPOINTS  Program to determine center points from a tacho signal
%
%INPUTS
%      SIG    Tacho Signal
%      TV     Trigger Value
%
%OUTPUTS
%      TP     Vector containing positions of center points from a tacho signal
%      NCP    Number of center points
%
%      EXAMPLE:     (CenterPoints,NumberPoints)=TriggerPoints(Tacho,3.4);
%      SEE ALSO:
%      REFERENCES:
%WRITTEN BY:      M.R. de Smidt
%DATE:      2005-09-29

Ex = find(SIG>=TV);                 %Determine all points exceeding the TV
a = 1;                              %Reset point counter
```

```
cp = 1;                              %Reset center points counter
while a <= length(Ex)-1;             %Work through all points
      avg = 0;                       %Reset average point number
      count = 0;                     %Reset number of points counter
      while (Ex(a+1)-Ex(a)) == 1;    %Work through series of points
            avg = avg + Ex(a);       %Add point to average
            count = count+1;         %Increase number of average points
            a = a + 1;               %Increase counter
            if a == length(Ex);      %If counter exceeds number of points
                  break              %Stop while loop
            end
      end
      avg = round(avg/count);        %Determine centre point
      if isnan(avg) == 0
            TP(cp)=avg;              %Record centre point as trigger point
            cp = cp+1;               %Increase number of trigger points
      end
      a = a+1;                       %Continue to next point
      if a >= length(Ex)             %If counter exceeds number of points
            break                    %Stop while loop
      end
end
NCP = cp - 1;                        %Assign total number of centre points
```

A3 MATLAB® Program – WindowExtract

To enable averaging of the signal measured from the epicyclic gearbox,windows of data must be extracted from the signal around a given point. This point is usually the point at which the gear passes the accelerometer and is determined using a tacho signal. The signal, from which windows must be extracted, as well as a vector containing the central point around which the data must be extracted, is used as input to the program in conjunction with the window size that is required.

It often occurs that the first window point requires signal values from before the start of the measured signal. Should this occur, the user is warned and when the user acknowledges the warning, the window data is adjusted to accommodate the missing data. If values are required after the last measured signal point, the user is warned and the window from the last signal point is ignored.

The output from the function is a matrix containing the windowed data around each centre point.

```
function[OData] = WindowExtract(SIG,CPoint,WSize);
%SIGDIV     Program to extract a window of data around a centre point
%           WSize must not be divisiable by 2
%
%INPUTS
%     SIG         Original Signal
%     CPoint      Central Point or Centre Point Vector
%     WSize       Window Size to be extracted
%
%OUTPUTS
%     OData       Output Data Vector
%
%     EXAMPLE:    (DataOut)=WindowExtract(Channel1,CentrePoint,WindowSize);
%     SEE ALSO:   TriggerPoints - Program to extract Centre Points
%     REFERENCES:
%WRITTEN BY:      M.R. de Smidt
%DATE:            2005-09-30
%MODIFIED:        2005-10-03  Modified to accept an CPoint vector and then
%                             output a vector containing points


%----------------------------INPUT VARIFICATION----------------------------
if rem(WSize,2) ~= 1                    %Ensure Window Size is an odd number
      disp('Window Size for Extraction not an odd number');
      OData = 'ERROR';
      break
end

%--------------------------POINT DETERMINATION----------------------------
```

```
OData = zeros(length(CPoint),WSize);      %Generate blank output window
Points = (WSize-1)/2;                     %Determine Lead in & Lead out length
%--------------------------FOR EACH CENTRE POINT--------------------------
for b = 1:1:length(CPoint);
      a = 1;                              %Reset window point
      Start = CPoint(b)-Points;           %Determine Starting Point of Window
      End = CPoint(b)+Points;             %Determine Ending Point of Window

      %---------------------------POINT VARIFICATION---------------------------
      if Start <= 0                       %Verify Starting Point not out of Range
            Error = 1-Start;              %Determine number of Points in error
            a = a + Error;                %Adjust Starting Point according to error
            Start = 1;                    %If out of range start at first point
            uiwait(warndlg('Start Window Error - Verify Input Data','W A R N I N
            G'));
      end;
      if End > length(SIG)                %Verify End Point not out of Range
            End = length(SIG);            %Adjust End Point
            uiwait(warndlg('End Window Error - Verify Input Data','W A R N I N
            G'));
      end;
      %---------------------------EXTRACT DATA POINTS---------------------------
      for c = Start:1:End;                %Window Points
            OData(b,a)=SIG(c);            %Record Window Points to Output
            a = a+1;
      end
end
```

A4 MATLAB® Program – ToothLookup

Every different epicyclic gearbox has an specific tooth mesh order which is dependant on the specific design of the gearbox. In order to successfully perform averaging on such a gearbox the teeth in mesh must be known. Thus, the tooth mesh sequence must be determined. The function ToothLookup generates as output a tooth vector consisting of the revolution number, planet number as well as the tooth number. Each of these factors must be known to accurately determine which teeth are currently in mesh. Due to the fact that the sequence will be specific to the gearbox under investigation, the function is developed specifically for the Bonfigligoli gearbox.

It is clear that this function is imperative to the correct averaging of the gearbox. Thus, the output from this function was tested by marking the gears of an open gearbox and rotating the sun gear as the mesh sequence at a specific point was monitored. The gears in mesh were recorded and this data was then checked to ensure that the function was in fact generating the correct sequencing data.

```
function[TV] = ToothLookup;
%ToothLookup      Program to determine tooth mesh order for
%                 Bonfiglogli Epicyclic Gearbox
%
%INPUTS
%
%OUTPUTS
%     TV    Tooth Vector in format:
%           [Rev# Planet#@Acc1 Planet#@Acc2 Tooth@Acc1 Tooth@Acc2]
%
%     EXAMPLE:    (ToothVector)=ToothLookup;
%     SEE ALSO:
%     REFERENCES:
%WRITTEN BY       M.R. de Smidt
%DATE:            2005-10-03
%MODIFIED:

TV = zeros(36,5);                                   %Generate Blank Matrix
a = 1;                                              %Reset Counter
A2GM = 0;                                           %Reset Acc # 2 Gear #
for REV = 1:1:12;                                   %For 12 Gearbox Revolution
      for A1 = 1:1:3;                               %For 3 Planet Gears
            TV(a,1)=REV;                            %Assign Rev #
```

```
            TV(a,2)=A1;                          %Assign Gear # @ Acc 1
            A1GM = mod((REV-1)*62,24)+1;         %Calculate Tooth # @ Acc 1
            TV(a,4)= A1GM;                       %Assign Tooth # @ Acc 1

            switch A1;                           %Calculate Gear # @ Acc 2
            case  1;
                  A2 = 3;                        %Planet 3 @ Acc 2
                  if A2GM == 0;
                        A2GM=((mod((REV-2)*62,24)+1)-3);    %Calculate Tooth # @
                                                            Acc 2
                  end
            case  2;                             %Planet 1 @ Acc 2
                  A2 = 1;
            case  3;
                  A2 = 2;                        %Planet 2 @ Acc 2
            end

            TV(a,3)=A2;                          %Assign Gear # @ Acc 1
            TV(a,5) = A2GM;                      %Assign Gear # @ Acc 2
            A2GM = A1GM + 21;                    %Calculate Tooth # @ Acc 2
            if A2GM > 24;
                  A2GM = A2GM - 24;              %Account for complete revolution
            end
            a = a + 1;                           %Increase counter
      end
end
```

A5 MATLAB® Program – ToothNumberVector

A program is required to determine the points at which the data obtained from a window is recorded. These points will be used as a basis for the averaging process and must be divided over an entire rotation of a planet gear. The window size over each tooth, as well as the number of points required is used as inputs to the function.

The output from the function is a vector containing positions around the planet gear, which are numbered, so that each whole number is the apex of a specific tooth of the planet gear. This vector can be equated to a pseudo epicyclic gear built out of a specific number of points around a real planet gear.

```
function[TNV] = ToothNumberVector(WSize,GP);
%ToothNumberVector      Program to calculate the Tooth Number Vector
%                       for a given Window Size and Number of Points
%
%INPUTS
%     WSize       Window Size in number of points
%     GP          Total number of discrete points
%
%OUTPUTS
%     TNV         Vector containing discrete points through gear rotation
%
%     EXAMPLE:    (ToothPosition)=ToothNumberVector(WindowSize,NumberOfPoints);
%     SEE ALSO:
%     REFERENCES:
%WRITTEN BY:      M.R. de Smidt
%DATE:            2005-10-03
%MODIFIED:

TNV = zeros(1,GP);                              %Empty Vector
PPT = GP/24;                                    %PointsPerTooth
Lead = (PPT-1)/2;
temp=linspace(0.5,1,Lead+1);                    %Half of the First tooth points
for a = 1:length(temp);
      TNV(a)=temp(a);                           %Assign Points
end
for b = 1:1:23;
      temp = linspace(b,b+1,PPT+1);             %Between Teeth
      for c = 2:1:length(temp);
```

```
            a = a+1;
            TNV(a)=temp(c);                         %Assign Points
      end
end
temp = linspace(24,24.5,Lead+1);                    %Last Half of last tooth
for d = 2:length(temp);
      a = a+1;
      TNV(a)=temp(d);                               %Assign Points
end
if length(TNV) ~= GP
      disp('Tooth Number Assignment Error');
end
```

A6 MATLAB® Program – EpiTSA

The function EpiTSA calculates the epicyclic time synchronous average for an epicyclic gearbox. The inputs to the function include a tacho and two accelerometer signals obtained during measurements on the gearbox under investigation. The sample rate at which the signals were sampled are required and is an additional input to the program. If the number of averages and window size is not defined, default values are used.

Trigger levels for the tacho signal must be defined during the program. As these values remain virtually constant during testing, these variables are not used as inputs to the program. The optimum window size and alpha values were determined using the optimization technique described in this document.

The rotational speed variation from an average value is determined to ensure that the averaging process is not corrupted by speed variations during the measurement process. The program determines if there is sufficient data contained in the input to complete the required number of averages. Once all the required confirmations have been received, the program continues to calculate the time synchronous average for the data. The condition indicators that are used are then calculated and can be displayed

```
function[SigAvg] = EpiTSA(Tacho,Acc1,Acc2,SR,NAvg,WSize);
%EpiTSA     Program to calculate the Time Synchronous Average of an
%           Bonfigliogli Epicyclic Gearbox
%
%INPUTS
%     Tacho Tacho signal, with pulse at each planet and increased
%           control pulse at 1 x per rev
%     Acc1  Accelerometer signal at position 1
%     Acc2  Accelerometer signal at position 2
%     SR    Sample Rate
%     NAvg  Number of Averages (Default = 8)
%     WSize Window Size in number of points (Default = 525);
%
%OUTPUTS
%     SigAvg      Built up signal average for planet 1 - 3
%
%     EXAMPLE:    (SignalAverage)=EpiTSA(Tacho,Channel1,Channel2,8,525);
%     SEE ALSO:   TRIGGERPOINTS, TOOTHLOOKUP, WINDOWEXTRACT, GETRPM,
%                 TOOTHNUMBERVECTOR
%     REFERENCES:
%WRITTEN BY       M.R. de Smidt
%DATE:            2005-10-03
```

```
%MODIFIED:        2006-01-30              %Modified to calculate req Win Size

%clc;

%----------D E F A U L T S   &   P R E   S E T   V A L U E S-----------
switch nargin                             %User notification
case 5
      WSize = 525;
      disp(['Number of averages defined: ',num2str(NAvg),' averages']);
      disp(['Default window size:        ',num2str(WSize),' points']);
case 4
      NAvg = 8;
      WSize = 525;
      disp(['Default number of averages: ',num2str(NAvg),'  averages']);
      disp(['Default window size:        ',num2str(WSize),' points']);

case 6
      disp(['Number of averages defined: ',num2str(NAvg),'  averages']);
      disp(['Window size defined:        ',num2str(WSize),' points']);
end

TLevel1 = 2.5;                                    %Trigger level all planets
TLevel2 = 7;                                      %Trigger level planet 1
TWa = 0.67;                                       %Tukey Window alpha
Window = (tukeywin(WSize,TWa))';                  %Generate Window
PPT=(WSize/3);                                    %Points Per tooth
if rem(WSize,3) ~= 0 | rem((PPT-1),2) ~= 0;
      disp('Alpha Value for Tukey Window incorrect for overlap');
end


%------D E T E R M I N E   T R I G G E R   P O I N T S & W I N D O W------
[CP,NCP] = TriggerPoints(Tacho,TLevel1);          %Determine center of planet
[IP,NIP] = TriggerPoints(Tacho,TLevel2);          %Determine pos of planet gear 1

%----------V A R I F Y   W I N D O W   S I Z E   R E Q U I R E D---------
for a = 1:(NCP-1)
      DNSP(a)=CP(a+1)-CP(a);
end
ADNSP=mean(DNSP);
SPT = ADNSP/14;
SPR = SPT*3;
if WSize >=(SPR*1.01)|WSize <= (SPR*0.9);
      button = questdlg('Window Size Variation Larger than 2% of Required',...
                        ' Size.  Do you wish to continue?',...
                        'Continue Operation','Yes','No','No');
      if strcmp(button,'Yes');
            disp(['Window Size Required:       ',num2str(SPR),' points']);
            disp('Continuing with Large Window Variation');
      elseif strcmp(button,'No');
            disp('Program Stopped due to Large Window Variation');
      end
else
      disp(['Window Size Required:       ',num2str(SPR),' points']);
end
```

```
%------------D E T E R M I N E   &   V A R I F Y   S P E E D------------
[rpm,trpm] = getrpm(Tacho,SR,TLevel1,1,3,SR);
rpm = rpm*5.77;
Avgrpm = mean(rpm);
Maxrpm = max(rpm);
Minrpm = min(rpm);
if (Maxrpm-Minrpm)>(Avgrpm*1.02);
      button = questdlg('Speed Variation Larger than 2% of RPM.  ',...
                        'Do you wish to continue?',...
                        'Continue Operation','Yes','No','No');
      if strcmp(button,'Yes');
            disp('Continuing with Large Speed Variation');
      elseif strcmp(button,'No');
            disp('Program Stopped due to Large Speed Variation');
      end
else
      disp(['Speed varified at:          ',num2str(Avgrpm),'[RPM] average']);
end


InitPoint = IP(2);                                  %Do not use first pass
StartP = 1;                                         %Start Point
er = 0;                                             %Initialize error term
while er == 0                                       %Repeat until match found
      if (InitPoint <= (CP(StartP)+2))...
                  &(InitPoint >= (CP(StartP)-2));
            er = 1;                                 %Point found
      else
            StartP = StartP + 1;                    %Increase counter
      end
end

BeginP = find(CP==CP(StartP));                      %Define beginning impulse
EndP = 36*NAvg;                                     %# of impulses (12rpmx3/rpm)
if EndP+1>(length(CP)-BeginP);                      %If insufficient Data impulses
      PAvg = floor((length(CP)-BeginP-3)/36);       %Possible number of averages
      uiwait(warndlg(['Insufficient Data For ',num2str(NAvg),' Averages'],...
             'W A R N I N G'));
      if PAvg == 0;
            disp(['Insufficeint data - No averages possible']);
            break
      else
            disp(['Insufficeint data - number of averages used: ',...
                  num2str(PAvg),' Averages']);
      end
      NAvg = PAvg;
end
for UsePoint = 1:1:(NAvg*36);
      GetPoints(UsePoint)=CP(BeginP+UsePoint-1);
end
Win1 = WindowExtract(Acc1,GetPoints,WSize);
Win2 = WindowExtract(Acc2,GetPoints-round(SPT),WSize);%
for a = 1:min(size(Win1))                           %length(Win1);
      O1 = Win1(a,:).*Window;
      O2 = Win2(a,:).*Window;
      TWin1(a,:)=O1;
```

```
      TWin2(a,:)=O2;
end
clear Win1 Win2 O1 O2;

%------R E A R A N G E   I N T O   T O O T H   N U M B E R S------

GP = 24*(WSize/3);
dpoints = (WSize-1)/2;
TNV = ToothNumberVector(WSize,GP);
TV = ToothLookup;
SigAvg = zeros(4,GP);
for ANum = 1:1:NAvg;
      disp(['Average # ',num2str(ANum)]);
      WS = ((ANum-1)*36)+1;
      WE = ANum*36;
      Pgear = zeros(3,GP);
      a = 0;
      for b = WS:WE;
            a = a+1;
            SWin1 = TWin1(b,:);           %First Window From Window Data Acc1
            SWin2 = TWin2(b,:);           %First Window From Window Data Acc2
            Rev = TV(a,1);                %Determine Rev number
            P1 = TV(a,2);                 %Determine Planet at acc 1
            P2 = TV(a,3);                 %Determine Planet at acc 2
            TN1 = TV(a,4);                %Determine Tooth in mesh at acc 1
            TN2 = TV(a,5);                %Determine Tooth in mesh at acc 2
            %-----------Acc 1------------ (Odd Teeth)
            Middle1 = find(TNV==TN1);           %Middle in output
            RecordStart1 = Middle1-dpoints;     %Start point
            RecordEnd1 = Middle1+dpoints;       %End point
            if RecordStart1>=0 & RecordEnd1 <= length(Pgear)%Apply no overlap
                  Pgear(P1,RecordStart1:RecordEnd1)=...
                  Pgear(P1,RecordStart1:RecordEnd1)+SWin1(1,:);
            elseif RecordStart1 < 0;                        %Apply start overlap
                  Pgear(P1,1:RecordEnd1)=Pgear(P1,1:RecordEnd1)+...
                  SWin1(1,(PPT+1):length(SWin1));
                  Pgl = length(Pgear);
                  Pgear(P1,Pgl-(PPT-1):Pgl)=Pgear(P1,Pgl-(PPT-1):Pgl)+...
                        SWin1(1,1:(PPT));
            elseif RecordEnd1 > length(Pgear) ;             %Apply end overlap
                  Pgl = length(Pgear);
                  Pgear(P1,RecordStart1:Pgl)=Pgear(P1,RecordStart1:Pgl)+...
                        SWin1(1,1:length(SWin1)-PPT);
                  Pgear(P1,1:PPT)=Pgear(P1,1:PPT)+SWin1(1,length(SWin1)-...
                        PPT:length(SWin1));
            end
            %-----------Acc 2------------ (Even Teeth)
            Middle2 = find(TNV==TN2);
            RecordStart2 = Middle2-dpoints;
            RecordEnd2 = Middle2+dpoints;
            if RecordStart2>=0 & RecordEnd2 <= length(Pgear)%Apply no overlap
                  Pgear(P2,RecordStart2:RecordEnd2)=...
                  Pgear(P2,RecordStart2:RecordEnd2)+SWin2(1,:);
            elseif RecordStart2 < 0;                        %Apply start overlap
                  Pgear(P2,1:RecordEnd2)=Pgear(P2,1:RecordEnd2)+...
                        SWin2(1,(PPT+1):length(SWin2));
```

```
                    Pgl = length(Pgear);
                    Pgear(P2,Pgl-(PPT-1):Pgl)=Pgear(P2,Pgl-(PPT-1):Pgl)+...
                          SWin2(1,1:(PPT));
              elseif RecordEnd2 > length(Pgear) ;              %Apply end overlap
                    Pgl = length(Pgear);
                    Pgear(P2,RecordStart2:Pgl)=Pgear(P2,RecordStart2:Pgl)+...
                          SWin2(1,1:length(SWin2)-PPT);
                    Pgear(P2,1:PPT)=Pgear(P2,1:PPT)+SWin2(1,length(SWin2)-...
                          PPT+1:length(SWin2));
              end
        end
        SigAvg(1,:)=(SigAvg(1,:)+(Pgear(1,:)/2));
        SigAvg(2,:)=(SigAvg(2,:)+(Pgear(2,:)/2));
        SigAvg(3,:)=(SigAvg(3,:)+(Pgear(3,:)/2));
end
SigAvg = SigAvg/NAvg;
for a = 1:3
        SigAvg(a,:) = detrend(SigAvg(a,:));
end
SigAvg(4,:)=TNV;

K1 = kurtosis(SigAvg(1,:))
K2 = kurtosis(SigAvg(2,:))
K3 = kurtosis(SigAvg(3,:))
CF1 = (max(abs(SigAvg(1,:))))/(rms(SigAvg(1,:)))
CF2 = (max(abs(SigAvg(2,:))))/(rms(SigAvg(2,:)))
CF3 = (max(abs(SigAvg(3,:))))/(rms(SigAvg(3,:)))
% figure(1);
% subplot(3,1,1);
% plot(SigAvg(4,:),SigAvg(1,:));
% axis tight;
% subplot(3,1,2);
% plot(SigAvg(4,:),SigAvg(2,:),'r');
% axis tight;
% subplot(3,1,3);
% plot(SigAvg(4,:),SigAvg(3,:),'m');
% axis tight;
% figure(2);
% plot(SigAvg(4,:),SigAvg(1,:));
% hold on;
% plot(SigAvg(4,:),SigAvg(2,:),'r');
% plot(SigAvg(4,:),SigAvg(3,:),'m');
% legend(['Planet 1 K=',num2str(K1)],['Planet 2 K=',num2str(K2)]...
%           ,['Planet 3 K=',num2str(K3)],0);
% figure(3);
% subplot(2,1,1);
% plot(SigAvg(4,:),SigAvg(1,:));
% title(['Undamaged planet  Kurtosis = ',num2str(K1)]);
% ylabel('Acceleration [g]');
% axis([0.5 24.5 -0.1 0.15]);
% subplot(2,1,2);
% plot(SigAvg(4,:),SigAvg(3,:));
% ylabel('Acceleration [g]');
% title(['Damaged planet  Kurtosis = ',num2str(K3)]);
% xlabel('Tooth #');
% axis([0.5 24.5 -0.1 0.15]);
```

A7 MATLAB® Program – IntPlanetExtract

Data measured from the internally mounted accelerometer must be extracted and processed. This process is implemented in the function IntPlanetExtract. Inputs to the function include the tacho signal and internal accelerometer signal. The sample rate and number of averages required are also given as inputs to the function. The signal is filtered using a butter filter. The signal average for planet gear 1 is given as output from the function.

```
function[SnlA,FreAvg] = IntPlanetExtract(Tacho,IA,SR,NAvg);
%IntPlanetExtract       Program to extract a window of data for a full planet
%                       gear on a Bonfigliogli Epicyclic Gearbox
%
%INPUTS
%     Tacho       Tacho signal, with pulse at each planet and increased
%                 control pulse at 1 x per rev
%     IA          Internal Accelerometer signal
%     SR          Sample Rate
%     NAvg        Number of Averages
%
%OUTPUTS
%     SnlA        Built up signal average for planet 1
%
%     EXAMPLE:    (SignalAverage)=IntPlanetExtract(Tacho,Channel3,8);
%     SEE ALSO:   TRIGGERPOINTS, TOOTHLOOKUP, WINDOWEXTRACT,
%                 TOOTHNUMBERVECTOR
%     REFERENCES:
%WRITTEN BY       M.R. de Smidt
%DATE:            2006-02-12
%MODIFIED:

%----------------------------V A R I A B L E S----------------------------
TLevel1 = 2.5;                          %Trigger level for all centre points
TLevel2 = 7;                            %Trigger level for P1 marker
[b,a] = butter(3,0.01,'high');


%------D E T E R M I N E   T R I G G E R   P O I N T S & W I N D O W------
[CP,NCP] = TriggerPoints(Tacho,TLevel1);        %Determine center of planet
[IP,NIP] = TriggerPoints(Tacho,TLevel2);        %Determine pos of planet gear 1

IA=filtfilt(b,a,IA);                            %Remove carrier freq
for a = 1:(NCP-1)                               %For all centre points
      DNSP(a)=CP(a+1)-CP(a);                    %Find delta points between
end
ADNSP=mean(DNSP);                               %Find average of delta points
SPT = ADNSP/14;                                 %Determine Sample Points / Tooth
SPP = ceil(SPT*24);                             %Sample Points / Planet
SPS = round((1/3)*SPP+SPP+110);                 %Adjust window size
MAvg = floor(NIP/12);                           %Maximum number of averages
b = 0;                                          %Reset counter
for a = 0:MAvg-1;                               %Max possible # of averages
```

```
        WCP = IP(2+(a*12));                          %Window Centre Point
        SP = WCP-ceil(SPT/2);                        %Start at beginning of T1
        Twin=IA(SP:(SP+(SPS)));                      %Extract window of Planet
        b = b+1;                                     %Increase counter
        Win(b,:)= Twin';                             %Store window
        FreAvg(b,1)=kurtosis(Twin);                  %Store kurtosis
        FreAvg(b,2)=(max(abs(Twin)))/(rms(Twin));    %Store Crest Factor
        FreAvg(b,3)=rms(Twin);                       %Store RMS
        if (a+1) == NAvg                             %Stop if desired #AVG
              break;
        end
end

SnlA=mean(Win);                                      %Determine average signal
FreAvg=mean(FreAvg);                                 %Determine average indicators
%FreAvg=max(FreAvg);                                 %Determine maximum indicators
```

Appendix B

Additional MATLAB® programs

Additional programs were developed and used during this study. These programs are attached in this section

B1 MATLAB® Program – BonfigFreq

During initial investigation on the Bonfigliogli gearbox, the frequencies that are generated during operation of the gearbox were required. This necessitated the calculation of these frequencies. This was implemented in the function BonfigFreq. As the level of complexity increased and the frequency domain data was investigated, different frequencies were identified and the program was expanded to determine frequencies found.

The program requires only the input speed to the gearbox as it is written for a specific gearbox. Outputs from the function is a list of frequencies and the sources of the frequencies. A modified form of the function is used when only specific frequencies must be calculated.

```
function[Freq,Source] = BonfigFreq(InS);
%BONFIGBOX              Program to determineall frequencies in the Bonfiglioli
                        300-L1-5.77-PC-V01B-E epicyclic gearbox
%
%     EXAMPLE:    [Freq,Source]=BonfigFreq(1600)
%     SEE ALSO:   FREQSORT, BONFIGBOX, C130BOX
%     REFERENCES: Mike Hoeper (Flender)
%                 FLENDER BOCHOLT "Planetengetriebe" pg 2-11
%                 (SHVA) The Simplified Handbook of Vibration Analysis, Vol 1,
%                 Arthur R. Crawford
%                 (AoEGV) Analysis of Epicyclic Gearbox Vibration, D. Forrester
%                 & D. Blunt HUMS2003
%                 (EAS)  An explanation for the asymmetry of the modulation
%                 sidebands about the tooth meshing frequency in epicyclic gear
%                 vibration, P.D. MacFadden
%
%WRITTEN BY:      M.R. de Smidt
%DATE:            2004-02-23
%MODIFIED:        2004-03-19, 2005-05-12
%                 2005-06-22  Modified to incorporate asymmetry of modulation
%                             sidebands

%-------------------------G E A R B O X   D E T A I L S-------------------------
Nr = 62;  Zb = Nr;                  %#T ring
Np = 24;                            %#T planet
Ns = 13;  Za = Ns;                  %#T sun

%-----------------------S P E E D S   A N D   R A T I O S----------------------
Inf = InS/60;                       %Input frequency
i = (Zb/Za)+1;                      %Actual ratio Flender -6- eq 7
io = -(Zb/Za                        %Flender -7- eq 8
ns = InS/(1-io); fc = (ns/60);      %Output (Carrier) speed Flender -7- eq 9
iof = io * (-1);                    %Adjustment for FAC Fold out
PS = InS*(iof/(1+iof))*(Ns/Np);     %Planet speed FAG Fold out: I A --> S, B fix
GMF = (PS/60)*Np;                   %[Hz] Gear Mesh Frequency SHVA Pg 81,
                                    %Formula 4-18
```

```
GMF3 = GMF*3;                       %[Hz] 3 x GMF (Identifiable frequency as
                                    %indicated by EAS)
PPM = 3*fc;                         %[Hz] Planet Pass Modulation (3 PLANETS)
                                    %AoEGV Pg 510-2
US1 = GMF+Inf;                      %[Hz] GMF Sun gear, Upper side band
                                    (m=1,n=1)
US2 = GMF+(PS/60);                  %[Hz] GMF Planet gear, Upper side band
                                    (m=1,n=1)
US3 = GMF+fc;                       %[Hz] GMF Carrier, Upper side band (m=1,n=1)
LS21 = GMF - 2 * Inf;               %[Hz] GMF Sun gear, 2 x Lower side band
                                    (m=1,n=-2)
LS22 = GMF - 2 * (PS/60);           %[Hz] GMF Planet gear, 2 x Lower side band
                                    (m=1,n=-2)
LS23 = GMF - 2 * fc;                %[Hz] GMF Carrier, 2 x Lower side band
                                    (m=1,n=-2)
L2S21 = (2*GMF)+ 2 * Inf;           %[Hz] 2 x GMF Sun gear, 2 x Upper side band
                                    (m=2,n=2)
L2S22 = (2*GMF)+ 2 * (PS/60);       %[Hz] 2 x GMF Planet gear, 2 x Upper side
                                    band (m=2,n=2)
L2S23 = (2*GMF)+ 2 * fc;            %[Hz] 2 x GMF Carrier, 2 x Upper side band
                                    (m=2,n=2)
L2S1 = (2*GMF)-Inf;                 %[Hz] 2 x GMF Sun gear, Lower side band
                                    (m=2,n=-1)
L2S2 = (2*GMF)-(PS/60);             %[Hz] 2 x GMF Planet gear, Lower side band
                                    (m=2,n=-1)
L2S3 = (2*GMF)-fc;                  %[Hz] 2 x GMF Carrier, Lower side band
                                    (m=2,n=-1)
Inf2 = 2*Inf;                       %[Hz] 2 x Input frequency;
Inf3 = 3*Inf;                       %[Hz] 3 x Input frequency;
Inf4 = 4*Inf;                       %[Hz] 4 x Input frequency;
Inf8 = 8*Inf;                       %[Hz] 8 x Input frequency;
fc2 = 2*fc;                         %[Hz] 2 x Output frequency;
fc3 = 3*fc;                         %[Hz] 3 x Output frequency;
fc4 = 4*fc;                         %[Hz] 4 x Output frequency;
FFS1 = (InS-PS)/Ns;                 %[Hz] Fault frequency Sun;
FFS2 = FFS1*2;                      %[Hz] 2 x Fault frequency Sun;
FFS3 = FFS1*3;                      %[Hz] 3 x Fault frequency Sun;
%Test section
LS1 = GMF-Inf;                      %[Hz] GMF Sun gear, Lower side band (m=1,n=-
                                    %1)
LS2 = GMF-(PS/60);                  %[Hz] GMF Planet gear, Lower side band
                                    %(m=1,n=-1)
LS3 = GMF-fc;                       %[Hz] GMF Carrier, Lower side band (m=1,n=-
                                    %1)
Source = ['Input F SUN         ';'Output F CARRIER    ';...
          'Planet Rev F        ';'3 x GMF             ';...
          'Planet Pass Mod     ';'GMF SUN USB         ';...
          'GMF PLANET USB      ';'GMF CARRIER USB     ';...
          '2 x GMF SUN LSB     ';'2 x GMF PLANET LSB  ';...
          '2 x GMF CARRIER LSB';'2 x Input F SUN     ';...
          '3 x Input F SUN     ';'4 x Input F SUN     ';...
          '2 x Output F        ';'3 x Output F        ';...
          '4 x Output F        ';'Fault F Sun         ';...
          '2 x Fault F Sun     ';'3 x Fault F Sun     ';...
          '8 x Input F SUN     ';'GMF SUN 2 x LSB     ';...
          'GMF PLANET 2 x LSB  ';'GMF CARRIER 2 x LSB';...
```

```
          'GMF                *';'GMF SUN LSB       *';...
          'GMF PLANET LSB     *';'GMF CARRIER LSB   *'];
Freq = [Inf;fc;(PS/60);GMF3;PPM;US1;US2;US3;L2S1;L2S2;L2S3;Inf2;Inf3;Inf4;...
      fc2;fc3;fc4;FFS1;FFS2;FFS3;Inf8;LS21;LS22;LS23;GMF;LS1;LS2;LS3];
[Freq,Source]=freqsort(Freq,Source);

for a = 1:length(Freq)
      disp([Source(a,:),' ',num2str(Freq(a,:))]);
end
```

B2 MATLAB® Program – CritFreq

When plotting the frequency data it is usefull to display the expected frequencies in the existing plot. These frequencies are calculated using the function BonfigFreq which has been discussed previously. The function CritFreq is then used to display the critical frequency in an existing plot. The frequency requires the rotational speed of the gearbox as well as the maximum frequency and maximum y-axis value in the plot to determine the values to be installed in the plot. This data is easily obtained from the data used to plot the original data.

```
function[] = CritFreq(Speed,FMAX,VMAX);
%FREQPLOT   Program to insert critical frequencies into an existing plot;
%
%INPUTS
%     Speed       Input speed for frequency calculations
%     FMAX        Maximum frequency in plot
%     VMAX        Maximum value in plot
%
%     EXAMPLE:    CritFreq(RotSpeed,max(Freq),max(Y));
%     SEE ALSO:   BONFIGFREQ
%     REFERENCES:
%WRITTEN BY:      M.R. de Smidt
%DATE:            22-06-2005
%MODIFIED:
hold on;

[Freqt,Sourcet]=BonfigFreq(Speed);
a = 1;                                      %Counter
while(Freqt(a)<FMAX) & (a<length(Freqt))
      a = a+1;
end
if a < length(Freqt)
      a=a-1;
end

hold on;
for b = 1:a;
      plot([Freqt(b),Freqt(b)],[0,VMAX],'r');
      text((Freqt(b)-0.7),(VMAX*(2/3)),(Sourcet(b,:))','FontSize',8);
      hold on;
end
```

B3 MATLAB® Program – C130Box

During the course of this research, the need arose at the SAAF VCC to determine the frequencies that are unique to the epicyclic set on the C130 gearbox. These frequencies were easily calculated using a modified version of the function BonfigFreq. This modified function was given the title C130Box. The input speed was required as input to the function. Data pertaining to the number of teeth was obtained from the literature concerning the gearbox, as well as correlation with practical gear counting on an open gearbox in the SAAF. The input speed was obtained from practical measurement during vibration testing on an actual aircraft. The data was logged and filtered using a Chadwick system. This enabled the frequencies from the gearbox to be determined. The frequency domain data measured from the gearbox during testing was then evaluated. A fault frequency not previously used for monitoring but which had been noticed in previous frequency data was found and incorporated into the SAAF vibration monitoring schedule. This frequency had been seen in damaged gearboxes in previous measurements but had never been incorporated as the users were unaware as to what was causing this frequency. This made a significant improvement in the reliability of the vibration monitoring in the VCC.

```
function[Freq,Source] = BonfigBox(InS);
%BONFIGBOX        Program to determineall frequencies in the Bonfiglioli
%                 300-L1-5.77-PC-V01B-E epicyclic gearbox
%
%     EXAMPLE:    [Freq,Source]=BonfigBox(1600)
%     SEE ALSO:   FREQSORT
%     REFERENCES: Mike Hoeper (Flender)
%                 John Hofmeyr (SAAF VCC)
%                 Div de Villiers (SAAF VCC)
%                 FLENDER BOCHOLT "Planetengetriebe" pg 2-11
%                 (SHVA) The Simplified Handbook of Vibration Analysis, Vol 1,
%                 Arthur R. Crawford
%                 (AoEGV) Analysis of Epicyclic Gearbox Vibration, K. Forrester
%                 & D. Blunt HUMS2003
%WRITTEN BY:      Capt M.R. de Smidt
%DATE:            2004-02-23
%MODIFIED:        2004-03-19, 2005-05-12

%-------------------------G E A R B O X   D E T A I L S-------------------------
Nr = 62;  Zb = Nr;                  %#T ring
Np = 24;                            %#T planet
```

```
Ns = 13;  Za = Ns;                    %#T sun

%----------------------S P E E D S   A N D   R A T I O S-----------------------
Inf = InS/60;                         %Input frequency
i = (Zb/Za)+1;                        %Actual ratio Flender
                                      %Planetengetriebe -6- eq7
io = -(Zb/Za);                        %Flender Planetengetriebe -7- eq 8
ns = InS/(1-io); fc = (ns/60);        %Output (Carrier) speed Flender
                                      %Planetengetriebe -7- eq 9
iof = io * (-1);                      %Adjustment for FAC Fold out
PS = InS*(iof/(1+iof))*(Ns/Np);       %Planet speed FAG Fold out:
                                      %I A --> S, B fixed
GMF = (PS/60)*Np;                     %[Hz] Gear Mesh Frequency SHVA Pg 81,
                                      %Formula 4-18
PPM = 3*fc;                           %[Hz] Planet Pass Modulation (3 PLANETS)
                                      %AoEGV Pg 510-2
FF1 = (PS/60)*2;                      %[Hz] Planet rotation fault frequency
FF2 = (InS-PS)/Ns;                    %From Mike Hoeper
Source = ['Input frequency (Sun gear):  ';'Output frequency (Carrier):  ';...
          'Planet revolution frequency: ';'Gear Mesh Frequency:         ';...
          'Planet Pass Modulation:      ';'Planet rotation fault freq:  ';...
          'Fault Frequency - Unknown    '];
Freq = [(InS/60);fc;(PS/60);GMF;PPM;FF1;FF2];
[Freq,Source]=freqsort(Freq,Source);
```